



HAL
open science

SUPRAMOLECULAR ENGINEERING OF VESICLES VIA SELF-ASSEMBLY: APPLICATION TO DRUG DELIVERY

Floraine M. Collette

► **To cite this version:**

Floraine M. Collette. SUPRAMOLECULAR ENGINEERING OF VESICLES VIA SELF-ASSEMBLY: APPLICATION TO DRUG DELIVERY. Material chemistry. University of New Hampshire, Durham, 2005. English. NNT : . tel-00359278

HAL Id: tel-00359278

<https://theses.hal.science/tel-00359278>

Submitted on 6 Feb 2009

HAL is a multi-disciplinary open access archive for the deposit and dissemination of scientific research documents, whether they are published or not. The documents may come from teaching and research institutions in France or abroad, or from public or private research centers.

L'archive ouverte pluridisciplinaire **HAL**, est destinée au dépôt et à la diffusion de documents scientifiques de niveau recherche, publiés ou non, émanant des établissements d'enseignement et de recherche français ou étrangers, des laboratoires publics ou privés.

THESIS

UNIVERSITY OF
NEW HAMPSHIRE

SUPRAMOLECULAR ENGINEERING OF VESICLES VIA
SELF-ASSEMBLY: APPLICATION TO DRUG DELIVERY

BY
FLORAINE M. COLLETTE

MASTER OF SCIENCE

2005

SUPRAMOLECULAR ENGINEERING OF VESICLES VIA SELF-ASSEMBLY:
APPLICATION TO DRUG DELIVERY

BY

FLORAINE M. COLLETTE

B.S., UNIVERSITY OF PARIS VI (FRANCE), 2003

Submitted to the University of New Hampshire

In Partial Fulfillment of

The Requirement for the Degree of

Master of Science

In

Chemistry

December, 2005

This thesis has been examined and approved.

Thesis Director,
Jerome P. Claverie
Associate Research Professor

Glen P. Miller
Associate Professor in Chemistry

Richard P. Johnson
Professor in Chemistry

Date 14/09/05

DEDICATION

This thesis is dedicated to my family. Without their love and support this work would not have been possible

ACKNOWLEDGEMENTS

First and foremost I would like to thank Jerome Claverie for letting me stay in his research group after my internship. The knowledge he has shared with me will surely help me in the future. I wanted also like to thank him for always pushing me to go further and for always showing a happy face when we obtained some encouraging results; for me that one of the main motivating factors. I also wanted to thank all the members of the NPRC for always being supportive and in particular Julien, Zac and Anne who have become great friends. I owe a huge thanks to Yvon and Don for always being so kind with me.

I owe a special thanks to all the faculty members and the students of the chemistry department, especially to Gary Weisman who shared his love for teaching and has always been extremely supportive. Thanks to all of you for your kindness and support.

I express my gratitude to Dr Johnson and Dr Miller for spending time reading this thesis and guiding me along my Master's degree.

I also thank Bentley Pharmaceutical Inc. for funding this project. I really appreciate the work we did with them, in particular with Robert Gyurik. Thanks to all of you.

TABLE OF CONTENTS

DEDICATION	iii
ACKNOWLEDGEMENTS.....	iv
TABLE OF CONTENTS.....	v
LIST OF FIGURES	ix
LIST OF TABLES	xiii
ABSTRACT	xiv
I. INTRODUCTION	1
1. Diabetes	1
2. Insulin Delivery Methods.....	7
A. Non-oral delivery methods.	7
B. Oral delivery of therapeutic proteins: Challenges.....	8
C. Oral delivery of therapeutic proteins and existing strategies for the oral delivery of insulin: Absorption enhancers.	10
D. Oral delivery of therapeutic proteins and existing strategies for the oral delivery of insulin: Coupling with a transport promoter.	11
E. Oral delivery of therapeutic proteins and existing strategies for the oral delivery of insulin: Proteases inhibitors.....	11
F. Oral delivery of therapeutic proteins and existing strategies for the oral delivery of insulin: Mucoadhesive polymers.....	12
G. Oral delivery of therapeutic proteins and existing strategies for the oral delivery of insulin: Prodrugs.....	13
H. Oral delivery of therapeutic proteins and existing strategies for the oral delivery of insulin: Microparticles and nanoparticles.....	14

I. Oral delivery of therapeutic proteins and existing strategies for the oral delivery of insulin: Liposomes and Niosomes.	15
J. Oral delivery of therapeutic proteins and existing strategies for the oral delivery of insulin: Delivery in the colon.	16
K. A new approach.	16
3. Design of the vesicles.....	19
II. BACKGROUND	22
1. Self-assembly with amphiphilic compounds	22
2. Selection of the components of the triblock copolymer.....	34
3. Synthetic Scheme.....	37
4. Synthesis of PEG-PLA diblock copolymer	38
5. Synthesis of polyglutamic acid.....	43
III. RESULTS AND DISCUSSION.....	52
1. Synthesis of the diblock copolymer PEG-PLA	52
2. Synthesis of the homopolymer poly(glutamic acid).....	67
3. Formation of the triblock copolymer PEG-PLA-PGlu	79
4. Formation of vesicles.....	85
A. Self-assembly of vesicles and characterization	85
B. Structure of the vesicles.	96
C. Insulin Encapsulation.	99
5. Pharmacokinetics and pharmacodynamics	102
IV. CONCLUSION	108
V. EXPERIMENTAL SECTION	112
1. General Methods	112
2. Solvents.....	113

3. Reagents	114
4. Synthesis	116
A. Typical preparation of a diblock copolymer.	116
B. Typical N-Carboxy Anhydride preparation.....	118
C. Typical polymerization of the NCA.	119
D. Typical deprotection of a poly(benzyl glutamate).	120
E. Five other methods of deprotection of the Poly(benzyl glutamate).....	121
F. Typical preparation of the branched triblock copolymer.	123
G. Typical preparation of the linear triblock copolymer, typical polymerization of the NCA and functionalisation of the P(Bn)Glu.	125
H. Typical coupling reaction.....	126
I. Typical deprotection of the linear triblock copolymers.	127
J. Typical CAC measurement experiment.	128
K. Typical insulin encapsulation experiment.	129
L. Animal experiments	130
LIST OF REFERENCES.....	134
APPENDICES	147
Appendix A: ^1H NMR of PEG-PLA in CDCl_3	148
Appendix B: ^{13}C NMR of PEG-PLA in CDCl_3	149
Appendix C: DSC spectrum of PEG-PLA	150
Appendix D: IR of the NCA polymerization at $t=0$	151
Appendix E: IR of the NCA polymerization at $t=3\text{h}17$	152
Appendix F: Maldi-tof spectrum of the P(Bn)Glu	153

Appendix G: Light scattering of the triblock copolymer PEG ₂₀₀₀ -PLA ₉₈₀₀ -PGlu ₁₃₀₀	154
Appendix H: ¹ H NMR of PEG-PLA-PGlu in TFA	155
Appendix I: Approval Letter 1 IACUC #030302	156
Appendix J: Approval Letter 2 IACUC #030302.....	157
Appendix K: Approval Letter 3 IACUC #030302	158

LIST OF FIGURES

Figure 1. Estimation of the prevalence of diabetes in the world, from reference 3	1
Figure 2. Scheme of the mechanism of the insulin and the glucagons ⁸	2
Figure 3. Figure of the islet of Langerhans ⁸	2
Figure 4. Amino Acid sequence of insulin (picture taken from reference 13).....	3
Figure 5. Molecule of Insulin (C ₂₅₄ H ₃₇₇ N ₆₅ O ₇₆ S ₆) ¹⁶	4
Figure 6. Hexamer of insulin coordinated with two Zinc atoms ¹⁷	4
Figure 7. Picture of an Insulin pen ¹⁸	5
Figure 8. Injection sites ¹⁹	6
Figure 9. TEM pictures of insulin fibrils ²¹	6
Figure 10. Different transports through the intestine ³⁶	10
Figure 11. Liposome section.....	15
Figure 12. SEM of intestinal microvilli of a mouse ⁷⁴	17
Figure 13. Picture showing villi, epithelial cells that cover the villi and the microvilli of the epithelial cells ⁷⁵	18
Figure 14. TEM picture of intracellular vesicle formation during endocytosis ⁷⁷ ..	19
Figure 15. Preparation of nanoparticles loaded with insulin.	20
Figure 16. Fate of the dosage form inside the small intestine	21
Figure 17. Figure of Vesicles (adapted from reference 78), Nanorod and Nanotube (adapted from reference 79) and Micelle (adapted from reference 80)	22
Figure 18. Scheme of extrusion process	23
Figure 19. Typical example of a bicontinuous optimal structure ⁸⁹	24
Figure 20. Geometries of self-assembled interfaces: (a) micellar (spheres), (b) hexagonal (cylinders), (c) lamellar (planes), (d) cubic bicontinuous (cubic minimal surfaces) and (e) disordered bicontinuous (random surfaces) ⁹⁰	24
Figure 21. Conjugation of DOX to poly(aspartic acid-b-ethylene glycol).....	25
Figure 22. Schematic structure of the nanoparticles NK911 ⁹³ (PEG (114 units) is used as a hydrophilic block and poly(aspartic acid) (30 units) coupled with Doxorubicin (DXR or DOX) as the hydrophobic part)	26
Figure 23. Figure of the formation of polymeric micelles (C) loaded with cisplatin (A) prepared from the complex formation of the diblock copolymer PEG-PGlu (B) and the cisplatin ⁹²	27
Figure 24. Picture of a shell crosslinked knedel. a. Formation of a micelle by self assembly. b. regioselective crosslimking. c. cleavage of core chains. d. extraction of the core ⁹⁶	27
Figure 25. Poly(styrene-b-p-chloromethyl styrene-quaternarized poly(4-vinyl pyridine)) ⁹⁷	28

Figure 26. PEG-PIBCA formula.....	29
Figure 27. triblock copolymer: PMBPS-b-PEO-b-PMBPS ¹¹⁵	31
Figure 28. triblock copolymer: PMOXA-PDMS-PMOXA ^{116,117,118}	31
Figure 29. triblock copolymer: PEO-b-PPO-b-PEO ¹¹⁹	32
Figure 30. Triblock copolymer: PEO-b-PDMS-b-PMOXA ¹²⁰	32
Figure 31. Formation of vesicles by direct self-assembly	34
Figure 32. Formation of vesicles by self-assembly after phase inversion.....	34
Figure 33. Biocompatible polymers used in drug delivery	35
Figure 34. Triblock copolymer: PEG-b-PLA-b-PGlu	36
Figure 35. Retrosynthesis for the triblock copolymer PEG-b-PLA-b-PGlu.....	37
Figure 36. Diblock copolymer PEG-b-PLA	38
Figure 37. L-Lactide (left), D-Lactide (middle) and meso-Lactide (right).....	39
Figure 38. Synthesis of PEG-b-PLA and PLA-b-PEG-b-PLA ^{107, 140}	40
Figure 39. Mechanism of metal alkoxide catalysis ¹⁴²	41
Figure 40. Mechanism of ring-opening polymerization using tin octoate and an alkoxide as initiator ¹⁴²	41
Figure 41. Catalyst for the polymerization of lactide: aluminium isopropoxide (left) and triethyl aluminium (right)	42
Figure 42. Poly(L-glutamic acid)	43
Figure 43. Phosgene	44
Figure 44. Triphosgene	44
Figure 45. Formation of the NCA of benzyl glutamic acid using either phosgene or triphosgene.....	44
Figure 46. Initiation of NCA using water, alcohols, primary amines or secondary amines	46
Figure 47. Initiation of NCA polymerization with tertiary amine or metal salts ...	47
Figure 48. Polymerization of high molecular weight PGlu using cobalt or nickel initiators	49
Figure 49. Mechanism of the NCA polymerization ¹⁵¹	50
Figure 50. ¹ H NMR spectra of the aliquots taken during the lactide polymerization (region of the methine proton)	53
Figure 51. ¹ H NMR spectrum of a diblock copolymer after 60 minutes at 60°C..	54
Figure 52. Transesterification occurring during the quenching of the polymerization with methanol	55
Figure 53. PLA polymerization.....	56
Figure 54. conversion of the molecular weight of the PLA block versus time (squares: MW _{PLA} =5000 g/mol; triangles: MW _{PLA} =15000)	58
Figure 55. Mechanism of the polymerization of the lactide by zinc alkoxide.....	59
Figure 56. Number average molecular weight vs the conversion ([Et ₂ Zn]=0.01mol/L, [lactide]=0.7mol/L, [PEG ₂₀₀₀]=0.02mol/L, 60°C)	60
Figure 57. GPC traces of a PEG-PLA copolymer, at different times. [PEG]=0.02mol/L, [lactide]=0.7mol/L	61
Figure 58. intramolecular and intermolecular transfers during the polymerization of lactide	62

Figure 59. DSC spectrum of a diblock copolymer (FMC 54) done with L-lactide (11.2mg of the sample was heated between -90°C and 220°C at a rate of 20°C/min).....	64
Figure 60. Quantitative ¹³ C NMR spectrum of a diblock copolymer made with L-lactide in CDCl ₃	64
Figure 61. DSC spectrum of a diblock copolymer (FMC 145) done with racemic lactide (15.1mg of the sample was heated between - 40°C and 220°C at a rate of 5°C/min, modulated).....	65
Figure 62. Quantitative ¹³ C NMR spectrum of a diblock copolymer (FMC 113) made with racemic lactide in CDCl ₃	66
Figure 63. Quantitative ¹³ C NMR spectrum of a diblock copolymer (FMC 113) made with racemic lactide in CDCl ₃ , zoom of the methyne signal (69ppm).....	67
Figure 64. NCA synthesis.....	68
Figure 65. zoom of the carbonyl region in IR before polymerization.....	69
Figure 66. zoom of the carbonyl region in IR after polymerization.....	69
Figure 67. Chromatogram of the NCA polymerization at 4 minutes.....	70
Figure 68. Chromatogram of the NCA polymerization at 180 minutes.....	70
Figure 69. NCA polymerization.....	71
Figure 70. Peak average molecular weight (measured by GPC) versus conversion (measured by HPLC).....	72
Figure 71. Formation of pyroglutamic end-groups ¹⁴⁸	72
Figure 72. α-helix ¹⁶¹	74
Figure 73. Parallel and antiparallel β-sheets ¹⁶¹ (vertical line: antiparallel, oblique line: parallel).....	74
Figure 74. Maldi-tof spectrum of poly(benzyl glutamate) (FMC 129) showing a bimodal distribution, sign of the β-sheets formation. This has been measured using MS ionization, positive reflectron mode, 80kV and 3-indoleacrylic acid (IAA) as a matrix. 1uL of poly(benzyl glutamate) in DMF/MeOH was deposited on the grid. Once dried, 1 uL of IAA in DMF/MeOH was added.	76
Figure 75. GPC chromatogram of polyglutamic acid (FMC 147, eluent phosphate buffer saline) showing low molecular weight chains, sign of the β-sheets formation in the poly(benzyl glutamate)	76
Figure 76. PGLu deprotection.....	77
Figure 77. Different methods to deprotect the poly(benzyl glutamic acid)	78
Figure 78. GPC trace of polyglutamic acid (eluent phosphate buffer saline) showing low molecular weight chains, sign of the hydrolysis of the PGLu.....	79
Figure 79. Coupling reaction between PGLu and the diblock copolymer.....	80
Figure 80. Side reaction occurring with DCC.....	81
Figure 81. ¹ H NMR spectrum of the branched triblock copolymer PEG ₂₀₀₀ -PLA ₅₄₇₅ -PGLu ₃₈₇₀ (FMC 95)	81
Figure 82. Functionalization of the poly(benzyl glutamate) prior coupling	83
Figure 83. Linear triblock copolymer.....	83
Figure 84. GPC chromatogram of the diblock copolymer PEG-PLA under deprotection condition at 20 minutes, 1 hour and 2 hours	84
Figure 85. ¹ H NMR of the vesicles in D ₂ O	86
Figure 86. Different processes applied on the triblock copolymer	88

Figure 87. TEM picture of particles formed by linear triblock copolymers.....	90
Figure 88. TEM pictures of the nanovesicles obtained by self-assembly in an HEPES buffer (The numbers correspond to the DP of each block).....	91
Figure 89. Cryo TEM of vesicles made by self-assembly of the triblock copolymer PEG-PLA-PGlu	92
Figure 90. Self-assembled monolayers SM1, SM2 ans SM3	92
Figure 91. AFM 3D view (1:1:1) of vesicles made by self-assembly of the triblock copolymer PEG-PLA-PGlu	93
Figure 92. Light scattering spectrum of the nanovesicles.....	94
Figure 93. Emission spectrum of pyrene in presence of PEG ₂₀₀₀ -PLA ₉₈₀₀ -PGlu ₁₂₉₀₀	95
Figure 94. Ratio of the intensity of the bands located at 332.5 and 338 nm vs pyrene concentration.	96
Figure 95. triblock copolymer in suspension in PBS in the presence (right side, vial labeled with a P) or without (left side) proteases	97
Figure 96. Formula of the Alexa fluor 350 hydrazide sodium salt.....	98
Figure 97. Formula of the Alexa fluor dyes 568 and 488.....	99
Figure 98. Amount of insulin, leaking from the vesicles (solid line) measured by HPLC, and calculated without vesicles (dash line)	101
Figure 99. Average insulin concentration vs time	103
Figure 100. Average glucose concentration vs time.....	104
Figure 101. Average insulin concentration vs time	106
Figure 102. Insulin concentrations in function of the time for the group 1.....	107

LIST OF TABLES

Table 1. Example of initiators which can be used for the NCA polymerization 148, 151	48
Table 2. Different type of catalysts prepared	57
Table 3. concentration of catalyst and of the ratio of monomer to catalyst in function of the molecular weight of the PEG.....	57
Table 4. Recapitulative table of the PEG-PLA synthesized	63
Table 5. Yield of the deprotection reaction	79
Table 6. Recapitulative table of the branched triblock copolymers synthesized .	82
Table 7. Recapitulative table of the linear triblock copolymers synthesized	84
Table 8. insulin encapsulation results.....	100
Table 9. Synthesis of diblock copolymers.....	117
Table 10. Synthesis of N-Carboxy Anhydride (NCA)	118
Table 11. Synthesis of Poly(Benzyl Glutamate) (PBnGlu)	119
Table 12. Synthesis of Poly(Glutamic acid) (PGlu).....	120
Table 13. Deprotection of PBnGlu with HBr	122
Table 14. Synthesis of triblock copolymers	124
Table 15. Preparation of functionalized PBnGlu prepared.....	126
Table 16. Formation of protected triblock copolymers	127
Table 17. Deprotection of protected triblock copolymers.....	128
Table 18. Intensities measured at 332.5 nm and 335 nm for different concentration of PEG-PLA-PGlu in the presence of pyrene (0.1674 g/L)	129
Table 19. Treatments given to the three groups of rats	130
Table 20. Treatments given to the three groups of rats	131

ABSTRACT

SUPRAMOLECULAR ENGINEERING OF VESICLES

VIA SELF-ASSEMBLY:

APPLICATION TO DRUG DELIVERY

By

Floraine M. Collette

University of New Hampshire, December, 2005

Sixteen millions of people are diabetics in the United States. Finding an oral way to deliver the insulin they need would improve the quality of their life. For this purpose biodegradable and biocompatible nanovesicles encapsulating some insulin have been synthesized. Those nanovesicles are made by self-assembly of a triblock copolymer poly(ethylene glycol)-b-poly(lactic acid)-b-poly(glutamic acid) (PEG-b-PLA-b-PGlu). The triblock copolymer has been prepared in several steps by multi-step anionic ring-opening polymerization. The first step consisted in the preparation of the diblock copolymer PEG-b-PLA. This diblock copolymer was synthesized by ring opening of racemic lactide, using a zinc alkoxide as an initiator. The second step was the synthesis of the poly(glutamic acid). The polybenzyl(glutamic acid) was obtained by ring opening polymerization of the N-Carboxyanhydride of the corresponding amino acid. Finally, the benzyl group was deprotected via protonolysis, to generate the homopolymer. This triblock was successfully obtained by coupling a diblock copolymer PEG-b-

PLA and a homopolymer poly(glutamic acid). In the presence of an aqueous solution of insulin where the pH is between 7 and 9, the triblock copolymer self-assembles in nanovesicles containing a part of the free insulin. In the intestine, the vesicles are highly solvated due to the deprotonated poly(glutamic acid) hair which are expected to be located on the outside. Moreover, to resist from the gastric acidity, the nanovesicles are protected with gastro resistant polymer, Eudragit, which stay solid at acidic pH but get dissolved in the intestine (where the pH is slightly basic), releasing the vesicles. All the polymers have been characterized using ^1H NMR and GPC. The percentage of encapsulation of insulin has been measured by HPLC some in-vivo experiments have been done on Sprague-Dawley rats.

I. INTRODUCTION

1. Diabetes

Diabetes is the fastest growing disease in the world¹ and currently affects 194 million people (Figure 1).²

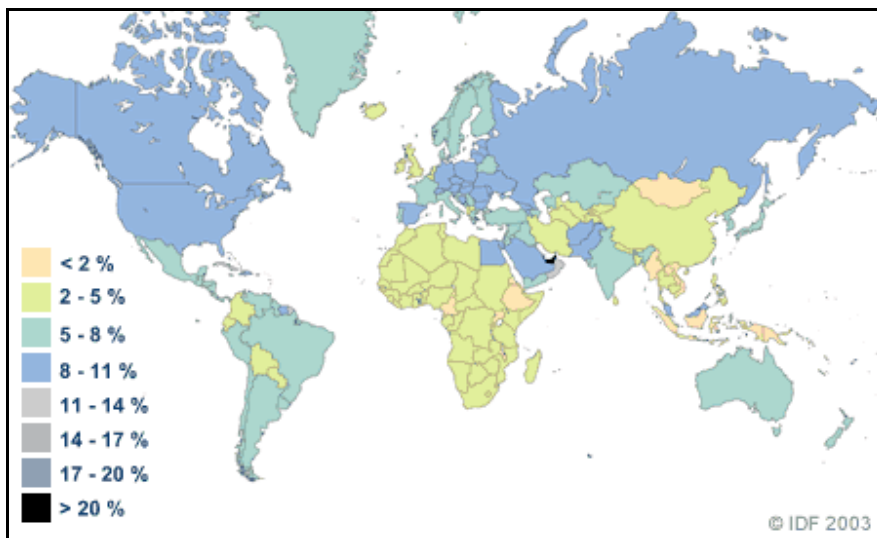


Figure 1. Estimation of the prevalence of diabetes in the world, from reference 3

In the United States, this disease was the sixth greatest cause of mortality in 2002.⁴ Currently 5 to 10% of the population⁵ has diabetes and it is expected that one out of three Americans born in 2000 will develop diabetes.⁶ From 1991 to 2004, in the United States, the number of cases has increased by 61%⁶ and it is expected that there will be 333 million diabetics in the world by 2025.² The annual American cost (direct and indirect) of diabetes represents 132 billion of dollars.⁶

Diabetes, also known as “high blood sugar”,⁶ is a leading cause of heart disease, stroke, blindness and kidney failure. This disease is caused by an inadequate regulation of the glucose level in the blood. The two main endocrine hormones responsible for glucose regulation are insulin and glucagon. They are both generated in the islets of Langerhans located in the pancreas (Figure 2).⁷ Insulin is synthesized in the beta-cells of the islets of Langerhans whereas glucagon is produced in the alpha-cells (Figure 3). When an excess of glucose is in the blood, the pancreas secretes insulin. Insulin activates a series of cell-receptors leading to the storage of glucose under the form of glycogen in the liver and to the uptake of glucose by other cells. Glucagon is the regulatory endocrine hormone for hypoglycemia (Figure 3).⁷

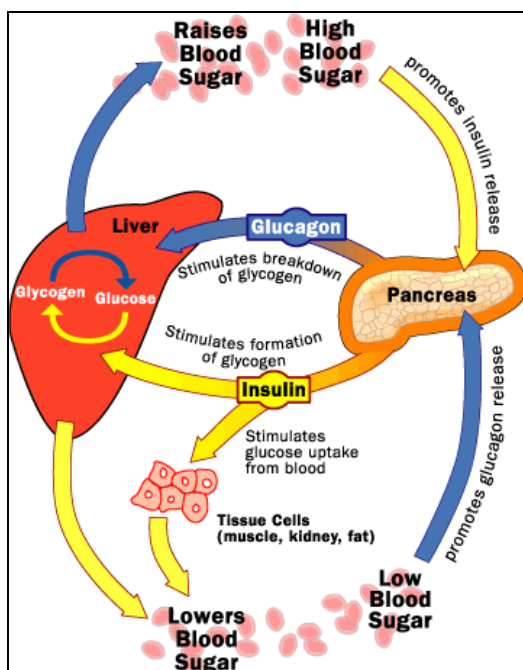


Figure 2. Scheme of the mechanism of the insulin and the glucagons⁸

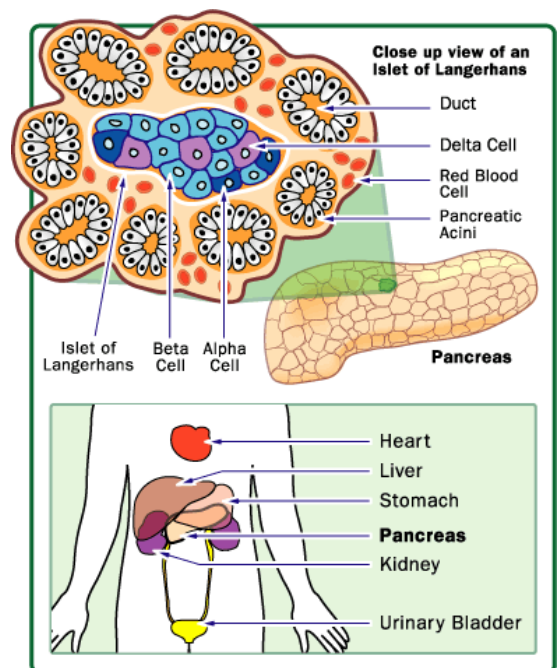


Figure 3. Figure of the islet of Langerhans⁸

Diabetes occurs in two different forms, classified as type one and type two. In the case of type one diabetes (also called juvenile diabetes), an autoimmune disease of genetic origin results in the eventual death of the beta-cells in the pancreas. This type of diabetes affects about 10% of the diabetics.⁹

Type two diabetes affects people over 30 or people who suffer from obesity. It often occurs when insulin is no longer efficiently recognized by cell receptors. The body becomes insulin-resistant and after several years, the production of insulin may even decrease.¹⁰ Besides a strict diet and physical exercise, therapeutic treatments include the use of “fat-burners” and injections of large doses of insulin. Therefore, insulin therapy is used in the treatment of both types of diabetes.

Insulin was discovered by Dr. Frederick Banting in 1922.¹¹ He was awarded the Nobel Prize in Physiology or Medicine one year later for this discovery. Insulin is a protein constituted of 51 amino acids (Figure 4): 2 peptide chains (the chain A of 21 and the chain B of 30 amino acids) are bonded together by two disulfide bridges.¹² An additional disulfide bridge link the residue A6 and A11. Its sequence was determined in 1955 by Frederick Sanger and it was the first protein to be sequenced.¹²



Figure 4. Amino Acid sequence of insulin (picture taken from reference 13)

In the presence of zinc ions, a zinc-containing hexameric aggregate is formed between two metal ions and six molecules of insulin, as shown in Figure 6. This complex is stabilized by the interaction of the zinc with the histidine residues located in position 10.¹⁴ In an aqueous medium, insulin adopts a globular conformation (Figure 5) with a volume of about 1.73 nm³ for the monomeric form and 14.71 nm³ for the hexameric form.¹⁵



Figure 5. Molecule of Insulin
(C₂₅₄H₃₇₇N₆₅O₇₆S₆)¹⁶

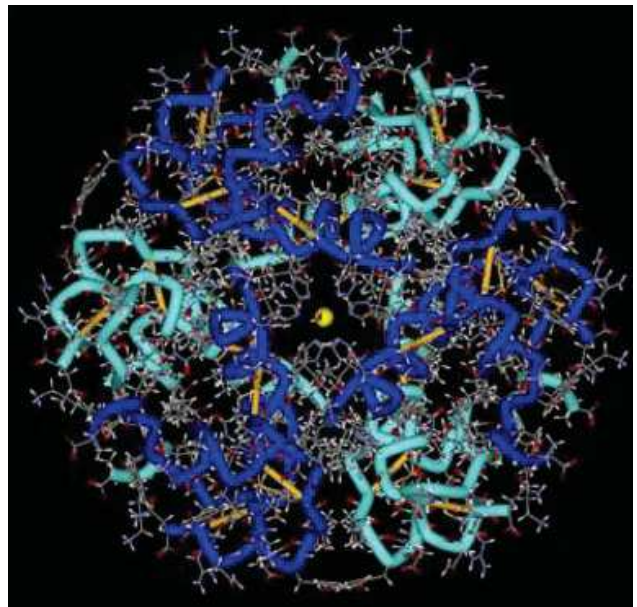


Figure 6. Hexamer of insulin coordinated with two Zinc atoms¹⁷

Insulin cannot be delivered orally since, as a protein, it is degraded in the stomach and intestine. Until April 2005, the only diabetes treatment accepted by the FDA (Food and Drug Administration) consisted of injecting therapeutic doses of insulin subcutaneously. In the majority of cases, a non-glycosylated human recombinant insulin

is used, although porcine or bovine insulin have been used in the past. As an alternative, pancreas transplant is an option for type one diabetics. No less than 33% of the people reject the transplant 5 years after this very heavy operation.³ The recently developed transplant of only the islets of Langerhans is a less intrusive procedure. Pancreatic cells are injected in the portal vein and are trapped in the liver. The rejection rate is still extremely high: 92% of the patients need to restart insulin injections after only one year.³

Diabetics inject insulin up to eight times a day using a subcutaneous needle. An insulin “pen” is often used to choose the right dosage (Figure 7).



Figure 7. Picture of an Insulin pen¹⁸



The injection sites are rotated to avoid the formation of painful dips in the skin (Figure 8) which are caused by the subcutaneously injected insulin which triggers an unwanted glucose digestion and cell apoptosis. A means of insulin delivery, that more uniformly distributes the drug throughout the body and favoring its uptake where needed, is currently unavailable and is highly desirable.

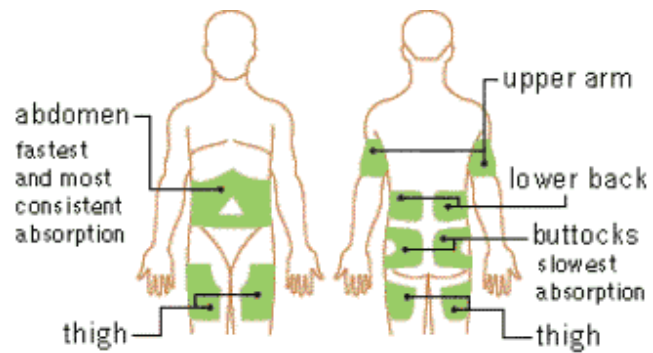


Figure 8. Injection sites¹⁹

In addition to the formation of dips, subcutaneous injection of insulin presents several other difficulties. Insulin, like most proteins, is prone to denaturation when kept as a solution (fibril formations: Figure 9). The insulin solutions cannot be kept more than 28 days either stored at room temperature (23°C) or 2 years refrigerated (4°C).²⁰

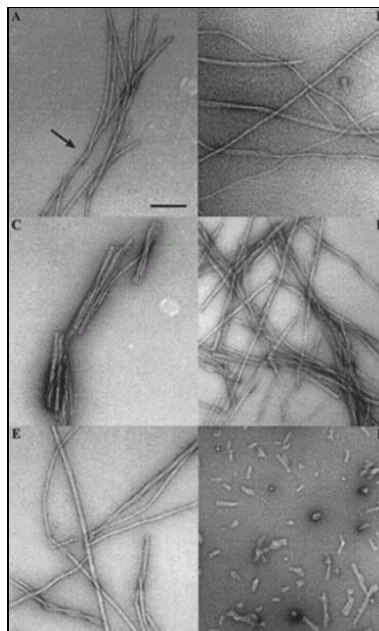


Figure 9. TEM pictures of insulin fibrils²¹

As a parenteral drug, the level of purity of insulin must be extremely high. In order to prevent the apparition of deadly pathogens (ie. bacteria), insulin solution is formulated with a significant quantity of biocides. Today, people typically use human recombinant insulin solutions containing no less than 1.5 g/L of phenol as biocide.²² Due to these disadvantages, there is a need to develop other methods of delivering insulin.

2. Insulin Delivery Methods

A. Non-oral delivery methods. There is a large body of academic and industrial work on insulin vectorization. Numerous delivery schemes have been investigated. Several methods can be envisaged, among those are oral, transdermal, buccal, nasal, ocular and parenteral administration routes.²³ For example, several biotechnology companies (Inhale, Generex, Emisphere) have been testing pulmonary delivery of insulin,²⁴ and are currently in Phase III clinical trials.²⁵ The first results indicated that there was a larger occurrence of cystic fibrosis, associated with lung infections, on patients using this pulmonary insulin.²⁶ Further testing of this method is currently underway. It has been argued that insulin, projected at the bottom of the lungs using a supersonic jet, causes fibril formation. This leads to a disease similar to the asbestosis triggered by asbestos inhalation. The company PowderJect (Oxford, UK) is interested in using a transdermal device²⁷ which propels insulin coated microparticles through the skin. Unfortunately, this mode of injection can be quite painful but is currently studied. Bentley Pharmaceuticals (Exeter, NH) is currently testing an intranasal formulation of

insulin which utilizes a non-toxic permeation enhancer to cross the nose epithelial barrier.²⁸ Phase I clinical trials have shown this method to be extremely effective.

Several attempts were made to deliver insulin orally without encapsulating it. Most of these attempts made use of an adsorption promoter which rendered the intestinal membrane permeable.²⁹ These promoters are usually quite toxic, since the epithelial cells lining the intestinal wall are damaged in their presence.²⁹ Therefore, encapsulation of insulin in a vesicle is necessary. In this dissertation, we investigate and develop oral delivery method.³⁰

B. Oral delivery of therapeutic proteins: Challenges. For most patients, the use of oral insulin is a painless method that would offer greater comfort and a better quality of life. It would be well received by patients who dislike injections. In addition, insulin would be delivered directly to the portal vein, where the pancreas naturally dumps insulin. There are several difficulties with the oral delivery of therapeutic proteins. First, peptide bond degradation is catalyzed by numerous enzymes present in the gastrointestinal track. Moreover the bonds are also pH-sensitive and the pH of the stomach can be as low as one.

Another difficulty in the delivery of therapeutic proteins is the intestinal wall which is an absorption barrier. It has been shown that under the best experimental conditions, less than 0.5% of insulin is absorbed through the intestinal mucosa.³¹ The intestine inner most layer is composed of epithelial cells covered by a viscous hydrophobic layer of mucus containing proteases. The epithelium is a physical barrier and prevents the absorption of any foreign compound. These epithelial cells, also named enterocytes,

host the cytochromes P450 and represent the first site for metabolism of orally ingested xenobiotics like therapeutic drugs.³² Therapeutic proteins can be recognized by cytochromes and can then undergo a variety of enzymatic reactions including epoxidation, N-dealkylation, O-dealkylation, S-oxidation and hydroxylation.³³ The cytochromes role is to detoxify substances that cross the membrane. However, as far as we know, insulin has not been reported to be a substrate of the Cytochrome P450.^{34,35}

Once the nutrient reaches the membrane intact, molecular transportation takes place via paracellular, transcellular or carrier-mediated transport (Figure 10).³⁶ Under natural conditions, most nutrient transport through the intestinal membrane is mediated by active ion-exchange mechanisms which are catalyzed by efflux mediated proteins (P-GP, Figure 10). Protein transport is not reported to be catalyzed by P-GP efflux mediated proteins.

Paracellular transport occurs when a nutrient channels through tight junctions between epithelial cells. The size of these tight junctions is small enough to exclude the passage of a protein (1.1 nm^{37, 38, 39}).

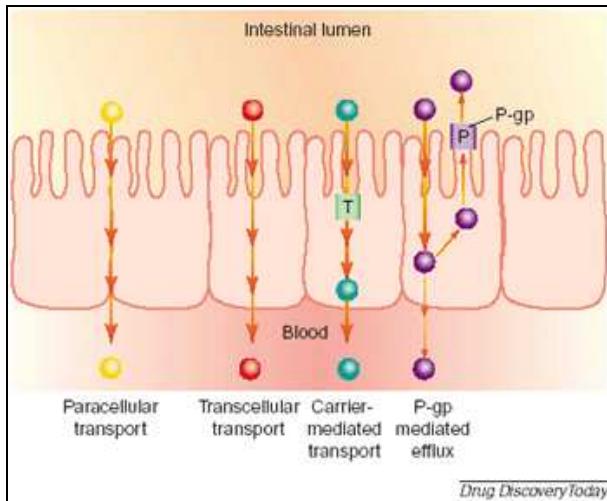


Figure 10. Different transports through the intestine³⁶

The last mode of transport is transcellular transport mediated by endocytosis (vide infra).

C. Oral delivery of therapeutic proteins and existing strategies for the oral delivery of insulin: Absorption enhancers. One of the strategies used to promote the permeation of proteins through the intestine consists of using permeation enhancers. Absorption enhancers change the properties of the intestinal wall and improve its permeability by creating a perturbation or increasing disorder in the intestinal membrane. Substances, such as bile salts, surfactants, cyclodextrins, saponin, sodium taurodihydrofusidate, sodium caprate, Na₂EDTA and sodium glycocholate, have been found to enhance the absorption of insulin.³⁹ Despite this, the insulin bioavailability is still low.⁴⁰ Calcium chelators are also used to provoke the opening of transcellular tight junctions³⁸ but interaction with sodium channels prevent its use for chronic administration. Beside their

toxicity toward the epithelial barrier,⁴¹ the absorption enhancers are not specific which can lead to the coabsorption of toxins.³⁸

D. Oral delivery of therapeutic proteins and existing strategies for the oral delivery of insulin: Coupling with a transport promoter. To improve the absorption of drugs, the protein can be coupled to a specific molecule which promotes intestinal transport, for example vitamin B₁₂. Once in the intestine, the transporter, located on the intestinal wall, recognizes the promoter like the vitamin, binds to it and allows the passage of the drug through the intestinal wall. In this case, the protein can still be subject to protease degradation.^{38, 42, 43}

E. Oral delivery of therapeutic proteins and existing strategies for the oral delivery of insulin: Proteases inhibitors. It is also possible to use proteases inhibitor to minimize enzymatic degradation. An inhibitor blocks the active site of the enzyme, either reversibly or irreversibly. Several protease inhibitors have been used, among others pepstatin, aprotinin, EDTA and ovomucoid.⁴⁴ A change of pH can also lead to inhibition as shown by the Unigene Laboratories (Fairfield, NJ). Salmon calcitonin is an excellent substrate for the pancreatic serine protease trypsin. With a decrease of pH, the activity of the enzyme decreases while the absorption, in the lower small intestine, is at a maximum.⁴⁵ Madsen *et al.* have demonstrated that the graft copolymer Poly(Methacrylic acid-g-Ethylene Glycol) (PMMA-g-PEG) can act as a protease inhibitor. In this case, poly(Methacrylic acid) chelates calcium ions, minimizing the activity of calcium dependent enzymes such as trypsin.⁴⁶ The more concentrated the inhibitor, the larger the bioavailability of the therapeutic protein. However this process interferes with the digestion of nutritive proteins and cannot be used for a long durations.^{38, 47, 48} A more

efficient method uses proteases inhibitors coupled with absorption enhancers as in the case of Oralject™ technology for oral vaccine delivery for salmonids.⁴⁹ Protease inhibitors can also be combined with mucoadhesive polymers.

F. Oral delivery of therapeutic proteins and existing strategies for the oral delivery of insulin: Mucoadhesive polymers. Mucoadhesive polymers have specific affinity for the mucin layer of a biological membrane. Mucin are high molecular weight glycosylated glycoproteins which form the mucus.⁵⁰ Mucoadhesive polymers adhere to the intestinal mucus because their low Tg (glass transition temperature) facilitates the diffusion of the polymer in the mucus resulting in the formation of favorable interactions (hydrophobic interactions, hydrogen bonds and electrostatic interactions). Mucoadhesion is greater for polymers with charged terminal groups (polyacrylate derivatives are often used) due to the formation of favorable interactions with the mucin functional groups (carboxyl, hydroxyl, amide, sulfate groups).⁵¹ Poly(acrylic acid) has been extensively tested for the release of therapeutic proteins in the close vicinity of the intestine wall.⁵¹ This acidic polymer locally decreases the pH, reducing topically the activity of the proteolytic enzymes present in the gastro-intestinal track. This polymer can also release either Ca²⁺ ions (which provoke the opening of transcellular tight junctions and enhance the absorption), enzyme inhibitors or absorption enhancers.³⁸ It has also been found by De Ascentiis *et al.* that the addition of free poly(ethylene glycol) chains increases the mucoadhesive properties of a polyacrylate derivative.⁵² Polymers having carboxylic groups and poly(ethylene glycol) fragments have been shown strong adhesion because of their propensity to form hydrogen-bonds with the hydroxyl groups of the mucin (present in the branched sugar chains).⁵³ The mucus also has a strong affinity with

hydrophobic materials. The mucoadhesion of polymers with thiol end-groups is enhanced by the formation of disulfide bonds with the cysteine-rich domains present in the mucus.⁵³

G. Oral delivery of therapeutic proteins and existing strategies for the oral delivery of insulin: Prodrugs. Another strategy to affect oral delivery consists in the use of prodrugs. In this case, the prodrug needs to be able to convert quantitatively into the protein to be delivered. The properties of the drug, such as stability, hydrophobicity, pharmacokinetics, polarity, etc..., are changed: The drug absorption increases and the drug becomes more resistant towards the proteases degradation. It has been shown that the cyclization of a therapeutic protein reduces its polarity and charge thereby increasing its membrane permeability.⁵⁴ The covalent coupling of the protein with a polymer, such as poly(ethylene glycol) (or PEG)⁵⁵ can improve biopharmaceutical and clinical properties of several therapeutic proteins. The solubility⁵⁶ and the stability⁵⁷ of the protein is increased, for example, which allows better pharmacokinetics properties.⁵⁶ Pegylated proteins can reduce adverse immune responses compare to the unpegylated equivalent therapeutic protein.⁵⁸ The digestion of pegylated proteins is believed to be slower because of the steric hindrance imparted by the PEG chain causes the therapeutic protein to become less accessible to the enzymes.⁵⁷ For example, pegylation increases the lifetime of a protein in circulation (stealth characteristics).⁵⁷ Such stealth proteins are not recognized by macrophages because their surface is devoid of hydrophobic patches. In practice, the use of prodrugs for the oral delivery of proteins has not been successful. However, Nobex has developed in phase II an oral version of insulin, Hexyl-insulin monoconjugated 2 (HIM2).^{59, 60} Moreover, by covalently

modifying a protein, a new molecule is created, which has unknown toxicity and side effects. The pharmacokinetics and pharmacodynamics activity can also significantly differ from the activity of the natural protein.

H. Oral delivery of therapeutic proteins and existing strategies for the oral delivery of insulin: Microparticles and nanoparticles. Microparticles and nanoparticles can also mediate the transport of drugs through the epithelium. It is thought that the particle protects the protein from gastric acidity and enzyme degradation allowing the intestinal wall to be crossed. The uptake of particles by the intestine has been the object of several studies, often with contradicting results. It has been shown that a polystyrene particle can cross the wall of the intestine without degradation.⁶¹ The amount of particles internalized decreases with increasing particle size. It is 6% for a 100 nm particle, 3% for a 300 nm particle and 0% for a 3µm particle.⁶¹ Using colloidal gold nanoparticles, Hillyer *et al.*⁶² has also shown that the absorption of particles with diameters comprised between 50 nm and 20 µm, occurs in the Peyer's Patch regions⁶³ of the small intestine (A Peyer's Patch is any of several lymph nodes in the walls of the intestines near the junction of the ileum and colon). This is size dependant with the smaller the particle size giving greater absorption rate. Desai *et al.* studied the effect of the particle size on the uptake of biodegradable microparticles made of poly(lactic-co-glycolic acid). Experiments were done on 100 nm, 500 nm, 1 µm and 10 µm particles. The uptake of 100 nm size nanoparticles was 4×10^6 times higher than for 10 µm microparticles and 6.7×10^3 times higher than for 1 µm microparticles. The concentration of the 100 nm size nanoparticles has been shown to be greater in the Peyer's Patch tissues.⁶⁴ However, it is known that Peyer's Patches are very few in number (~0.1%) and it is unknown if the

particles are released in the lymphatic system, in the blood or if the particles stay in the Peyer's Patch. Also, an increase of the hydrophobic character of the particle increases the absorption.⁶⁵

I. Oral delivery of therapeutic proteins and existing strategies for the oral delivery of insulin: Liposomes and Niosomes. The use of liposomes⁶⁶ and niosomes^{67, 68} seems to be promising. A liposome is an artificial microscopic vesicle consisting of an aqueous core enclosed in a phospholipid bilayer, used to convey vaccines, drugs, enzymes, or other substances to target cells or organs (Figure 11).⁶⁹

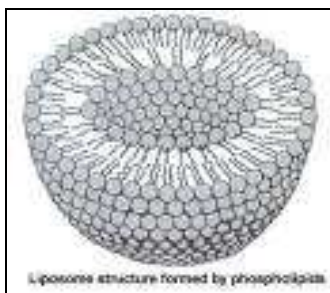


Figure 11. Liposome section

Niosomes are artificial vesicles made of non-ionic surfactants which can also be used in drug delivery. Niosomes are formed with fatty acids which are pegylated.⁶⁸ In these systems, the therapeutic proteins are protected against the enzymatic degradation, not only in the intestinal lumen but also in the mucus. The surfactants, with which the vesicles are formed, can enhance the penetration in the mucus. However, they are much less stable than polymeric particles and can easily undergo degradation in the gastro-intestinal track.³⁸ Moreover, the use of organic solvent is necessary for their formation and they are quite large (10 μ m).⁷⁰

J. Oral delivery of therapeutic proteins and existing strategies for the oral delivery of insulin: Delivery in the colon. Finally, drugs can be delivered in the colon. Some polymers like Eudragit or cellulose acetate phthalate are pH sensible and will only become solvated in the colon where the pH is slightly more alkaline than in the intestine.⁷¹ Once the polymer is dissolved, the therapeutic protein is released. As the proteolytic enzymes concentration is smaller in the colon, the protein is less likely to be hydrolyzed. Thus, the bioavailability is higher than in the small intestine.

K. A new approach. None of the techniques mentioned have been very successful, since they do not combine high bioavailability and low toxicity, the requirements for drug delivery. There are a wide variety of nanosize objects, the most common ones being nanovesicles and nanoparticles. Insulin in nanoparticles is not well protected from the action of intestinal proteases. The driving force for the encapsulation of insulin is the formation of hydrophobic interactions between the nanoparticle and insulin. In this dissertation, we will reserve the use of the word vesicles to “nano” objects (with size < 1 μm). It is well known that proteins irreversibly adsorb on hydrophobic surfaces leading to protein denaturation (rearrangement of the tertiary structure).⁷² Therefore, insulin must be encapsulated in vesicles. As seen below, vesicles are stabilized by a hydrophilic external layer which is essential to ensure colloidal stability. If the hydrophilic layer is too small, the vesicles aggregate together under the form of a macroscopic powder. Usually vesicles which are colloidally stable in water are protected by a charged layer. However, mucus has been shown to be an

“hydrophobic” environment,⁷³ and charged objects (even if they have mucoadhesive properties) usually do not permeate the intestinal membrane. This yields an intrinsic contradiction between colloidal stabilization and intestinal permeation.

We propose to encapsulate insulin in polymeric vesicles of nanometer scale, so called nanovesicles. Of course, those nanovesicles need to possess special characteristics. First, they need to be biocompatible as they are orally administrated and then partially absorbed. They must be resistant to the gastrointestinal environment (low pH in the stomach and pH = 7.4 in the intestine), in order to cross the intestinal wall and to deliver the insulin into the blood. To cross the intestine between the microvilli by endocytosis, the nanovesicles need to be small enough. The intestine surface is covered by villi, composed of epithelial cells. On the surface of those epithelial cells, microvilli (also called “brush border”⁷⁴) increase the surface area of the intestine to almost 200 square meters⁷⁴ (Figure 12 and Figure 13).

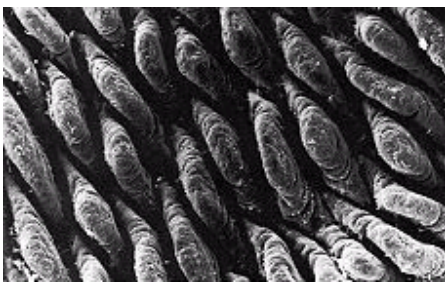


Figure 12. SEM of intestinal microvilli of a mouse⁷⁴

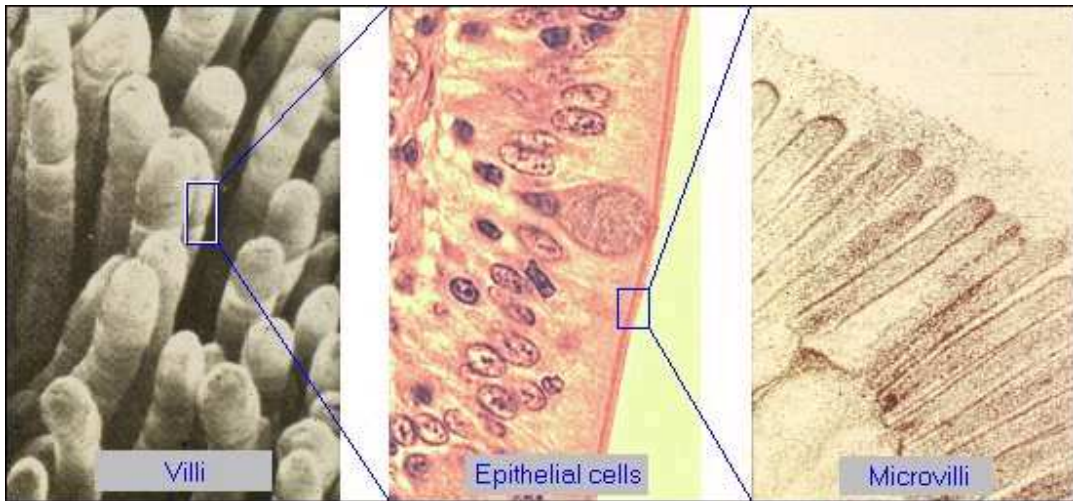


Figure 13. Picture showing villi, epithelial cells that cover the villi and the microvilli of the epithelial cells⁷⁵

The distance between microvilli is around 80nm.⁷⁶ If the diameter of the vesicles is too large, the vesicles will probably not be able to approach the surface of the enterocyte where absorption occurs. Endocytosis is a process whereby any cell internalizes material. In the gastrointestinal track, the epithelial cells (Figure 14) internalize material and release it into the blood. This material can be, among a large number of possibilities, amino acids, proteins, vitamins, sugar and lipids. In the endocytosis process, after activation of receptors present on the surface of the epithelial cells, an invagination of the plasma membrane is created and the substance becomes internalized in an intracellular vesicle (endosome). This intracellular vesicle is transported by the cytoskeleton until the substance gets released in the blood by fusion of the vesicle with the plasma membrane (exocytosis).

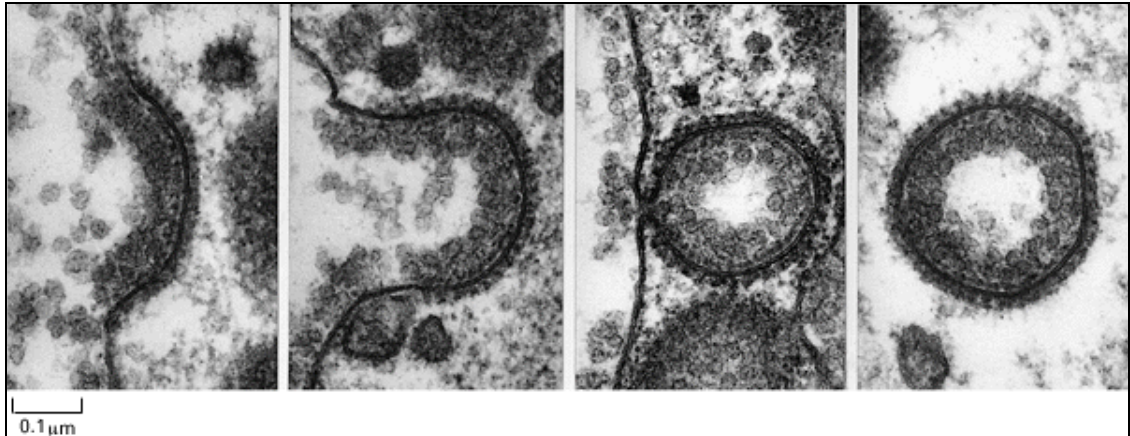


Figure 14. TEM picture of intracellular vesicle formation during endocytosis ⁷⁷

3. Design of the vesicles

The nanovesicles we have prepared are formed by the self assembly of a triblock copolymer, as illustrated in Figure 15. This triblock copolymer is composed of a block of poly(ethylene glycol) (PEG), a block of poly(lactide) (PLA), and a block of poly(glutamic acid) (PGlu), where the hydrophobic block (PLA) is the inner block. This triblock PEG-PLA-PGlu is prepared by multi-step anionic ring-opening polymerization. We show that vesicles are spontaneously formed in an aqueous solution of insulin ($7 < \text{pH} < 9$, Figure 15). We also bring indirect proof that the PEG block is mostly oriented towards the internal compartment, whereas the PGlu is oriented toward the outside. In the nanovesicles, the inner hydrophilic PEG prevents the adsorption of the insulin on the hydrophobic layer of PLA. The PLA prevents the leakage of the protein to the

outside. In the intestine, where the pH is about 7.4, PGlu is partially deprotonated. This allows the vesicle to become highly solvated, prevents the formation of aggregates due to high electrostatic repulsions between vesicles, and imports the vesicles with mucoadhesive properties.

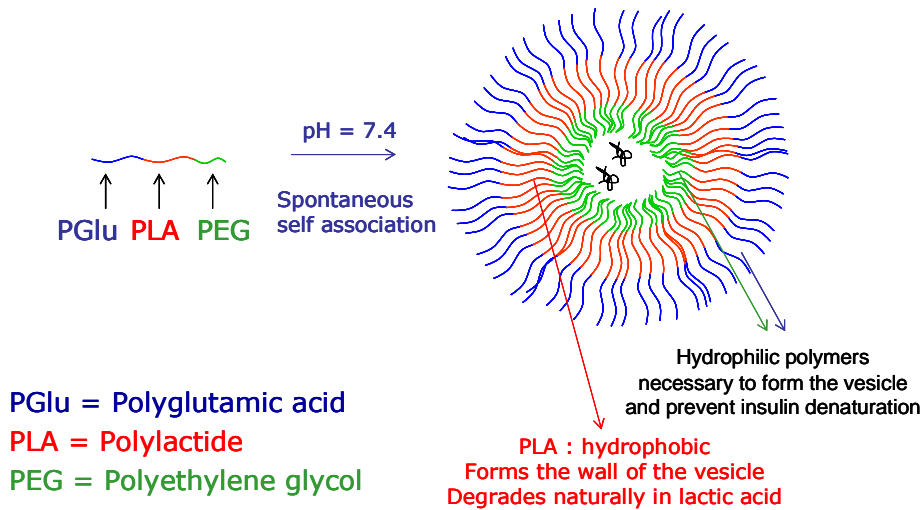


Figure 15. Preparation of nanoparticles loaded with insulin.

The vesicles containing the insulin are microencapsulated in Eudragit, a commercial polymer which is insoluble in the acidic environment of the stomach. Eudragit is used to form gastro-resistant pills which are not degraded in the stomach, but are solubilized in the intestine, thus releasing the vesicles. The vesicles have been designed so that the external PGlu, once exposed to the cocktail of intestinal proteases (which are in the lumen and in the mucus), is degraded (PGlu is also a “protein”). Thus, the vesicle surface becomes more hydrophobic as patches of PLA are exposed at the surface. The unsolvated vesicles are expected to “precipitate” at the surface of the intestine, be trapped in the microvilli or in the Peyer’s patch regions and be internalized via endocytosis

in an endosome. In the acidic endosome (pH=4-5), the polylactide is degraded, leaving water-soluble PEG and insulin (Figure 16).

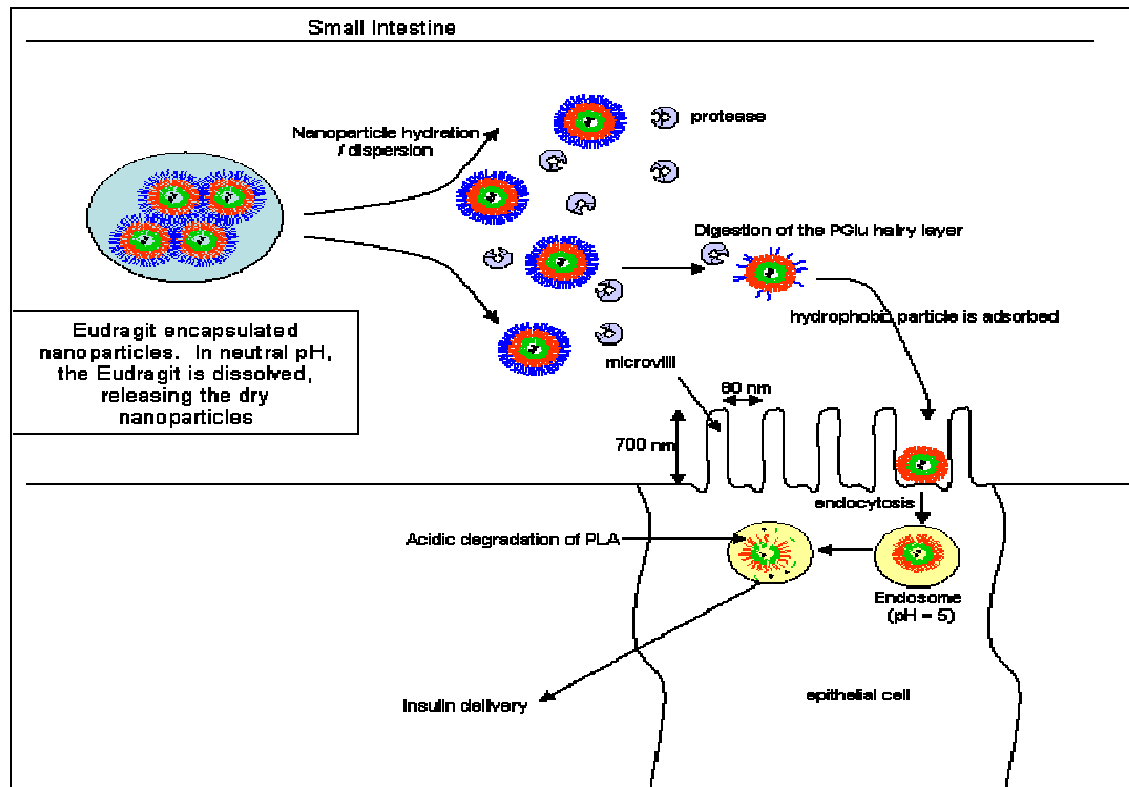


Figure 16. Fate of the dosage form inside the small intestine

To the best of our knowledge, triblock copolymers PEG-PLA-PGLu have never been synthesized prior this work, and the preparation of such compounds will be presented in detail in Section III. In a subsequent chapter, elements on the formation of vesicles, structure of vesicles and encapsulation of insulin in these vesicles will be presented. Finally, the results of the insulin delivery in rats, mediated by the vesicles, will be discussed.

II. BACKGROUND

1. Self-assembly with amphiphilic compounds

Amphiphilic compounds (also called surface active compounds or surfactants) possess at least one hydrophilic part and one hydrophobic part. Such compounds spontaneously self-organize in the presence of a selective solvent, such as water, which dissolves only one of the parts. Depending upon the nature of the amphiphile and the conditions (temperature, ionic strength, concentration, etc.), a variety of supramolecular aggregates can be formed, such as micelles, vesicles, lamellar structures, rods or bicontinuous structures (Figure 17 and Figure 20).

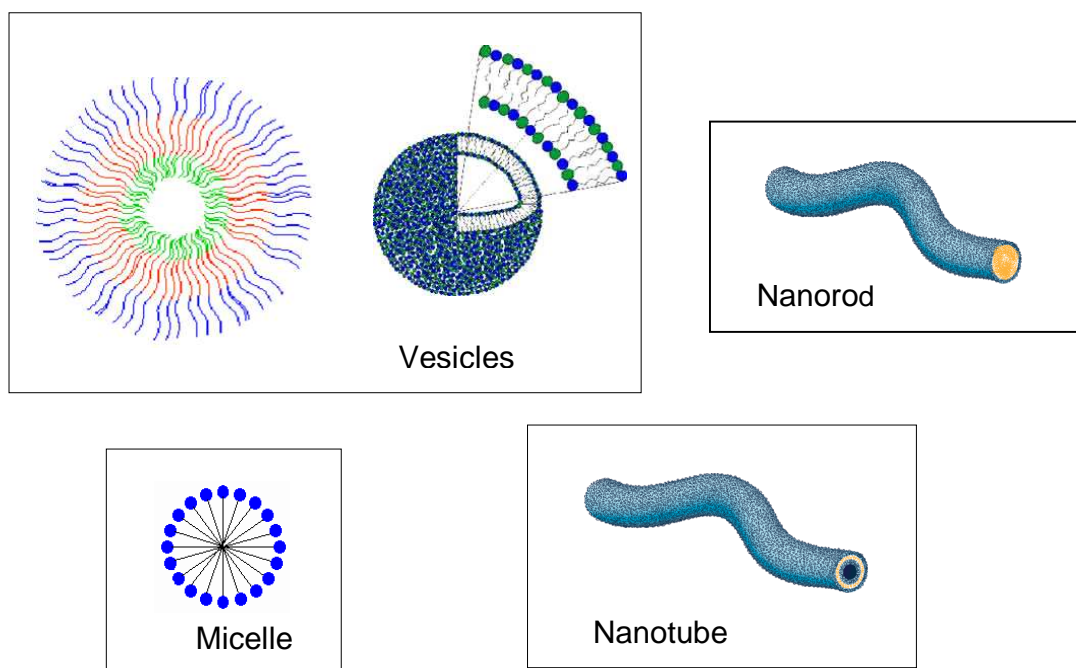


Figure 17. Figure of Vesicles (adapted from reference 78), Nanorod and Nanotube (adapted from reference 79) and Micelle (adapted from reference 80)

Micelles (Figure 17) are supramolecular objects, the inside of which consists of hydrophobic moieties and the outside of which is decorated by the polar heads. In general, micelles are spherical, although elongated micelles have been reported.^{81, 82, 83} The average diameter of a micelle is approximately twice the size of a surfactant molecule. By contrast, vesicles are supramolecular objects in which an aqueous cavity is enclosed by a continuous layer of amphiphilic compounds.⁸⁴ Most of the time, vesicles are spherical. At the molecular level, vesicles (Figure 17) have flat interfaces. For a molecule in the bilayer, the environment is the same in a sphere of radius 100 nm, 200 nm, 300 nm, etc.... Basically, the molecule “feels” that it is in a flat environment. Therefore, there is no thermodynamic preference for one size or another (as long as the size is large enough). Size is usually controlled by processing of the vesicles, such as extrusion (Figure 18).^{85,86,87}

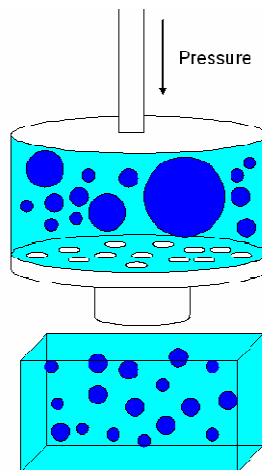


Figure 18. Scheme of extrusion process

Liposomes are vesicles which are formed via the assembly of phospholipids and other surfactants with one polar head and two hydrophobic

tails.⁸⁸ The phospholipids are arranged in a bilayer which is the main constituent of cell walls. In this case, the polar heads of the surfactant point towards either the inside or the outside of the vesicle while the hydrophobic tails are forming the membrane of the vesicle. Other structures such as rods and lamellar phases are often encountered in concentrated “solutions” of surfactants. Bicontinuous structures (Figure 19 and Figure 20) are special supramolecular objects which can be ordered (like cubic bicontinuous) or disordered. In a bicontinuous phase, it is possible to go continuously from one point to another point by taking a “hydrophobic” only or “hydrophilic” only pathway. It is not possible to define an inside or an outside for such phases.

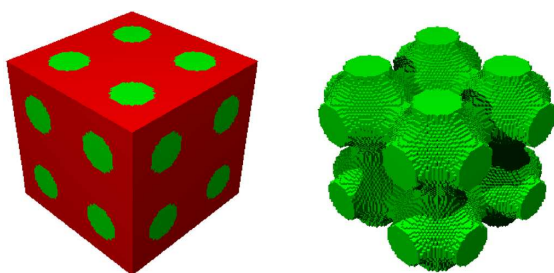


Figure 19. Typical example of a bicontinuous optimal structure⁸⁹

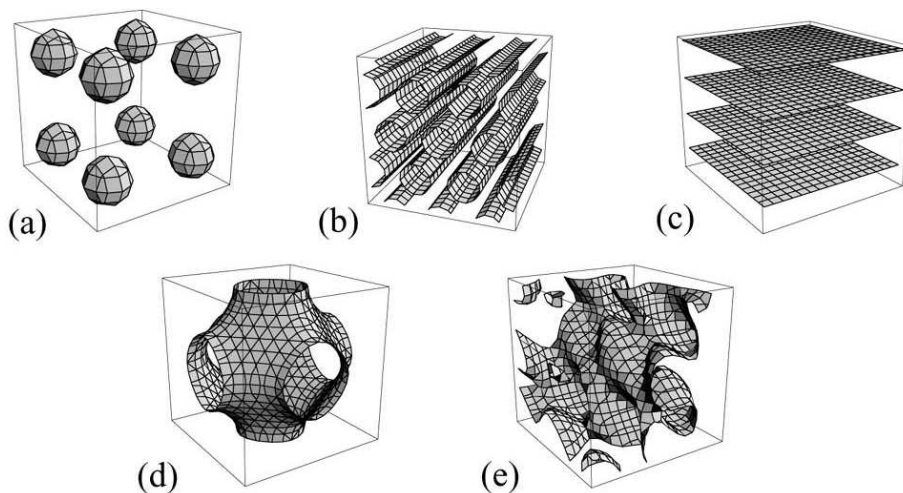


Figure 20. Geometries of self-assembled interfaces: (a) micellar (spheres), (b) hexagonal (cylinders), (c) lamellar (planes), (d) cubic bicontinuous (cubic minimal surfaces) and (e) disordered bicontinuous (random surfaces)⁹⁰

A polymer micelle is a micelle composed by an amphiphilic copolymer, while a polymer vesicle is a vesicle made from an amphiphilic copolymer. Some of them are designed to mimic a biological system. Kataoka *et al.* have been working extensively on the use of polymeric micelles for the encapsulation of hydrophobic chemotherapeutics. For example, the block copolymer poly(aspartic acid-b-ethylene glycol) was conjugated to doxorubicin (DOX or DXR)^{91, 92} (Figure 22). In the presence of water, nanoparticles were formed where the hydrophobic core poly(aspartic acid-doxorubicin) was stabilized by poly(ethylene glycol) hairs.

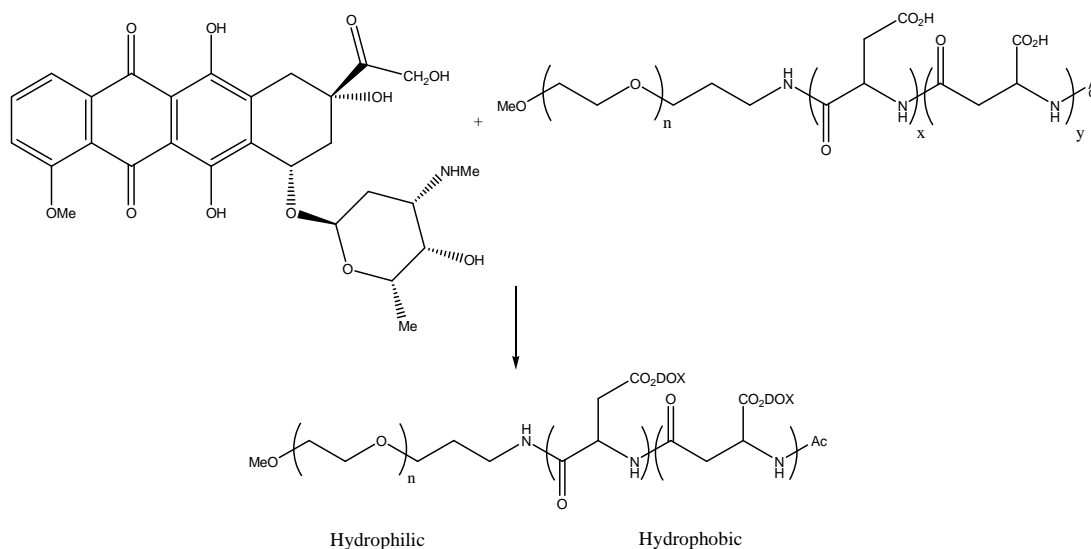


Figure 21. Conjugation of DOX to poly(aspartic acid-b-ethylene glycol)

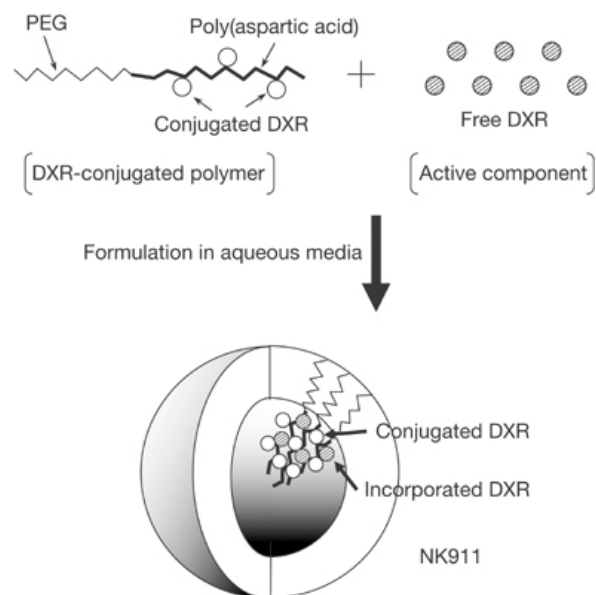


Figure 22. Schematic structure of the nanoparticles NK911⁹³ (PEG (114 units) is used as a hydrophilic block and poly(aspartic acid) (30 units) coupled with Doxorubicin (DXR or DOX) as the hydrophobic part)

The micelles can be loaded with doxorubicin at the time of formation (Figure 21 and Figure 22). These polymeric micelles have been injected into animal^{92, 94} and human cancer patients.⁹⁵ Compared to injections of doxorubicin, the micelle system shows prolonged circulation time and a greater adsorption by the tumor. Because of its hydrophobicity, doxorubicin does not readily circulate in the blood to reach the tumor site. Thus, the use of a polymeric micelle as a carrier is advantageous.

Other polymeric micelles have been formed by complexation of cisplatin to the copolymer PEG-poly(glutamic acid) or PEG-poly(aspartic acid). In this case, the platinum complex acts as a crosslinker of the poly(glutamic acid) (Figure 23) or poly(aspartic acid) fragment (Figure 27).

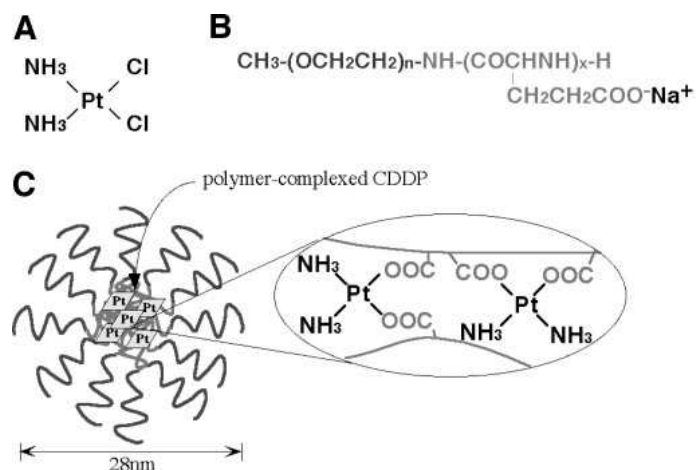


Figure 23. Figure of the formation of polymeric micelles (C) loaded with cisplatin (A) prepared from the complex formation of the diblock copolymer PEG-PGlu (B) and the cisplatin⁹²

Another type of polymeric micelles are shell-crosslinked knedels (SCK) prepared by Wooley *et al.* (Figure 24). The SCK are micelles formed by self-assembly of an amphiphilic diblock copolymer followed by the cross-linking of the shell layer.

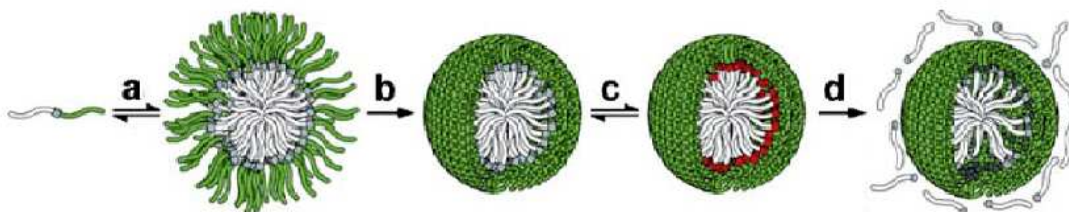


Figure 24. Picture of a shell crosslinked knedel. a. Formation of a micelle by self assembly. b. regioselective crosslinking. c. cleavage of core chains. d. extraction of the core⁹⁶

These diblock copolymers are composed of a hydrophobic poly(styrene) segment and a hydrophilic P4VP(CIMeS) (poly(styrene-*b*-*p*-chloromethyl styrene-*q*-quaternarized poly(4-vinyl pyridine)))segment.

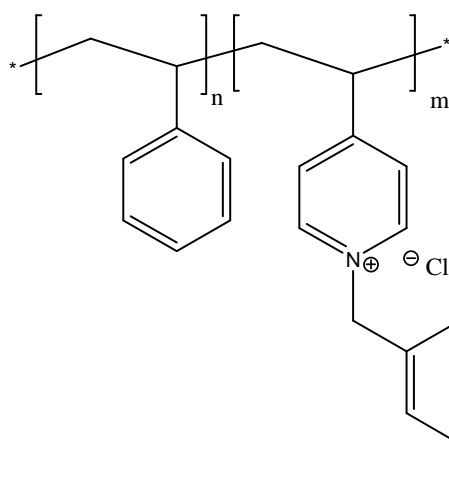


Figure 25. Poly(styrene-b-p-chloromethyl styrene-quaternarized poly(4-vinyl pyridine))⁹⁷

Once the shell formed by the P4VP(CIMeS) is crosslinked, the core chains are cleaved to give a crosslinked shell. These objects can be used to transport and deliver DNA⁹⁷ or lipoproteins (groups of conjugated proteins where at least one of the components is a lipid⁹⁸). Those SCK can also be used as a model of histone core of nucleosomes (arrangements of 146 base pairs of DNA wrapped around an octamer of core histone, forming regular spherical structures in eukaryotic chromatin⁹⁹).¹⁰⁰

Although not really amphiphilic in nature, the work of Couvreur *et al.* on polycyanoacrylate nanoparticles is worth being cited. For example, the diblock copolymer PEG-poly(isobutyl 2-cyanoacrylate) (or PEG-b-PIBCA) (Figure 26) forms PEG-coated PIBCA nanoparticles which can be used for insulin administration.

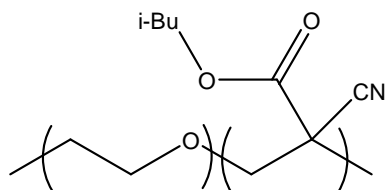


Figure 26. PEG-PIBCA formula

The mechanism of degradation of the nanoparticle in the gastrointestinal track is not yet well understood, but the preferred hypothetical “key step” is the enzymatic hydrolysis of the ester on the pendant chain. This hydrolysis leads to the formation of an alcohol and a polycyanoacrylic acid which is water soluble and excreted. Formaldehyde and cyanoacetate are minor degradation products.³¹ The mechanism of the liberation of insulin is unknown, but it has been proven that these nanospheres partially protect the insulin from protease degradation: 75 to 85% of the initial insulin associated with the nanosphere was recovered when the nanospheres were dispersed in miglyol 812 (medium-chain triglycerides, not very well defined oil) containing pepsin. When the suspension medium was pure water, only 25% of the initial insulin was recovered.³¹

Liposomes are also used for drug delivery purposes but they cannot be used for oral delivery of insulin because amphipathic substances secreted in bile (such as glycocholic acid) disrupt their organization, thus releasing the payload.⁷⁵ We believe that polymeric vesicles are best suited for the oral delivery of insulin, because the leakage of the drug is less rapid.⁸⁴

Vesicles can be prepared from diblock copolymers and triblock copolymers. In general, diblock copolymers lead to the formation of micelles.^{101,102} However, polymersomes¹⁰³ have been shown to yield vesicles.¹⁰⁴

Polymersomes are amphiphilic diblock copolymers which are stuffed with a hydrophobic polymer. This hydrophobic polymer intercalates between block-copolymers, thus favoring the formation of polymeric vesicles, called polymersomes. An example of polymersomes is poly(ethylene glycol-b-ethylethylene) stuffed with poly(ethylethylene).³⁰ It is also important to note that numerous authors have reported the formation of polymeric vesicles via self-assembly of polymers in organic solvents.¹⁰⁵ Such vesicles are not covered in this short review because they are not colloiddally stable in water.

Triblock copolymers lead to the formation of a large variety of structures such as micelles,^{106,107,108,109,110} nanotubes,⁷⁹ membrane-like superstructures,¹¹¹ particles¹¹² (suspension of a solid in a liquid), vesicles,¹¹³ nanostructured hydrogels,¹¹⁴ lamellar structures,¹⁰⁹ and film.¹¹⁴ There is no general rule on the object formed by a triblock ABC where the blocks A and C are hydrophilic and B is hydrophobic. That is why, in our case, once the conditions were optimized for the different synthetic steps, different compositions of the triblock copolymer PEG-b-PLA-b-PGlu were tried in order to form vesicles.

Only a handful of examples of polymeric vesicles based on triblock copolymers have been reported. Zhang *et al* have shown that by using the triblock copolymer PMBPS-b-PEO-b-PMBPS (Figure 27),¹¹⁵ it is possible to form vesicles in a mixture of water and dioxane, followed by dialysis in order to remove the dioxane.

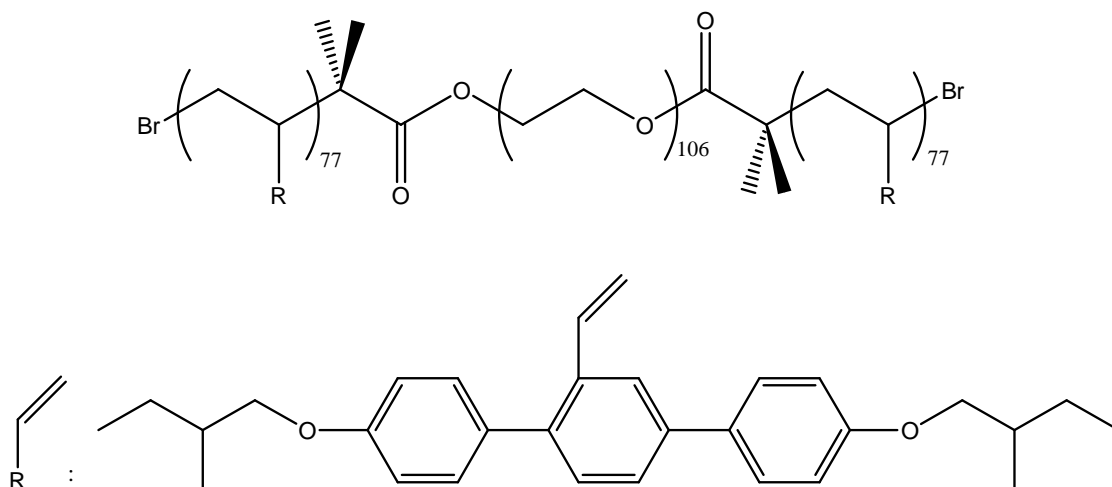


Figure 27. triblock copolymer: PMBPS-*b*-PEO-*b*-PMBPS¹¹⁵

In this case, the vesicles are formed by a phase inversion process, using dioxane as a good solvent for both the PMBPS block and the PEO block. In such a process, the polymer is dissolved in a good solvent and a selective bad solvent is slowly added until one of the blocks is segregated and forms self-assembled objects.¹¹⁵ However, no vesicles are formed by direct self-assembly in water. The group of Meier has studied in detail the self-assembly of the triblock copolymer poly[(2-methyloxazoline)-*b*-dimethylsiloxane-*b*-(2-methyloxazoline)] in water (Figure 28).^{116,117,118}

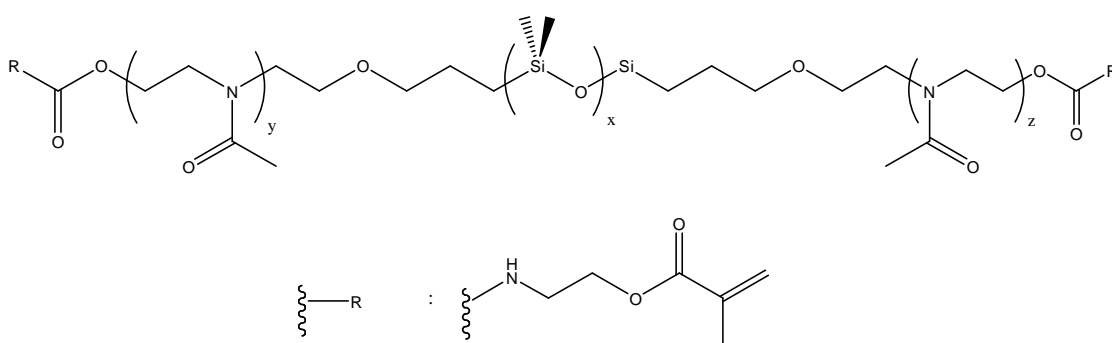


Figure 28. triblock copolymer: PMOXA-PDMS-PMOXA^{116,117,118}

The polymer spontaneously formed vesicles in water (the diameter of these vesicles was ranging from 50 to 500 nm). These vesicles were used to encapsulate phosphate anions. The vesicles were constituted of only neutral polymers. It is important to note that the PDMS is not biodegradable, so such vesicles would not be suitable for insulin delivery. Schillen *et al.* also formed vesicles by self-assembly using PEO-b-PPO-b-PEO (Figure 29).¹¹⁹ However, once again the central block is not biodegradable. In addition, these vesicles have a tendency to spontaneously invert to a lamellar structure.

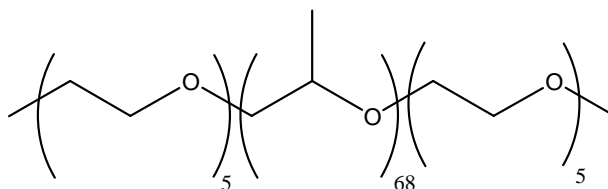


Figure 29. triblock copolymer: PEO-b-PPO-b-PEO¹¹⁹

Asymmetric vesicles were prepared by the Meier group, using poly[(ethylene oxide)-*b*-dimethylsiloxane-*b*-(2-methyloxazoline)] as a building block (Figure 30).¹²⁰ In this case, the vesicles were spontaneously formed in water via self-assembly.

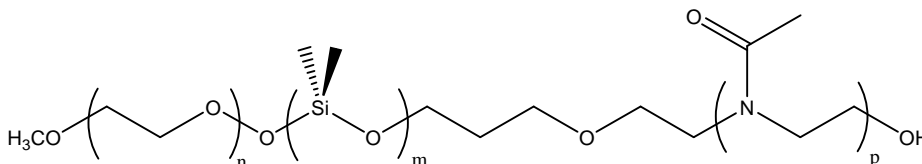


Figure 30. Triblock copolymer: PEO-b-PDMS-b-PMOXA¹²⁰

The interest for asymmetric vesicles lies in the fact that, as in natural membranes, the inside environment is different from the outside environment.¹¹⁴

The asymmetry can also be generated by using blocks of similar nature but varying lengths. In the case of the poly(2-methyloxazoline)-*b*-poly(dimethylsiloxane)-*b*-poly(2-methyloxazoline), synthesized by the Meier group (Figure 28), the shorter block ends up inside the vesicle.¹²¹ Because this segregation phenomenon is based on the difference in lengths of the two poly(2-methyloxazoline) blocks, it is important to prepare triblock copolymers made of monodisperse blocks.

There exist two main methods to prepare self-assembled objects from amphiphilic copolymers: direct self-assembly¹²² in water and self-assembly after phase inversion.^{123,124,125,126} Formation of vesicles by electroforming¹²⁷ or film rehydration¹²⁸ are sometimes used as well. As the name states in the method of direct self-assembly, the triblock copolymers self-assemble to form vesicles directly (Figure 31). In the phase inversion process, the triblock copolymer is first dissolved in a solvent which is good for all the blocks and then a selective solvent (water in our case) is added in excess (Figure 32). Here, the method of direct self-assembly is used because it prevents the use of organic solvents in the last step, since the organic solvent could induce insulin denaturation.

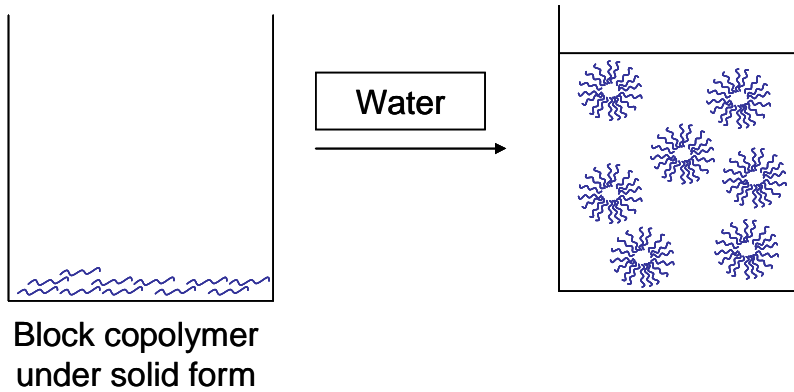


Figure 31. Formation of vesicles by direct self-assembly

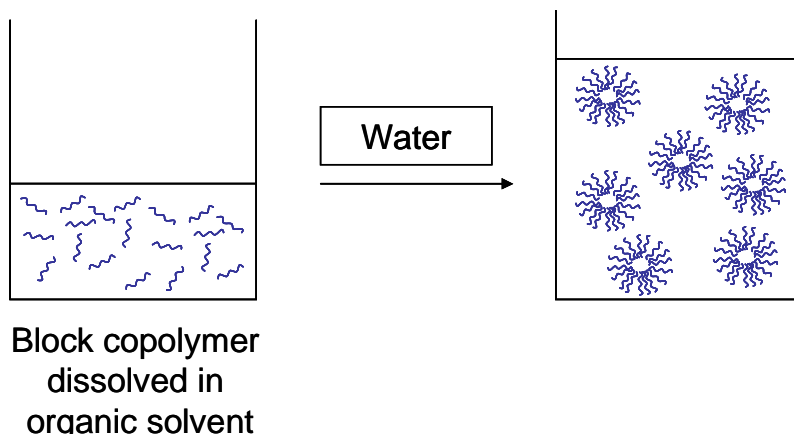


Figure 32. Formation of vesicles by self-assembly after phase inversion

With the solvent inversion method, the nature of the object depends upon the amount of solvent that is present.^{123, 129}

2. Selection of the components of the triblock copolymer

Biodegradable means capable of being decomposed by natural biological processes.¹³⁰ In our case, the polymer should be decomposed by the enzymes present in the body or in the gastrointestinal tract. A substance is considered biocompatible if it does not produce toxic, injurious, or other harmful

immunological responses in living tissue.¹³¹ The preparation of vesicles with biocompatible polymers limits our choice of raw materials. Poly(ethylene oxide), also called poly(ethylene glycol),¹⁰⁶ and poly(lactic acid)¹¹² are considered safe and biocompatible (Figure 33).

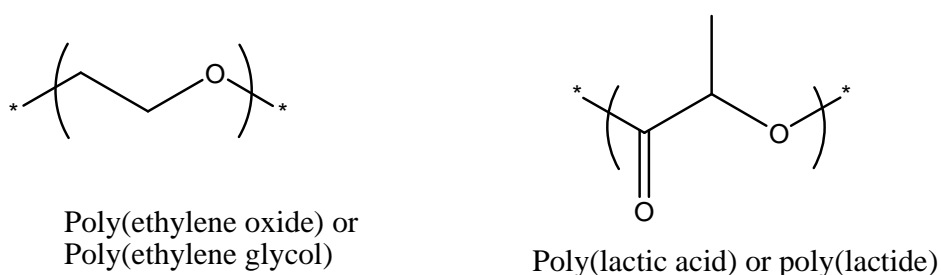


Figure 33. Biocompatible polymers used in drug delivery

Both PEG and PLA are approved by the FDA and so can be used for the purpose of drug delivery. They possess a low toxicity in animals and humans. Also, the polymeric polylactide chains are degraded by hydrolysis to lactic acid. The PLA is a bioresorbable material:^{132, 133} it is degraded by hydrolysis at a slightly acidic pH.¹³⁴

Poly(amino acids)¹³⁵ are also considered safe, as long as no more than two amino acids¹³⁶ are used in their backbone, as a higher number of amino acids can be recognized by the immune system (the immunogenicity increases with an increase in the molecular complexity). Therefore, the triblock copolymer PEG-PLA-PGlu (Figure 34) can be considered as biocompatible, knowing that

the byproducts are lactic acid, glutamic acid and poly(ethylene glycol) which can be eliminated via the kidneys.

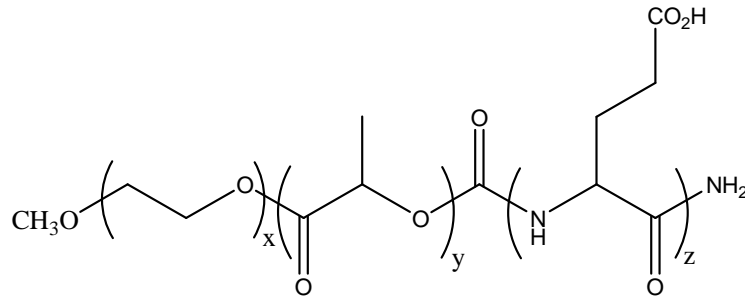


Figure 34. Triblock copolymer: PEG-b-PLA-b-PGlu

It is important to note also that PEG is excreted by the urine only if its molecular weight is less than 10,000 g/mol.^{137, 106}

3. Synthetic Scheme

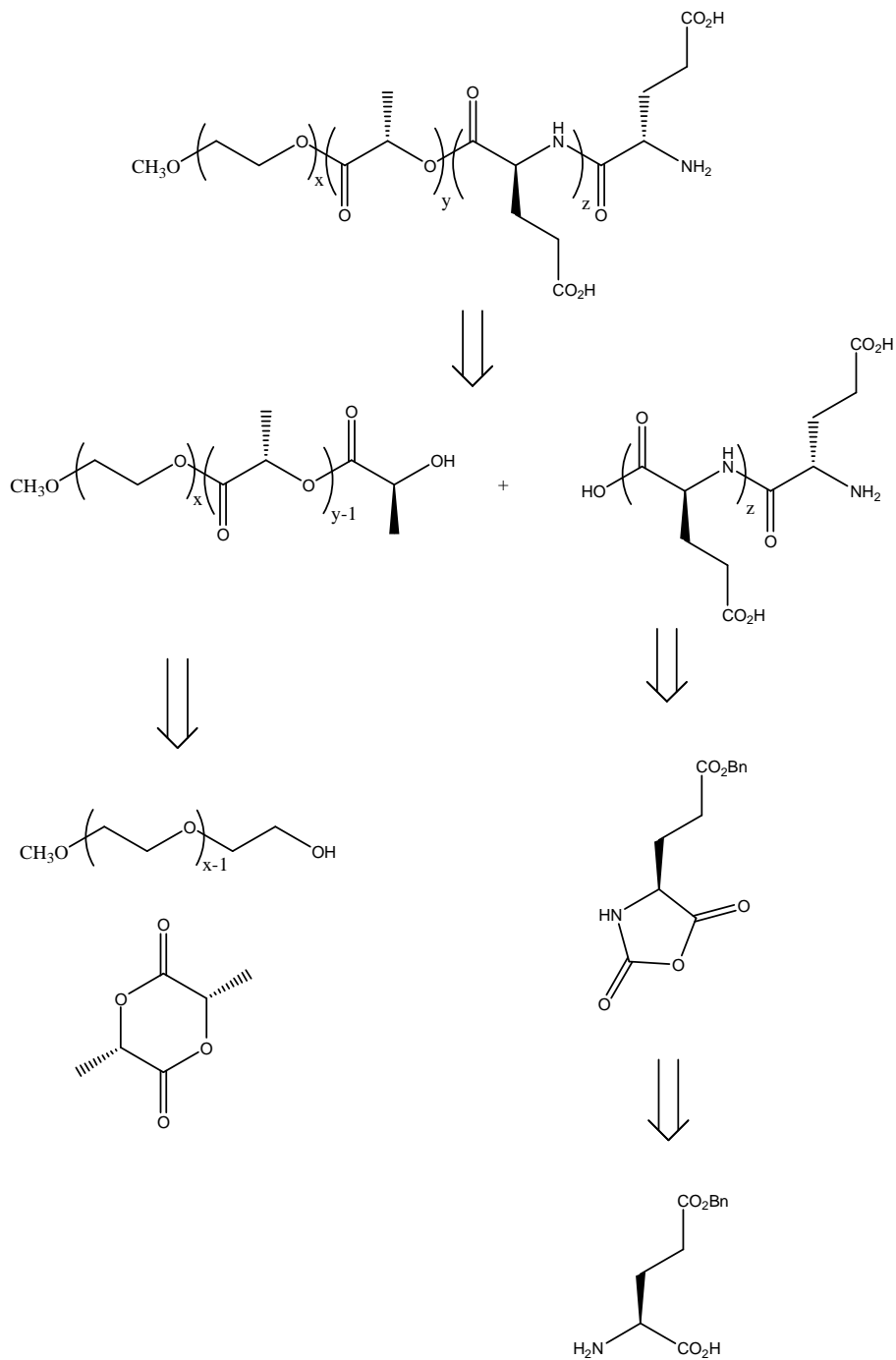


Figure 35. Retrosynthesis for the triblock copolymer PEG-b-PLA-b-PGlu

We have decided to synthesize the triblock copolymer sequentially from the PEG to PGLu. In most cases, the polymerization of the lactides is initiated by metal alkoxy complexes.¹³⁸ In our case, the alkoxy complex can easily be formed upon reaction of monomethoxy PEG on diethyl zinc. If the copolymer was synthesized by starting with the PGLu, the deprotection of the poly(benzyl glutamate) block, which is usually done in an acidic medium, may hydrolyze the PLA block. In our hands, hydrogenolysis of poly(benzyl glutamate) catalyzed by palladium on carbon was not successful (*vide infra*). Starting the triblock copolymer from the PEG moiety also presents the advantage of being able to synthesize both branched and linear triblock copolymers (see section “coupling and formation of vesicles”).

4. Synthesis of PEG-PLA diblock copolymer

In order to form the triblock copolymer, the first step is to form the diblock copolymer PEG-b-PLA (Figure 36).

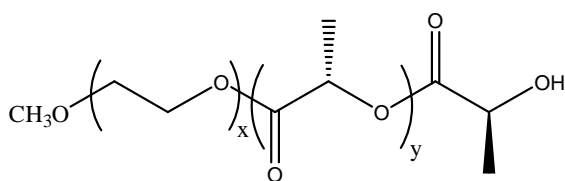


Figure 36. Diblock copolymer PEG-b-PLA

The PLA is a polyester which can be synthesized either by polycondensation of lactic acid or by ring-opening polymerization^{101,139} of its cyclic dimer: the lactide (Figure 37).

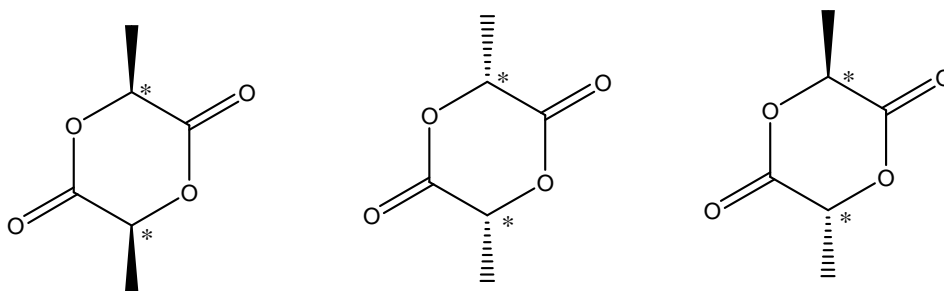


Figure 37. L-Lactide (left), D-Lactide (middle) and meso-Lactide (right)

However, the ring-opening polymerization is the only method which gives access to a controlled/living polymerization.¹³⁹ A living polymerization is a polymerization devoid of termination or transfer reactions. Thus, the architecture of the PLA can be controlled. Lactide polymerization can be initiated by alcohols such as a PEG containing two hydroxy ends yielding a symmetrical triblock copolymer PLA-b-PEG-b-PLA,¹⁰⁷ or using a monomethoxy PEG, which generates a diblock copolymer PEG-b-PLA.¹⁰⁷ In the presence of a catalyst, the PEG becomes a macromolecular initiator¹⁴⁰ of the polymerization. For example, Dai *et al.*¹⁰⁷ synthesized a diblock copolymer PEG-PLLA using L-Lactide as monomer, PEG as initiator and the coordination compound calcium ammoniate as catalyst.

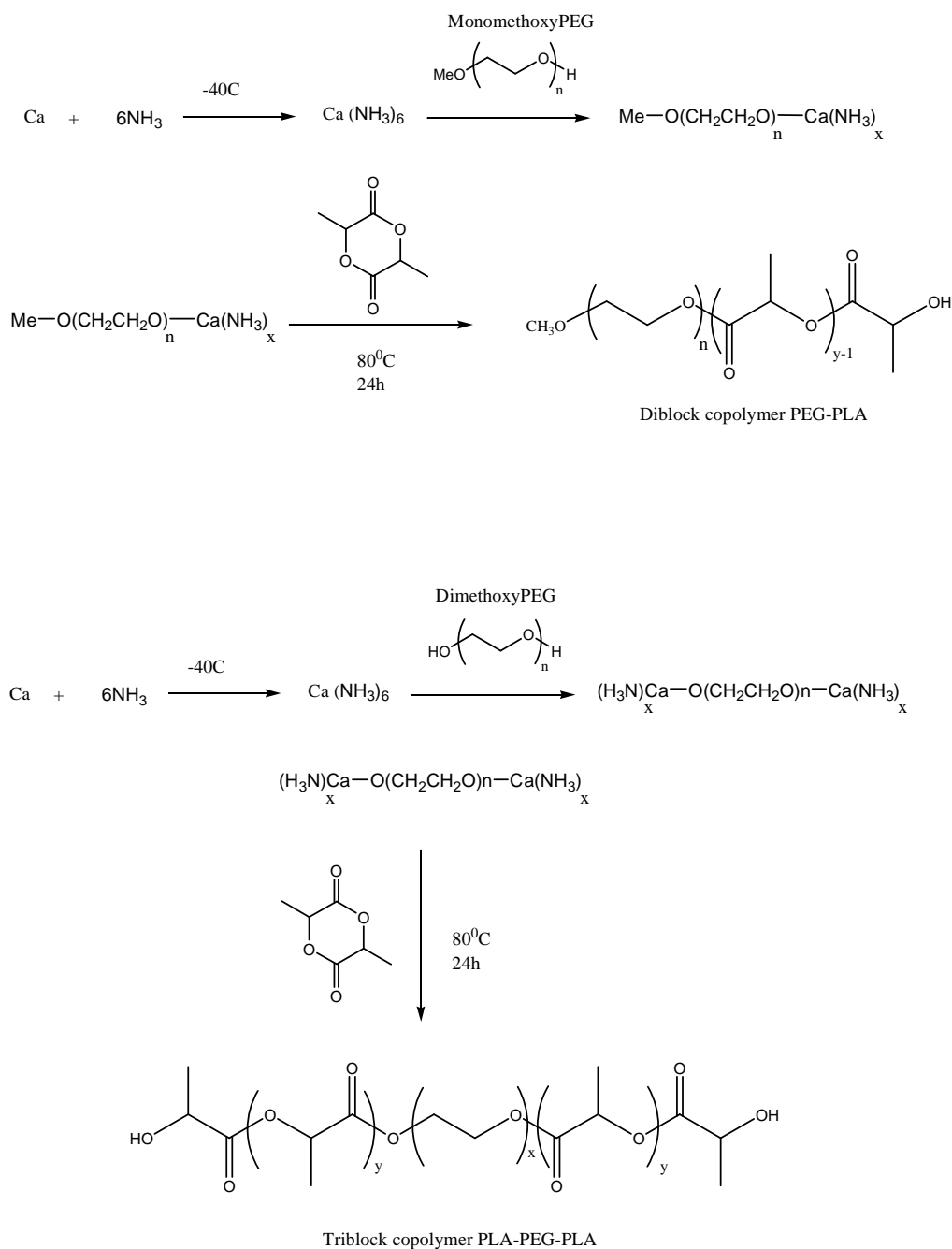


Figure 38. Synthesis of PEG-b-PLA and PLA-b-PEG-b-PLA^{107, 140}

Lactide polymerization is most frequently initiated by metal carboxylates or alkoxides.^{101,102,141} If the initiator is very basic (potassium methoxide or potassium *tert*-butoxide, e.g.), the initiation occurs by monomer deprotonation. In this case, the polymerization is not controlled.

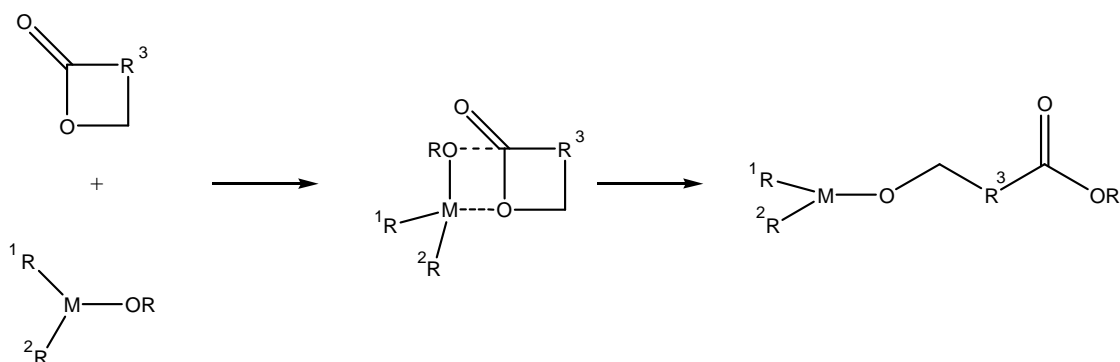
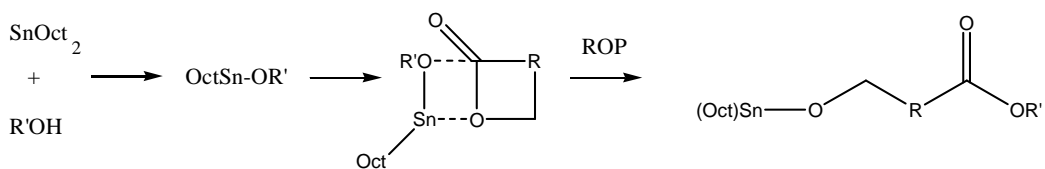


Figure 39. Mechanism of metal alkoxide catalysis¹⁴²

Numerous less basic catalysts have been reported, the most classic catalyst being stannous octoate ($\text{Sn}(\text{Oct})_2$).¹⁰² With this catalyst, the polymerization is usually slow, even at a high temperature. For example, the Wang group¹⁴³ reported that at 140°C , the lactide polymerization initiated by PEG lasted 20 hours.

a) Formation of the tin-alkoxide complex before the ring-opening polymerization (ROP)



b) Complexation of a monomer and alcohol before the ring-opening polymerization (ROP)

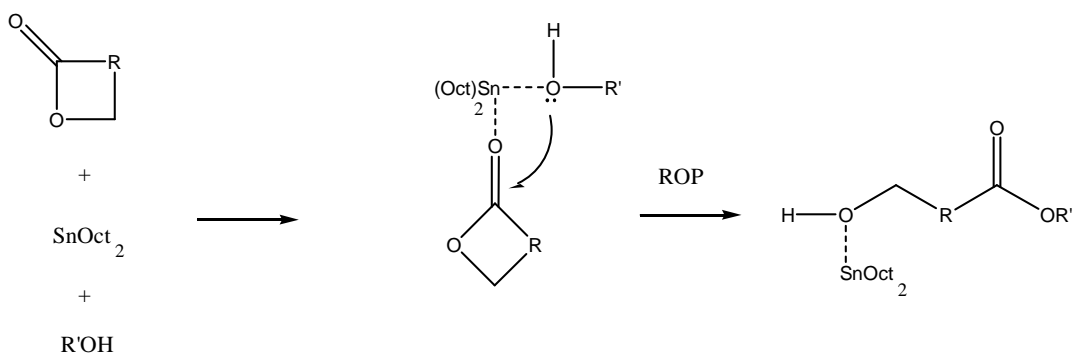


Figure 40. Mechanism of ring-opening polymerization using tin octoate and an alkoxide as initiator¹⁴²

Bero *et al.* studied the coordination polymerization of lactides catalyzed by various zinc and aluminum compounds. The most efficient catalysts were found to be diethyl zinc and its complex with either aluminum isopropoxide or with the hydrolysis product of the diethyl zinc/triethyl aluminium equimolar mixture (Figure 41).¹³²

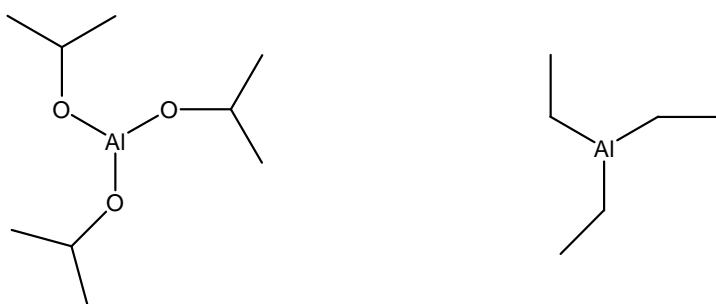


Figure 41. Catalyst for the polymerization of lactide: aluminium isopropoxide (left) and triethyl aluminium (right)

Williams *et al.* have reported a highly active Zn(II) alkoxide (L_1ZnOEt) which has been shown to be active for polymerization of lactide. This controlled polymerization yields to high molecular weight PLA at fast rates.¹⁴⁴

The stereochemistry of the PLA has long been studied and found to depend on the nature of the monomer: racemic lactide¹⁴⁵, L-lactide or D-lactide¹⁴⁶ and meso-lactide (Figure 41).¹⁴⁵ The L-lactide polymerization yields a highly crystalline PLA which is predominantly isotactic¹³³ and the racemic lactide yields a predominantly atactic polymer.¹⁴⁷ For those polymerizations, it is assumed that transesterification does not occur and that the addition of a monomer on the growing polymeric chain follows a Bernoullian statistics.¹³² However, the theoretical percentage of each kind of sequence type (diads, triads, tetrads,

pentads, etc.) and the percentage obtained by NMR are different due to the unavoidable transesterifications which occur at the ester bonds and which redistribute the sequences. This point will be treated in more details in section “synthesis of the diblock copolymer PEG-PLA”).

5. Synthesis of polyglutamic acid

The second step of the synthesis of the triblock copolymer is the formation of poly(L-glutamic acid) (Figure 42).

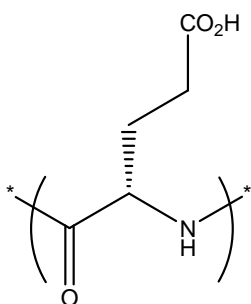


Figure 42. Poly(L-glutamic acid)

Its monomer, L-glutamic acid, is one of the twenty essential amino acids. Poly(glutamic acid) (PGlu) can then be considered as a particular polypeptide or as a particular protein composed only by glutamic acid. Homopoly(amino acids) are usually prepared by the ring-opening polymerization of the N-Carboxyanhydrides (NCA) of the corresponding α -amino acid. Except for a handful of reports where the polymer of Glu-NCA is presented, PGlu is always prepared from a protected Glu-NCA, usually using the benzyl group as a protecting group.

NCA are usually synthesized by phosgenation of the amino acid. However, phosgene (Figure 43) is a poisonous gas which was used massively during World War I as a chemical weapon.

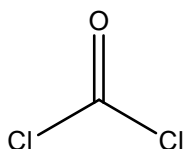


Figure 43. Phosgene

Triphosgene, [Bis(trichloromethyl) carbonate] (Figure 44), is a phosgene alternative which is safer to use, because it is a solid.¹⁴⁸

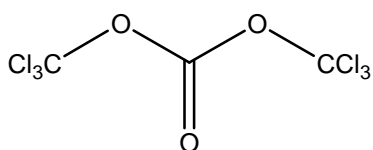


Figure 44. Triphosgene

Moreover, Cornille *et al.* have showed that triphosgene can react with several α -amino acids to give the corresponding NCA in good yields.¹⁴⁹

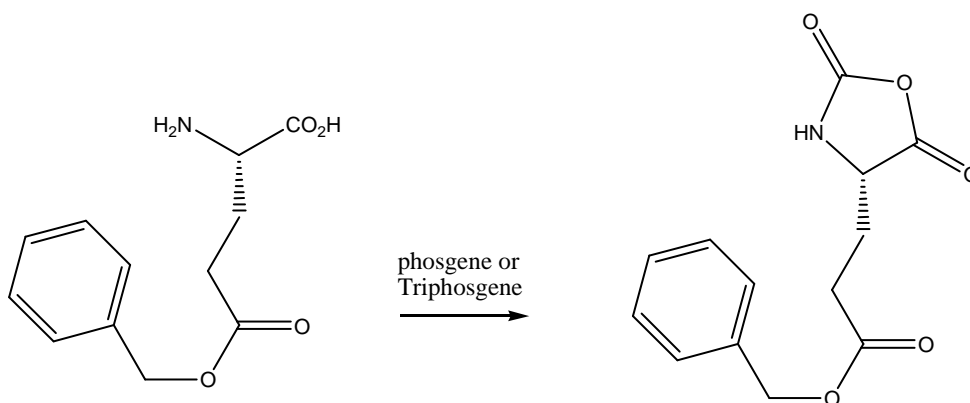
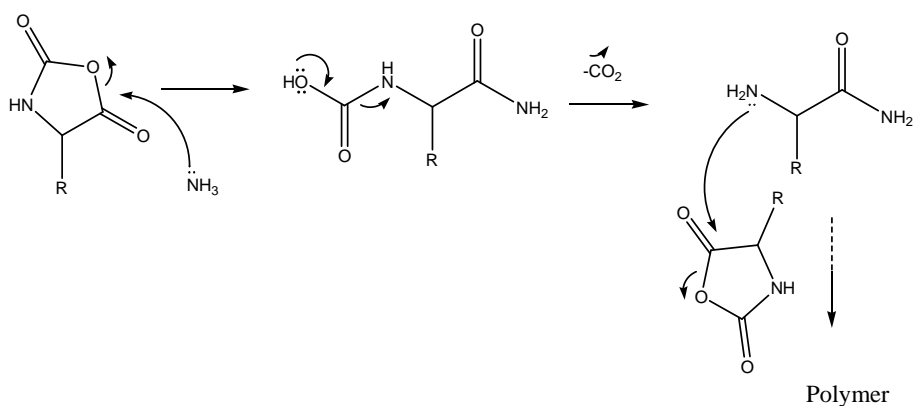


Figure 45. Formation of the NCA of benzyl glutamic acid using either phosgene or triphosgene

An NCA is a five-member ring which possesses two electrophilic centers: an anhydride site and a carbamate site. There are four main classes of initiators for the polymerization of N-carboxyanhydrides: protic and aprotic nucleophiles, aprotic bases and organometallic compounds (Table 1).¹⁴⁸ there exist two main classes of polymerization mechanism: one where the N-terminus of the growing poly(amino acid) is the active site of the polymerization and the other one where the N-acyl carboxyanhydride is the active site of the polymerization. When water or a primary amine is initiating the polymerization (Figure 46), nucleophilic attack of the amine on the ester side (the more electrophilic carbonyl) results in the formation of a ring-opened carbamate which spontaneously loses CO₂, to regenerate an amine. Under this mechanism, the reaction is slow and living, under certain conditions (see section "Synthesis of the homopolymer poly(glutamic acid)").

a. Initiation with a primary amine, water or alcohol



b. Initiation with a secondary amine

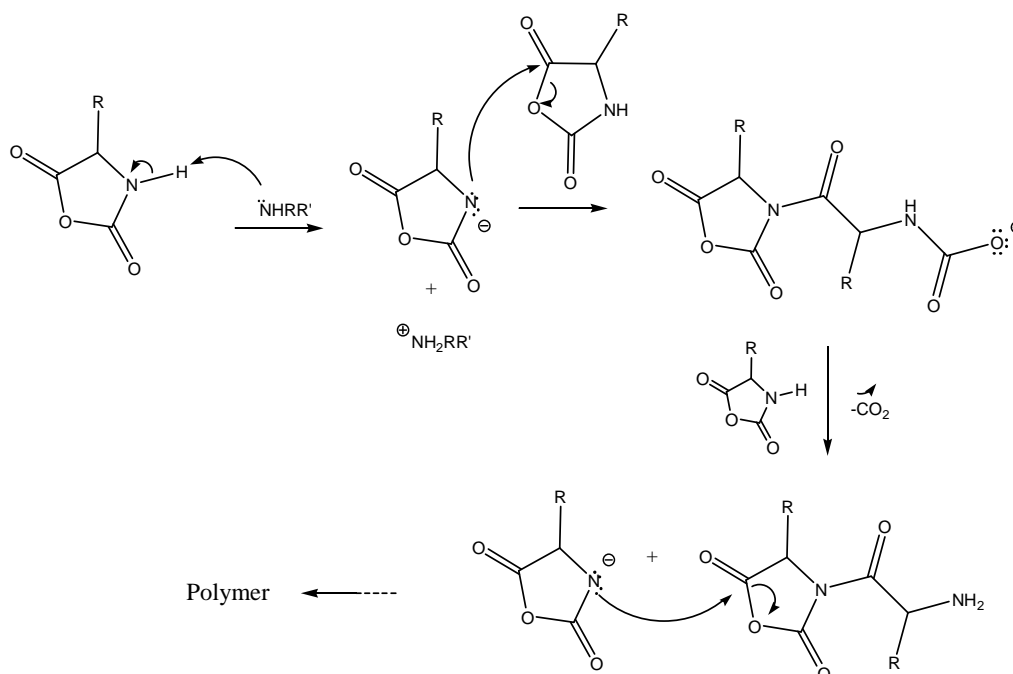


Figure 46. Initiation of NCA using water, alcohols, primary amines or secondary amines

When using tertiary amines and metal salts, the first step is the formation of an amide anion. This reaction is slow with tertiary amines and rapid with metal salts (Figure 47).

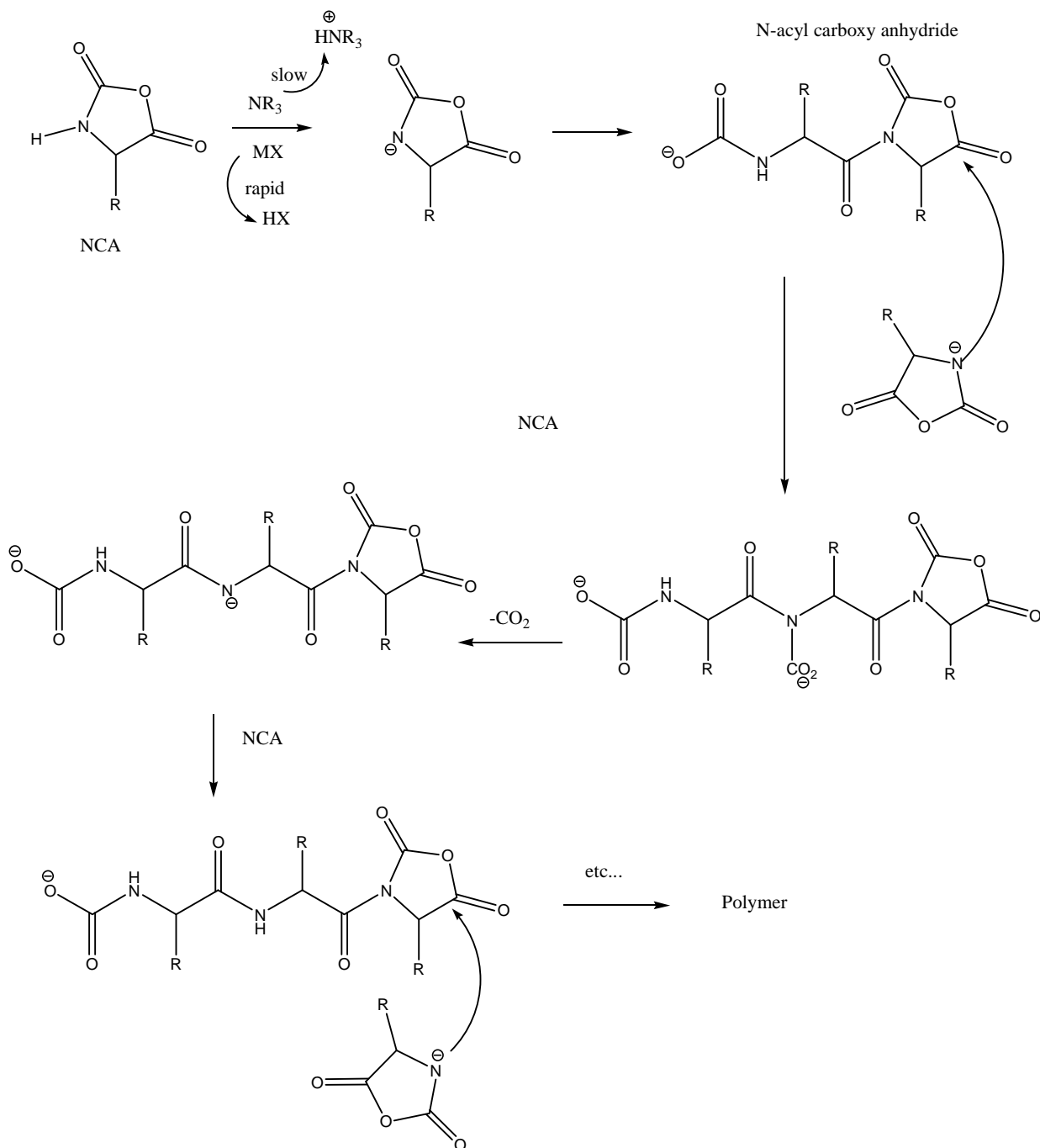


Figure 47. Initiation of NCA polymerization with tertiary amine or metal salts

This anion is very reactive and is believed to ring open the NCA to generate a N-acyl carboxy anhydride with a pendant carbamate, which is stable in the absence

of proton donors. The N-acyl carboxy anhydride being very electrophilic, it is immediately ring opened by another amide anion, to generate again an elongated N-acyl carboxy anhydride and a carbamate amide which spontaneously decarboxylate into an amide anion and CO₂. The amide anion can either undergo proton exchange with a monomer, or attack a monomer to generate a branched urea. The former reaction is favored because of the high pKa of the linear amide compared to NCA amide. In the type of polymerization, the rate limiting step is the formation of the initial amide. All the other steps are very rapid. Consequently, it is impossible to control the number of growing chains and the reaction yields a high molecular weight polymer with a broad molecular weight distribution. When a secondary amine is used for the polymerization, both mechanisms can occur at the same time (Figure 46 and Figure 47), yielding ill-defined polymers.

H. Kricheldorf^{148, 150, 151} was the first one to report the mechanism of the polymerization (Figure 46, Figure 47).

Table 1. Example of initiators which can be used for the NCA polymerization^{148, 151}

Primary amines	Secondary amines	Tertiary amines	Metal salt
Amonia	n-hexylamine	Triethyl amine	n-Butyl lithium
t-butylamine	Dicyclohexyl amine	Methyl diisopropyl amine	Diethyl Zinc
i-propylamine	Isopropylamine	Pyridine	Diethyl Cadmium
ethylamine	Diethylamine	Tributyl amine	Triethyl aluminum
Benzyl amine	Diisopropylamine		

A truly living polymerization of the NCA has been described using nickel and cobalt catalysts (Figure 48).¹⁵² However, both nickel and cobalt are not compatible with the synthesis of a polymer for pharmaceutical usages.

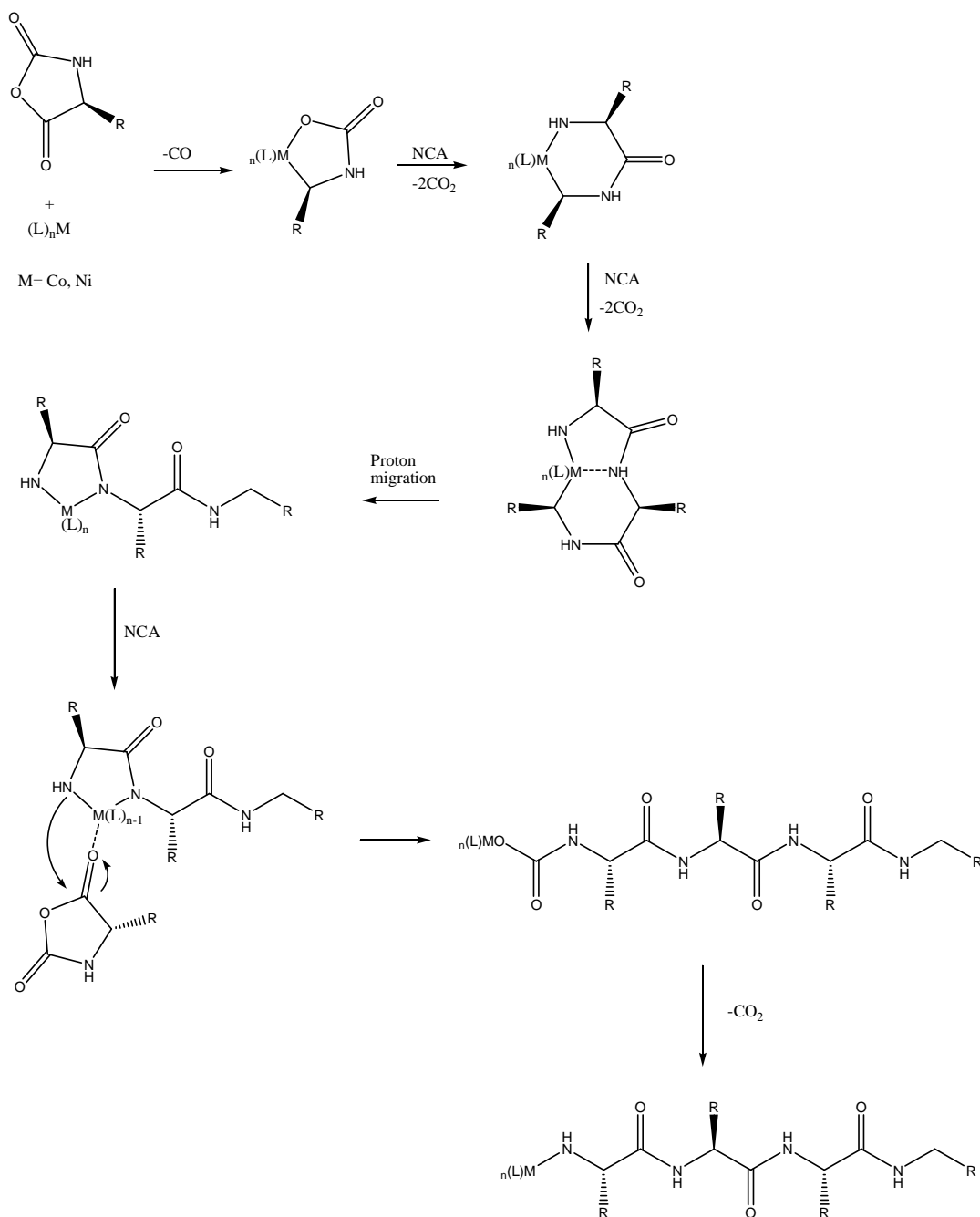


Figure 48. Polymerization of high molecular weight PGLu using cobalt or nickel initiators

By oxidative addition across the anhydride bond of the NCA, a metallacyclic complex is formed. This reaction is followed by the addition of a

second NCA which leads to the six-membered amino-alkyl metallacycle. This six membered-ring has been found to further contract to a five-membered amido-amidate metallacycles while it reacts on another NCA. It is believed that this ring contraction occurs via migration of the amide proton to the metal-bound carbon, liberating the chain-end from the metal. During the polymerization, one of the carbonyl of the NCA chelates the metal allowing the terminal amine to ring-open the NCA. As the metal complexes the terminal amine, the amine is less nucleophilic and does not react to form pyroglutamic acid end-groups, allowing the polymerization to be living: no dead chains are formed.

When the growing polymeric chain reaches a certain length, a hydrogen bond is easily formed between the oxygen of one of the carbonyl groups on the growing polymeric chain and the hydrogen of the NCA amide group (Figure 49).

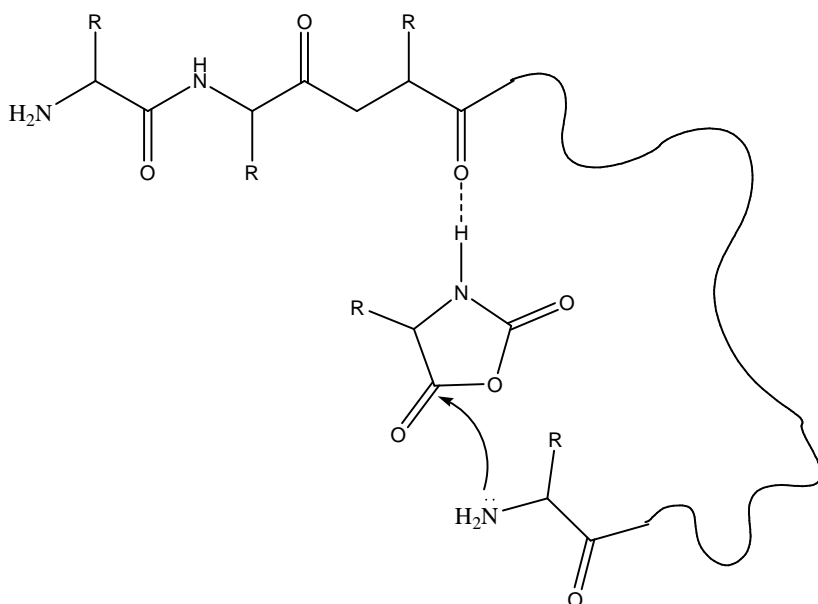


Figure 49. Mechanism of the NCA polymerization¹⁵¹

This intermediate state is called a “microcyclic transition state” by Kricheldorf.¹⁵¹ Once the NCA is maintained near the terminal amine group of the polymeric growing chain, the nucleophilic nitrogen attacks the most electrophilic carbonyl group (the ester group) and provokes the opening of the five-membered NCA, releasing one equivalent of carbon dioxide.¹⁵¹ It has been found that the initial rates of polymerization increase while the chain grows. This kinetic effect is called chain-effect polymerization and has been partially proved by infrared spectroscopy where the NCA associates with various amides via H bonds formation. This phenomenon can influence significantly the polymerization rate depending of the distance between the binding site and the amino chain.

L-glutamic acid is often protected with a benzyl group.¹⁵³ The protecting group increases the electrophilic character of the carbonyl¹⁵⁴ and allows the amine to react with it. That leads to the formation of a five-membered imide (also called a pyroglutamic group, Figure 71), stops the propagation of the chain and prevents the polymerization from being controlled. In other words, the control of the polymerization is lost when too many pyroglutamic groups are formed.

III. RESULTS AND DISCUSSION

1. Synthesis of the diblock copolymer PEG-PLA

Lactide, also called 3,6-dimethyl-1,4-dioxane-2,5-dione, is a white solid obtained by the cyclic dimerization of lactic acid. Often, lactide is contaminated by lactic acid, or dimers of lactic acid generated by the reaction of lactide with water. These impurities have been shown to react with the polymerization catalyst, leading to reactions with a lower degree of control. There exist several methods to purify lactides such as recrystallization,¹⁰² sublimation¹⁵⁵ and distillation.¹⁵⁶ In our case, lactide was recrystallized from hot toluene prior use and then washed with the same solvent. Lactide is soluble in hot toluene (above 40 °C), in chloroform and in THF.¹⁵⁷ We chose toluene as reaction solvent, because it allows to obtain a poly(lactic acid) with a higher molecular weight and a higher monomer conversion (no poisoning due to coordination of THF on the catalyst, e.g.).¹⁵⁷ Once recrystallized, the monomer could be ring-opened by a zinc-alkoxide. The polymerization was followed by ¹H NMR. At different times, a small aliquot of the reacting medium was quenched with a 35% solution of hydrogen chloride in toluene, the solvent was evaporated and the residue was analyzed by NMR. In CDCl₃, the methine proton of the monomer (5.05 ppm) is clearly different from the resonance of the methine proton of the polymer (5.2 ppm, Figure 50). After 60 min, at 60°C, and for a 10000g/mol PLA block, the resonance of the lactide monomer is no more observed, indicating that the reaction is complete.

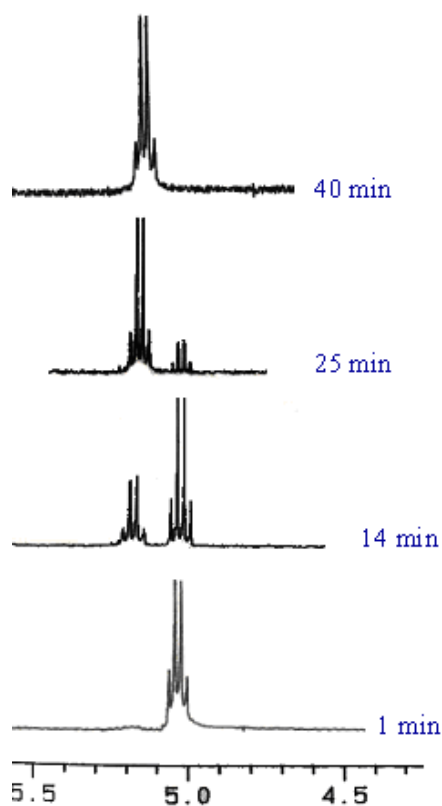


Figure 50. ^1H NMR spectra of the aliquots taken during the lactide polymerization (region of the methine proton)

All the diblock copolymers synthesized were characterized by ^1H NMR (Figure 51). The ^1H NMR gives access to the conversion of the polymerization as well as the molecular weight of the PLA block, knowing the molecular weight of the PEG block used. On Figure 51, the integration value of the PEG is 16.88 which correspond to 4.72/H. The average integration value of the PLA is 19.44/H. Knowing that the PEG is composed by 45 units, it is found that the PLA is composed by 187 units.

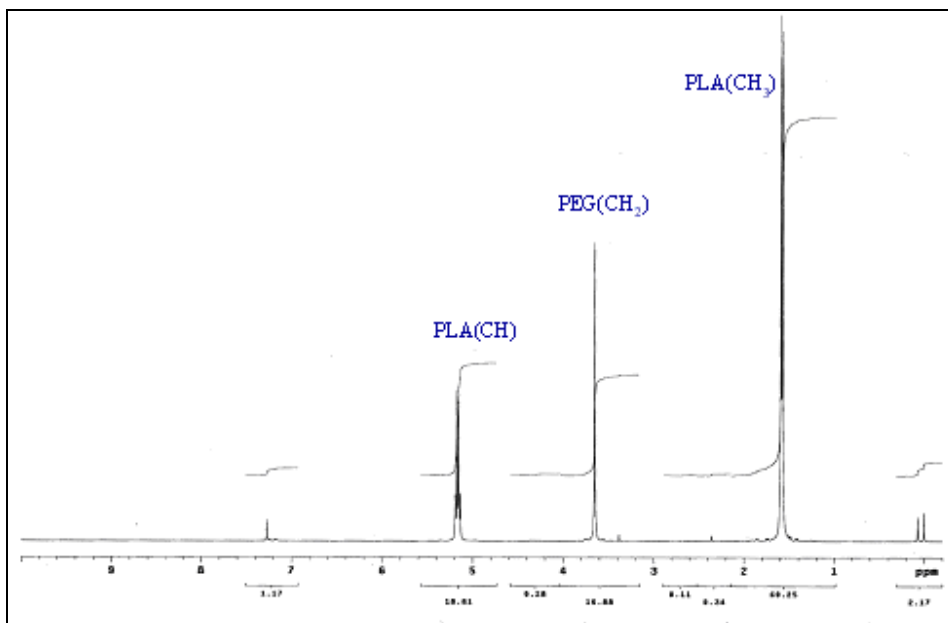


Figure 51. ¹H NMR spectrum of a diblock copolymer after 60 minutes at 60°C

The active site in our polymerization is a zinc alkoxide. This species is readily hydrolyzed into zinc oxide and an alcohol. Thus, all the reactions were carried out under inert atmosphere using dried reagents. The facile hydrolysis (and methanolysis) of the Zn-O bond was used to quench the polymerization reaction. When a large excess of methanol is used to quench the polymerization, the polymeric product is contaminated by a series of low molecular weight products, as shown by gel permeation chromatography. Analysis by ¹H NMR of these impurities indicates that they result from the ring-opening of residual lactide initiated by methanol (likely catalyzed by the zinc based catalyst) (Figure 52).

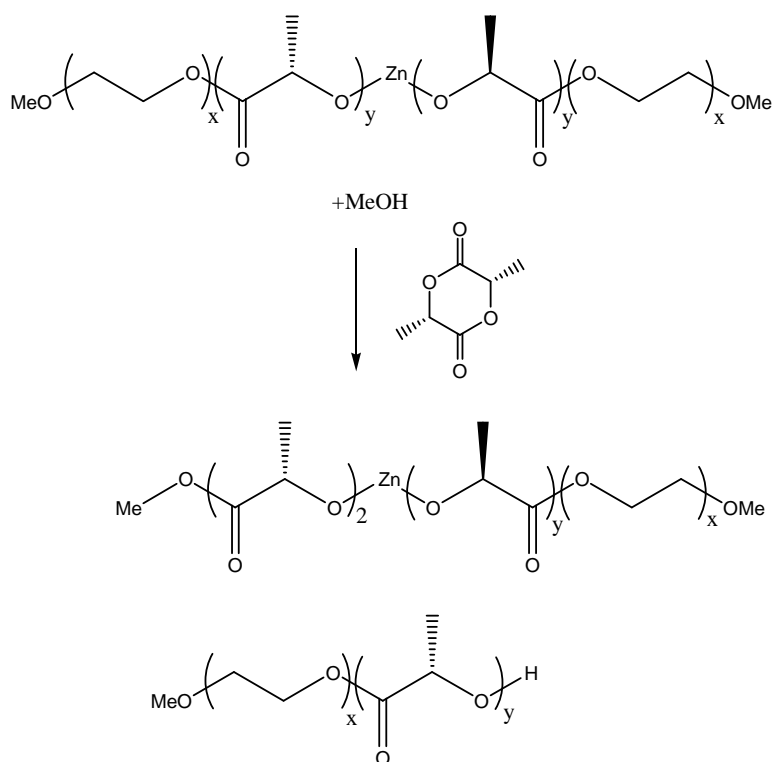


Figure 52. Transesterification occurring during the quenching of the polymerization with methanol

The polymerization could also be quenched by addition of 0.11 % of concentrated HCl (5 equivalents, compared to the diethyl zinc) (Figure 53). The by-product of this reaction is ZnCl_2 , which does not further react with lactide. After quenching and evaporation of the solvent, the polymer was redispersed in THF and separated from residual monomer by precipitation in ether, followed by filtration.

Once prepared and purified, the polymers were analyzed by gel permeation chromatography. This technique gives access to a molecular weight value which is relative to the molecular weight of the standards used to calibrate the instrument. In our case, polystyrene standards were used, leading to an

offset between experimental and theoretical molecular weights calculated from the conversion and the reaction stoichiometry.

Numerous catalysts exist for the polymerization of lactide. In fact, it is believed that any metal alkoxide can be used for this purpose. In our case, we decided to use a zinc based catalyst because such catalysts are reported to lead to fast and quantitative reactions and because residual zinc in the polymer (degree of oxidation II) is assumed to be non toxic.¹³² Moreover, the zinc alkoxide promotes the coordinated anionic ring-opening polymerization of lactide which is a controlled polymerization, as shown below. The catalyst is prepared by adding half of an equivalent of diethyl zinc at room temperature to a toluene solution of monomethoxy PEG (Figure 53).

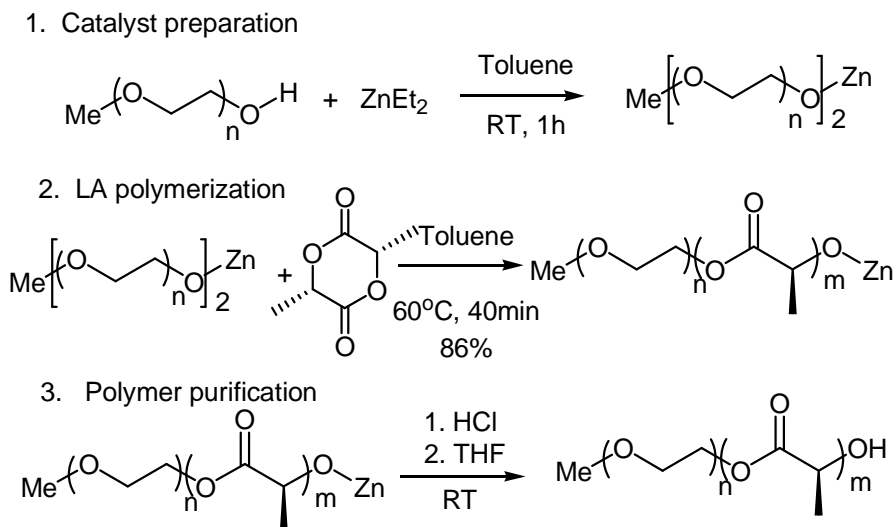


Figure 53. PLA polymerization

This reaction is believed to be rapid and quantitative and was not studied. Several catalysts were prepared by this method (Table 2).

Table 2. Different type of catalysts prepared

MW _{PEG} (g/mol)	T _{polymerization} (°C)
350	80
5000	80
750	60
2000	60

The two preferential molecular weights chosen for the PEG were 750 and 2000 g/mol as the 350 g/mol PEG would not give a triblock copolymer hydrophilic enough and as the 5000 g/mol PEG is harder to dissolve in hot toluene.

As soon as it was prepared, the catalytic solution was then transferred to a toluene solution of lactide. In our conditions, high conversions were reached within minutes when the polymerization temperature was 80°C. However, for reasons which become apparent below, the reaction temperature was set at 60°C. In this case, the reaction time depends on the concentration of catalyst and the ratio of monomer to catalyst. When a PEG chain of high molecular weight is used (Table 3), the catalyst concentration is relatively low, leading to long polymerization times (2 hours).

Table 3. concentration of catalyst and of the ratio of monomer to catalyst in function of the molecular weight of the PEG

FMC	Mn _{PEG} (g/mol)	Mn _{PLA} (g/mol)	[lactide]/[catalyst]	[catalyst] (mol/L)	T (°C)	t _{reaction} (min)
22	750	5000(theoretical)	68	0.0137	80	120
27	5000	5000(theoretical)	68	0.00092	80	120
49	2000	5100	35	0.0000133	60	40
89	2000	4300	208	0.00456	60	40
102	2000	16000	208	0.00456	60	180
145	2000	9800	139	0.00625	60	60

The lactide Mn have been calculated from the NMR spectra (measured by the disappearance of the monomer by ¹H NMR), knowing the PEG molecular weight. (T: Temperature; t_{reaction}: time of reaction)

When PLA chains of high molecular weight are targeted, the initial ratio of monomer to catalyst is relatively high, also leading to long polymerization times. The lactide polymerization time was modified in order to obtain PLA blocks with different length: three different molecular weights targeted were tested for the PLA: 5000, 15000 and 10000 g/mol. For the main diblock copolymers, PEG₂₀₀₀-PLA_x, the reaction is quenched after 40 minutes when x=5000g/mol, after 90 minutes when x=15000g/mol and after 60 minutes when x=10000g/mol (Figure 54).

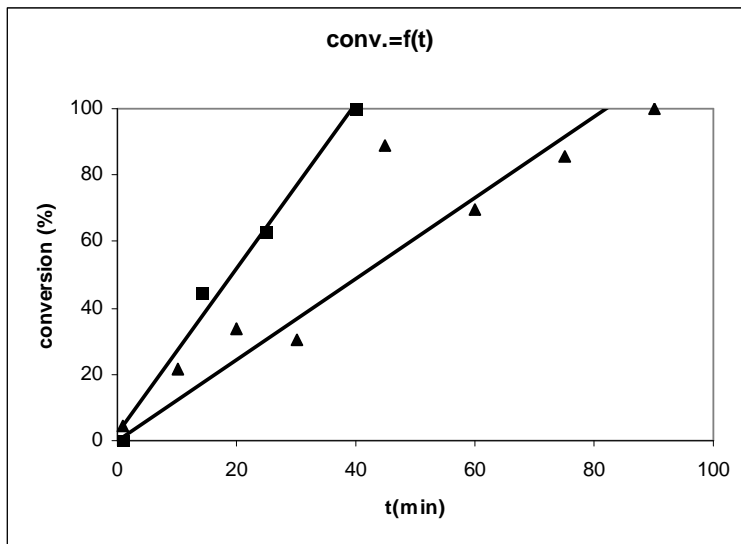


Figure 54. conversion of the molecular weight of the PLA block versus time (squares: MW_{PLA}=5000 g/mol; triangles: MW_{PLA}=15000)

At first sight, the kinetics of polymerizations were found to be of zero-order in lactide (Figure 54), as shown by the linear evolution of the monomer conversion with time. This behavior could illustrate the importance of the coordination step in the polymerization mechanism (Figure 55). However, these results need a further investigation with a larger number of data points as they

contradict the data found in the literature which show a first-order law in monomer.¹⁵⁸

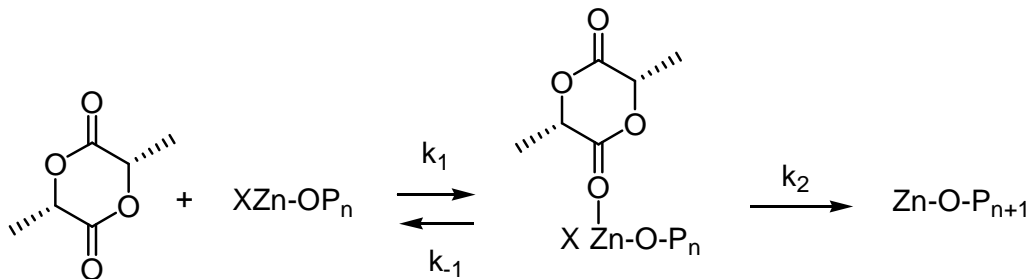


Figure 55. Mechanism of the polymerization of the lactide by zinc alkoxide

The polymerization mechanism involves two steps: the coordination of the monomer onto the zinc atom, followed by the insertion of the coordinated monomer into the metal alkoxide bond (transesterification) (Figure 55). Depending on which step is rate determining, the polymerization is either first or zero order law in monomer. If the first step is rate limiting, the polymerization rate is $k_1 \cdot [\text{Zn}] \cdot [\text{lactide}]$, leading to a first order kinetics. If the second step is rate limiting, the polymerization rate is then given by $k_2 \cdot [\text{Zn.lactide}]$, where the concentration of the complex zinc-lactide is given by the equilibrium constant between zinc and lactide. Because a polymerization is always carried with a large excess of lactide vs zinc, one may expect to see that the majority of the zinc sites are complexed by lactide (provided the equilibrium constant is not too small). In this case $[\text{Zn.lactide}] = [\text{Zn}]_0$, and the rate of polymerization is independent of the lactide concentration.

Besides reaching high conversion, we measure the success of the polymerization reaction by its ability to form block copolymers (all PEG chains

are extended by PLA) and by the fact that the chains have a narrow molecular weight distribution. Such characteristics are reached when the polymerization is living (or controlled), which means that the polymerization is devoid of termination or transfer reactions. In this case, each catalyst grows one single chain, the chains have on average the same length and the molecular weight grows linearly with conversion (Figure 56). At 80°C, the polymerization seems to level off at 74% conversion. As indicated by GPC, the polymerization is not living because the molecular weight does not increase linearly with the conversion, and the polydispersity is broad (above 1.4). The temperature is likely too high, and termination and transfer reactions occur at this temperature. Furthermore, there is a large discrepancy between the predicted molecular weight and the experimental molecular weight.

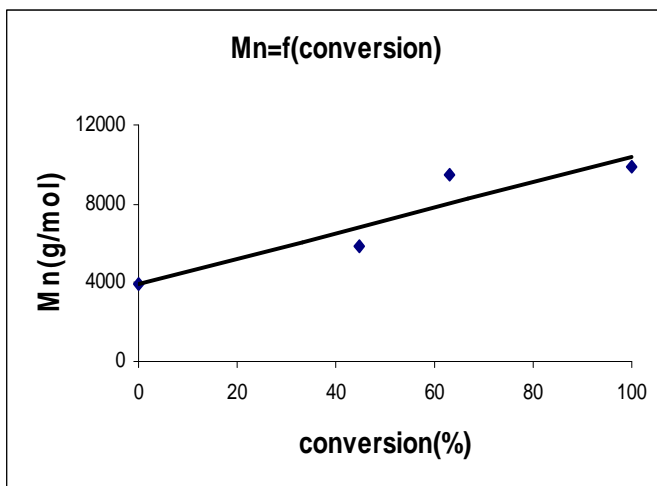


Figure 56. Number average molecular weight vs the conversion ([Et₂Zn]=0.01mol/L, [lactide]=0.7mol/L, [PEG₂₀₀₀]=0.02mol/L, 60°C)

At 60°C, the number average molecular weight increases linearly with conversion (Figure 56), up to nearly quantitative conversion (reached in 40 minutes for a

PLA molecular weight of 5000 g/mol and 90 minutes for a PLA molecular weight of 15000 g/mol). Therefore, all the polymerizations were done at 60°C. At zero conversion, the molecular weight is not zero, but corresponds to the molecular weight of the PEG chain. The molecular weight distribution of the polymer remains narrow (Figure 57) and all the PEG chains seem to be extended, as shown by the complete disappearance of the PEG chains in the GPC chromatogram. The broadness of the distribution is usually characterized by its polydispersity index, PDI, which in our case is found to be less than 1.2 (if the reaction is quenched with HCl and not with MeOH). Such low PDIs are also characteristic of living processes.

Interestingly, when the polymerization is not quenched as soon as a high conversion is reached, the molecular weight distribution becomes broader (Figure 57).

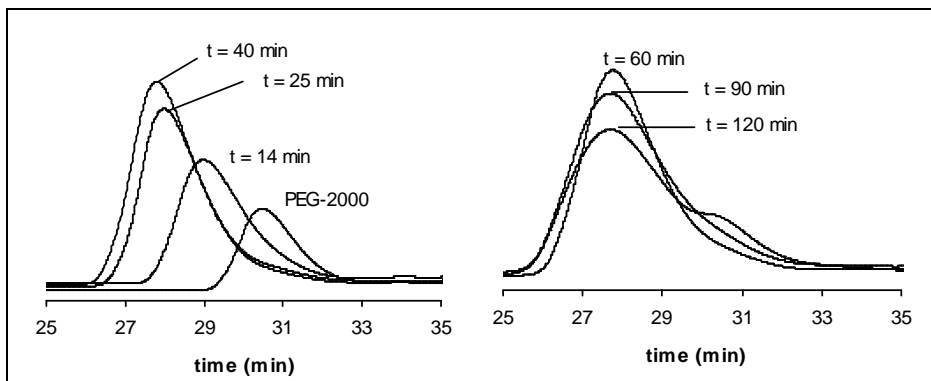


Figure 57. GPC traces of a PEG-PLA copolymer, at different times. [PEG]=0.02mol/L, [lactide]=0.7mol/L

The increase of the polydispersity index (PDI) can easily be explained by the presence of transfer to polymer. Intermolecular transfer “redistributes” the

molecular weight distribution into a most probable distribution (final PDI = 2), and intramolecular transfer (also called backbiting) generates low molecular weight macrocycles (Figure 58). At 120 minutes on the GPC chromatogram, a new peak located in the low molecular weight area appears, a sign of those low molecular weight macrocycles.¹⁵⁹ Although they are both transesterifications catalyzed by a zinc alkoxide, the reaction of transfer is slower than the polymerization (it only becomes apparent once the polymerization is completed). This probably results from the fact the driving force for the polymerization is the loss of ring strain from the lactide cycle, which, albeit small, is enough to ensure a rapid polymerization reaction

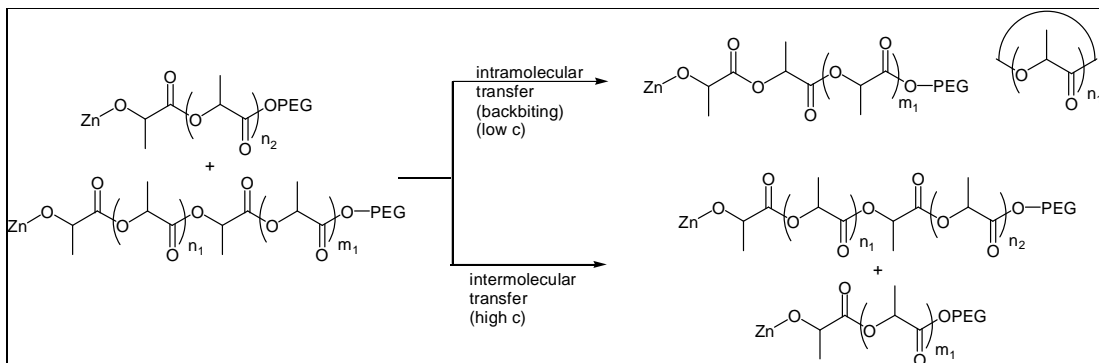


Figure 58. intramolecular and intermolecular transfers during the polymerization of lactide

Table 4. Recapitulative table of the PEG-PLA synthesized

FMC		MW _{PEG} (g/mol)	MW _{PLA} (g/mol)	PDI	T(°C)	[lactide]/[Et ₂ Zn]	[Et ₂ Zn] (mol/L)	Quencher
2	C	350	5000	1.4	80	51	0.014	M
3a	C	5000	5000	1.27	80	6	0.225	M
3b	C	5000	1000	1.7	80	9	0.15	M
3d	C	5000	3000	1.79	80	3.5	0.62	M
24	C	5000	5000	1.18	80	68	0.006	M
32	C	750	3000	1.39	80	42	0.013	M
42	C	2000	5000	1.59	60	70	0.01	M
49a	C	2000	5000	1.16	60	35	0.013	M
49b	C	2000	10000	1.19	60	70	0.013	M
54	C	750	7600	1.29	60	70	0.013	M
55	C	750	13900	1.09	60	208	0.007	M
105	C	2000	15800	1.19	60	208	0.004	HCl
113	A	2000	9700	1.17	60	139	0.006	HCl
117	SC	2000	10000	1.17	60	139	0.006	HCl
145	A	2000	9800	1.14	60	139	0.006	HCl

A: Amorphous, SC: Semi-Crystalline, C: Crystalline
M: Methanol, HCL: Hydrochloric acid

The synthesis of the diblock copolymer was first done using L-lactide. This leads to an isotactic polymer which is highly crystalline as shown in the DSC trace (Figure 59). The ΔH of melting given by the literature is 93 J/g.¹⁶⁰ The experimental ΔH of melting of the diblock copolymer PEG-PLA (FMC 54, Table 4) synthesized exclusively with L-lactide is 54.26 J/g. This value was obtained by conventional DSC and not modulated DSC and should be taken with a grain of salt. The percentage of crystallinity was found to be 58% which is high for a polymer.

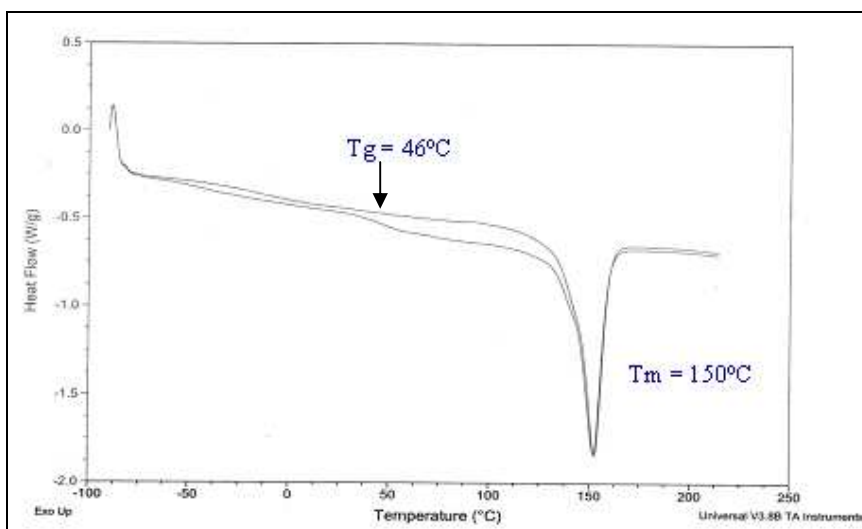


Figure 59. DSC spectrum of a diblock copolymer (FMC 54) done with L-lactide (11.2mg of the sample was heated between -90°C and 220°C at a rate of $20^{\circ}\text{C}/\text{min}$)

As expected, the quantitative ^{13}C NMR spectrum is consistent with a polymer which is 100% isotactic: there is only one peak per carbon (Figure 60).

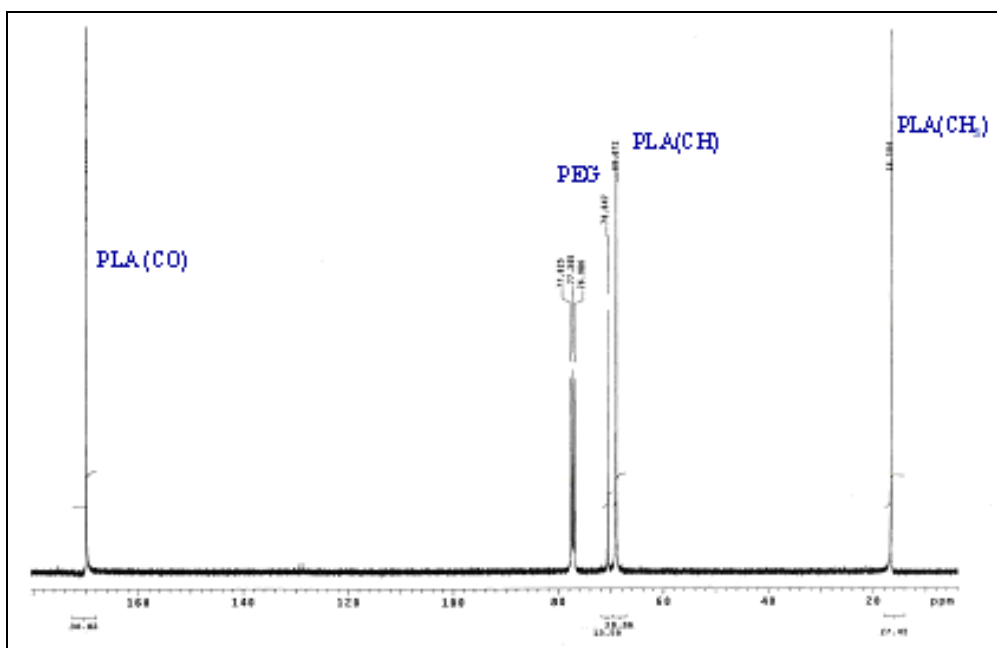


Figure 60. Quantitative ^{13}C NMR spectrum of a diblock copolymer made with L-lactide in CDCl_3

It is shown below that the crystallinity of the polymer is detrimental to the formation of the vesicles. Thus, later experiments were done using racemic lactide (experiment FMC113 and FMC145, Table 4. FMC 117 is carried with 10% of racemic lactide). No separate kinetics study has been done with racemic lactide. Considering the time of reaction and the polydispersity of the diblock copolymers, it seems that neither the kinetics nor the livingness of the polymerization are affected by using racemic lactide instead of L-lactide. This polymerization leads to an atactic polymer which is amorphous, as shown in the DSC trace (Figure 61). Indeed only a T_g (4.44°C) can be seen and there is no trace of crystallinity peak.

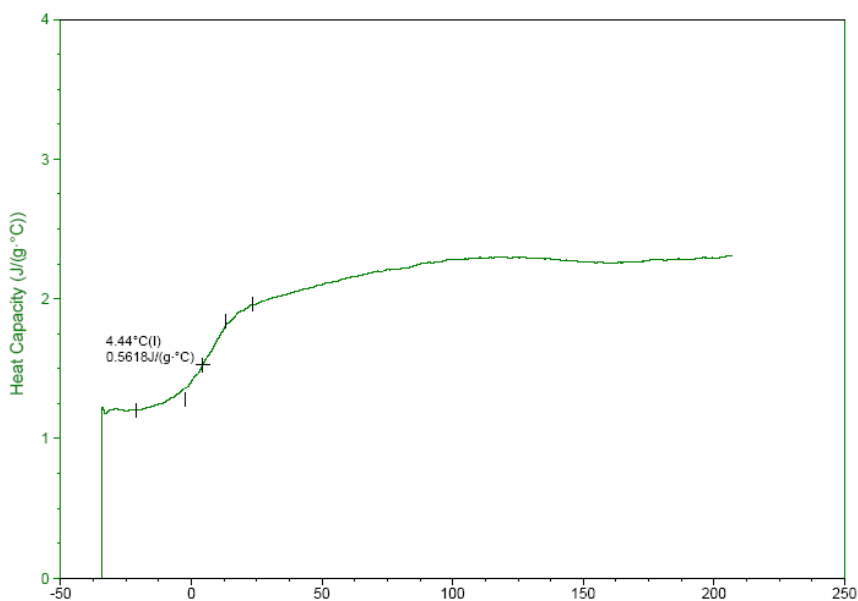


Figure 61. DSC spectrum of a diblock copolymer (FMC 145) done with racemic lactide (15.1mg of the sample was heated between - 40°C and 220°C at a rate of 5°C/min, modulated)

As expected, the quantitative ¹³C NMR spectrum (Figure 62) is consistent with a polymer which is 100% atactic. There are several resonances per carbon,

corresponding to several microstructures. The integrals measured for each tetrads corresponds to the ones expected with a Bernoullian statistics (iii=37.5%; isi=25%; iis=isi=sii=12.5% where i means isotactic and s syndiotactic). Accordingly, the catalyst does not show any preference for isotactic or syndiotactic linkages and the polymer is not crystalline.

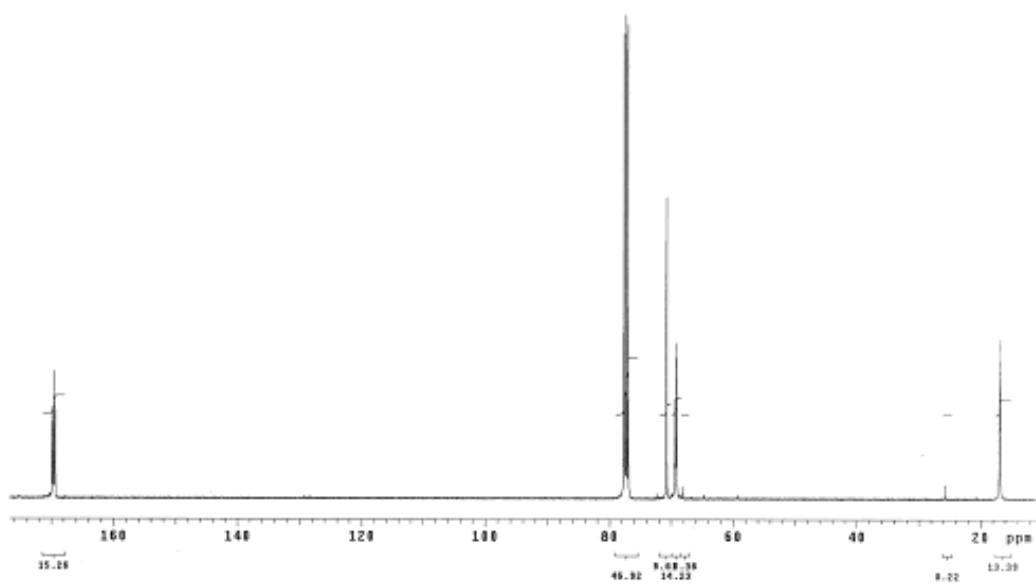


Figure 62. Quantitative ¹³C NMR spectrum of a diblock copolymer (FMC 113) made with racemic lactide in CDCl₃

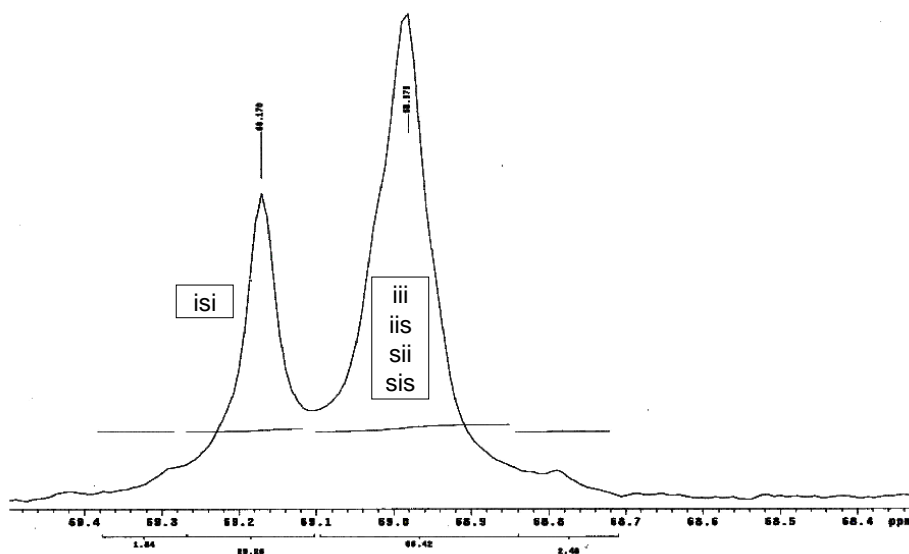


Figure 63. Quantitative ¹³C NMR spectrum of a diblock copolymer (FMC 113) made with racemic lactide in CDCl₃, zoom of the methyne signal (69ppm)

2. Synthesis of the homopolymer poly(glutamic acid)

Poly(benzyl glutamate), a protected poly(glutamic acid), is obtained from the polymerization of the corresponding N-carboxyanhydride (NCA).¹⁵¹ This NCA is produced by phosgenation of the corresponding amino acid, benzyl glutamate.¹⁴⁹ The procedure we followed was adapted from a direct phosgenation procedure (Figure 64) described in reference ¹⁴⁹. Instead of 2.16 equivalents of phosgene gas, one equivalent of triphosgene was used for the sake of facility and safety. After synthesis, the product is recrystallized and obtained as a pure white solid.

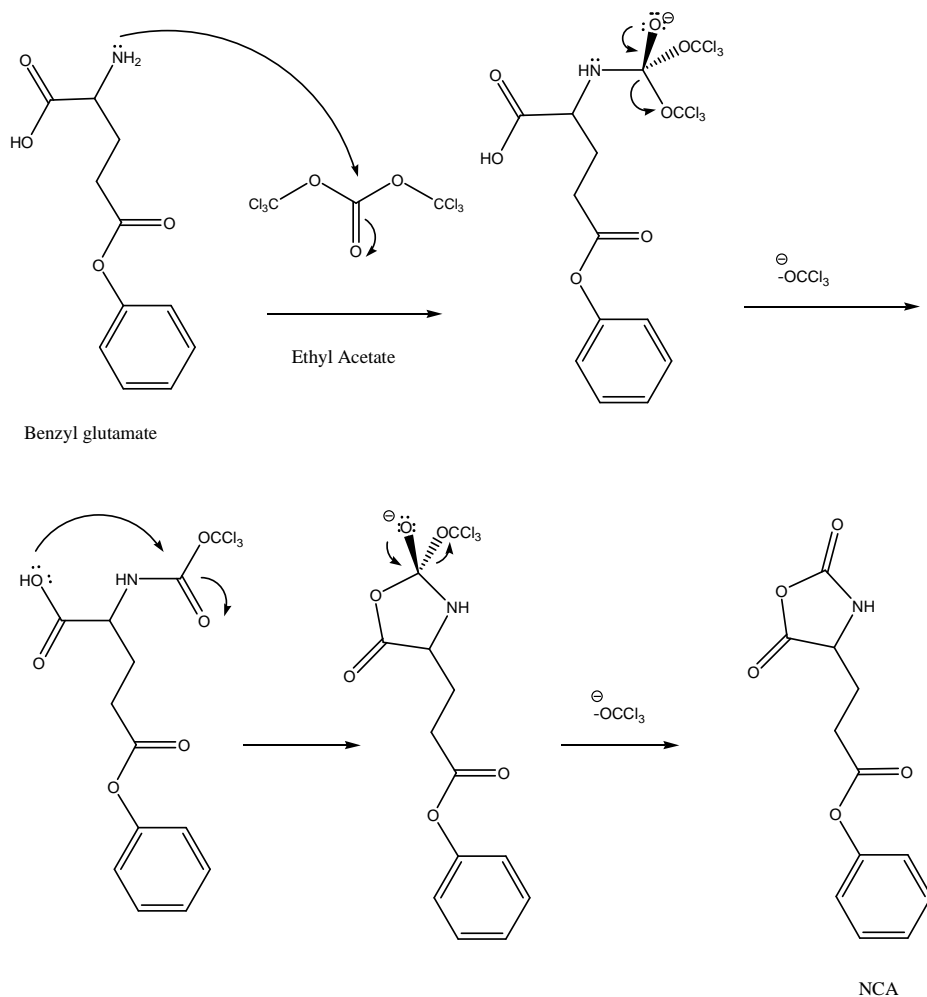


Figure 64. NCA synthesis

The polymerization of the NCA was performed in N-methyl pyrrolidinone (NMP) as solvent and the conversion was followed by two different methods: infra-red spectroscopy and HPLC. Indeed, two IR bands (1786 cm^{-1} and at 1853 cm^{-1}) are characteristic of the NCA¹⁴⁸ (Figure 65 and Figure 66). These bands correspond to the two carbonyl located on the five-membered ring (carbonyl stretch of the ester side and of the amide side of the NCA). These bands are obscured by the signal of NMP, which was subtracted for quantification purpose.

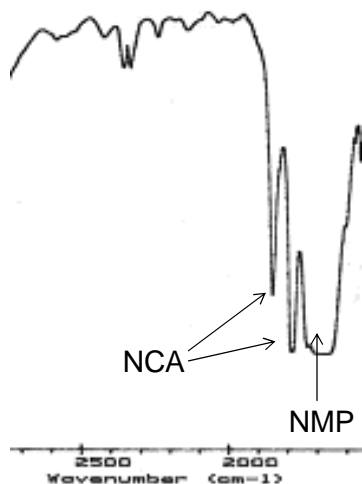


Figure 65. zoom of the carbonyl region in IR before polymerization

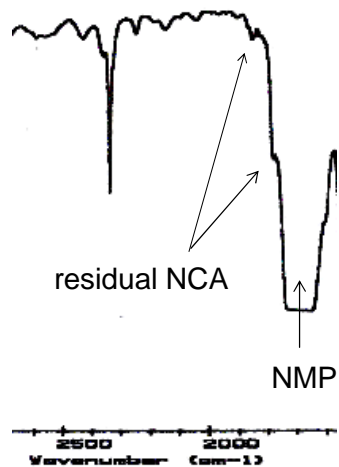


Figure 66. zoom of the carbonyl region in IR after polymerization

The conversion can also be followed via HPLC. At different times, a small aliquot of the reacting medium was precipitated in ultra pure water, filtered and dissolved in a phosphate buffer. A peak characteristic of the NCA is observed at 4.4 minutes in the chromatogram. This peak disappears as time progresses (Figure 67 and Figure 68). Although not checked, it is likely this peak corresponds to the signal of benzyl glutamate, the hydrolysis product of the NCA.

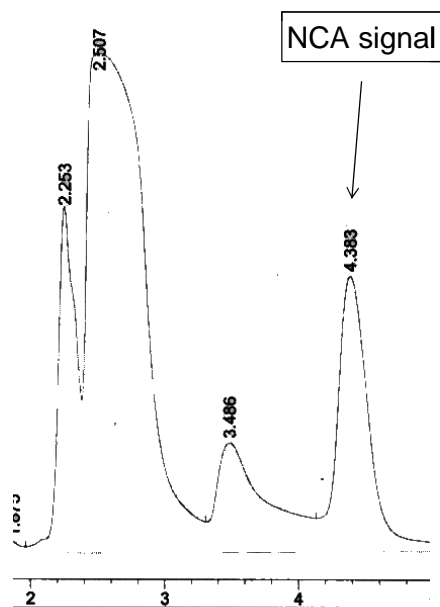


Figure 67. Chromatogram of the NCA polymerization at 4 minutes

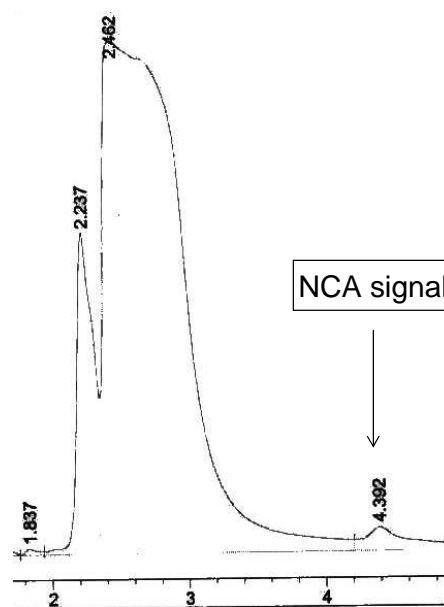


Figure 68. Chromatogram of the NCA polymerization at 180 minutes

The initiator chosen for this ring opening polymerization of the NCA is either ammonia or benzyl amine. The amine attacks the most electrophilic carbonyl group (ester side), generating a carbamate which spontaneously releases CO_2 and regenerates an amine¹⁴⁸ (Figure 69). The advantage of using benzyl amine is that, once deprotected, the degree of polymerization of the PGlu can be obtained by integrating the resonances of the aromatic region relative to those of the glutamic acid units in the ^1H NMR spectrum. On the contrary, the advantage of choosing ammonia is that, once deprotected, the percentage of deprotection can be calculated by integrating the residual aromatic protons in the ^1H NMR spectrum. Both polymerizations with ammonia and benzyl amine were followed by HPLC. The choice of initiator does not seem to make a difference in terms of kinetics or polydispersity.

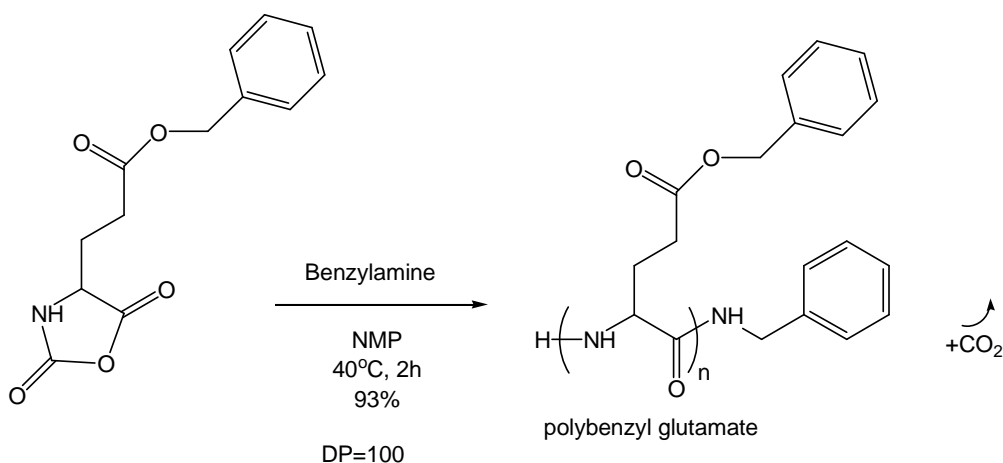


Figure 69. NCA polymerization

Initially, the degree of polymerization (ratio monomer to initiator) was arbitrarily fixed at 30. However, it turned out that the triblock copolymer formed by coupling between the PEG-PLA and the PGLu was not hydrophilic enough to allow for vesicle formation. For the latest experiments, the degree of polymerization was increased from 30 to 100.

The polymerization was found to be living, as shown by the linear evolution of the peak average molecular weight vs conversion (Figure 70). However, this behavior is only true for polymers of low degree of polymerization (up to 200, corresponding to a Mn of 25800 g/mol)

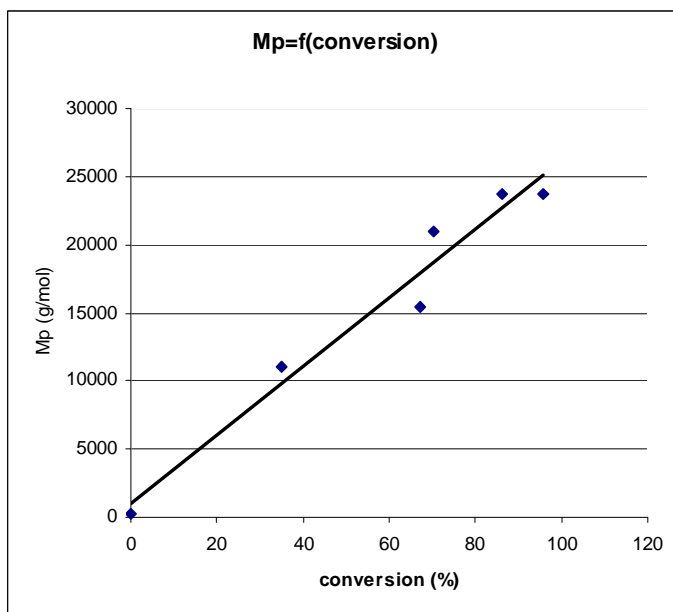


Figure 70. Peak average molecular weight (measured by GPC) versus conversion (measured by HPLC)

Indeed, the polymerization of benzyl glutamate polymerization is plagued by the formation of pyroglutamic end-groups (Figure 71) issued from the nucleophilic attack of the amino terminus on the electrophilic carbonyl of the pendant chain. Due to the adequate distance between the nitrogen and the carbonyl, this reaction forms a stable five-member ring¹⁵⁴ and stops the propagation of the chain.

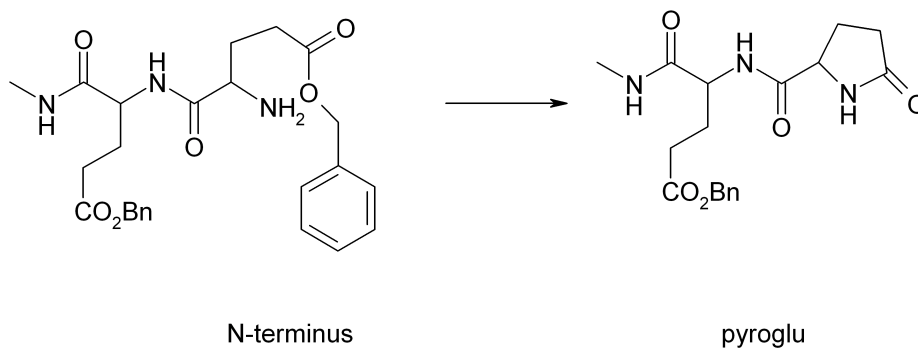


Figure 71. Formation of pyroglutamic end-groups¹⁴⁸

However, under the experimental conditions used here, the polydispersity stays low and the molecular weight increases linearly with the conversion. Even if dead chains are observed on GPC spectrum (Figure 75) and on maldi-tof spectrum (Figure 74), the polymerization can then be assumed to be living: the rate of formation of pyroglutamic end-groups is most likely much slower than the polymerization rate. When long chains of poly(benzyl glutamate) are targeted, then the formation of pyroglutamic end-groups becomes predominant and the chains terminate before the polymerization is over. Thus, it is not possible to prepare long chains of poly(benzyl glutamate) by an anionic ring-opening polymerization using ammonia or benzyl amine as initiator.

Besides the formation of pyroglutamic end-groups, the formation of β -sheets during the polymerization leads to the premature loss of propagating species.¹⁴⁸ Indeed, as a poly(amino acid), the polybenzyl glutamate chain adopts a secondary structure while it grows. There are two main kinds of secondary structures for polypeptides: α -helix (Figure 72) and β -sheet (parallel and anti-parallel) (Figure 73).

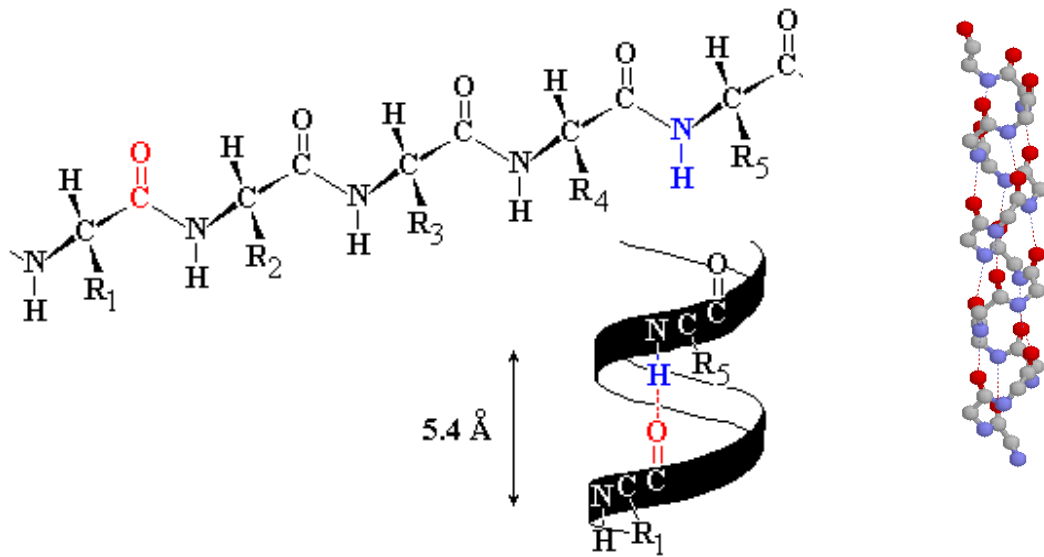


Figure 72. α -helix¹⁶¹

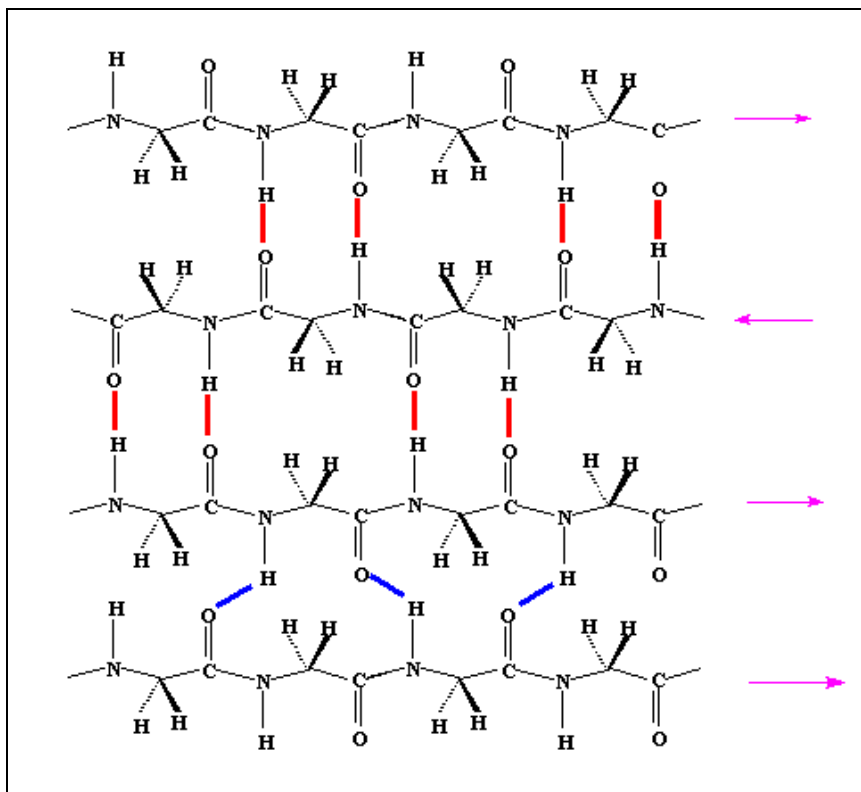


Figure 73. Parallel and antiparallel β -sheets¹⁶¹ (vertical line: antiparallel, oblique line: parallel)

Initially the chain grows under a random coil conformation. When the chain becomes long enough, or when the concentration of chains becomes large

enough, the chain may fold into a secondary structure. If a α -helix conformation is adopted, the N-terminus of the chain (which is the active site of the polymerization) is accessible. However, if β -sheets are formed, several chains aggregate, causing the precipitation of several chains or at least the immobilization of the N-terminus in larger macromolecular structures.¹⁴⁸ It is well known that high molecular weight poly(benzyl glutamate) adopts an α -helix conformation,¹⁴⁸ but low molecular weight poly(benzyl glutamate) may either stay under a random coil conformation or may form β -sheets.¹⁴⁸ Such β -sheets can be observed in the low molecular area of the GPC chromatogram (Figure 75) and on a Maldi-Tof spectrum (Figure 74). This former technique indicates that the chains which precipitate under the form of β -sheets have an average molecular weight of 1500g/mol, corresponding to 12 units. The presence of β -sheets in the Maldi-Tof spectrum is artificially enhanced because in Maldi-Tof, low molecular weight chains are preferably desorbed and ionized in comparison to higher molecular weight chains. In GPC, we observe that the amount of low molecular weight “dead” chains (Figure 76) is small relative to the main peak of the living chains. Therefore, under our conditions, most of the chains are propagating, and the polymerization can be considered as living.

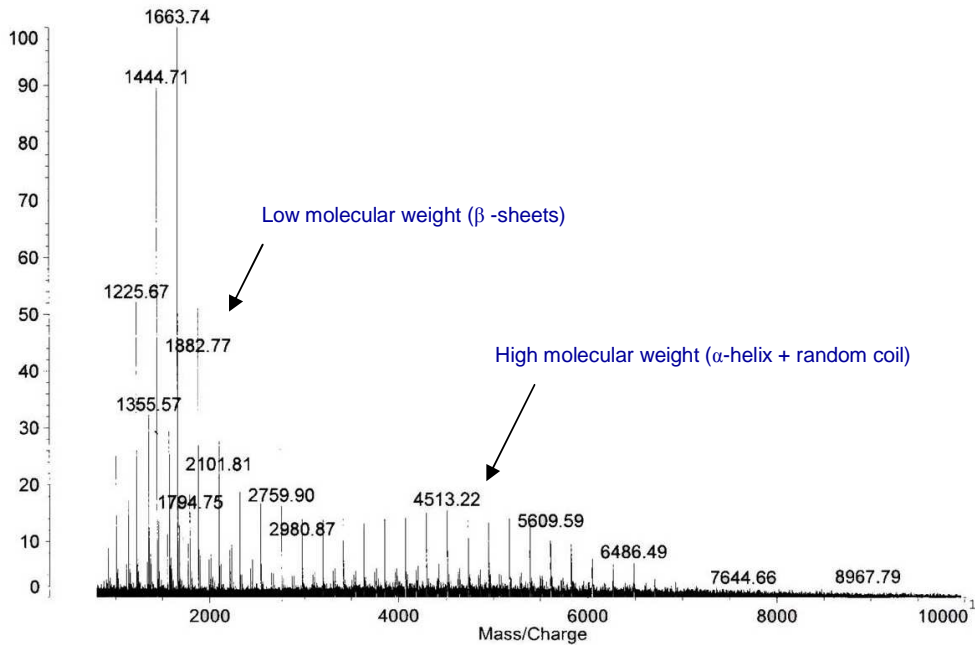


Figure 74. Maldi-tof spectrum of poly(benzyl glutamate) (FMC 129) showing a bimodal distribution, sign of the β -sheets formation. This has been measured using MS ionization, positive reflectron mode, 80kV and 3-indoleacrylic acid (IAA) as a matrix. 1 μ L of poly(benzyl glutamate) in DMF/MeOH was deposited on the grid. Once dried, 1 μ L of IAA in DMF/MeOH was added.

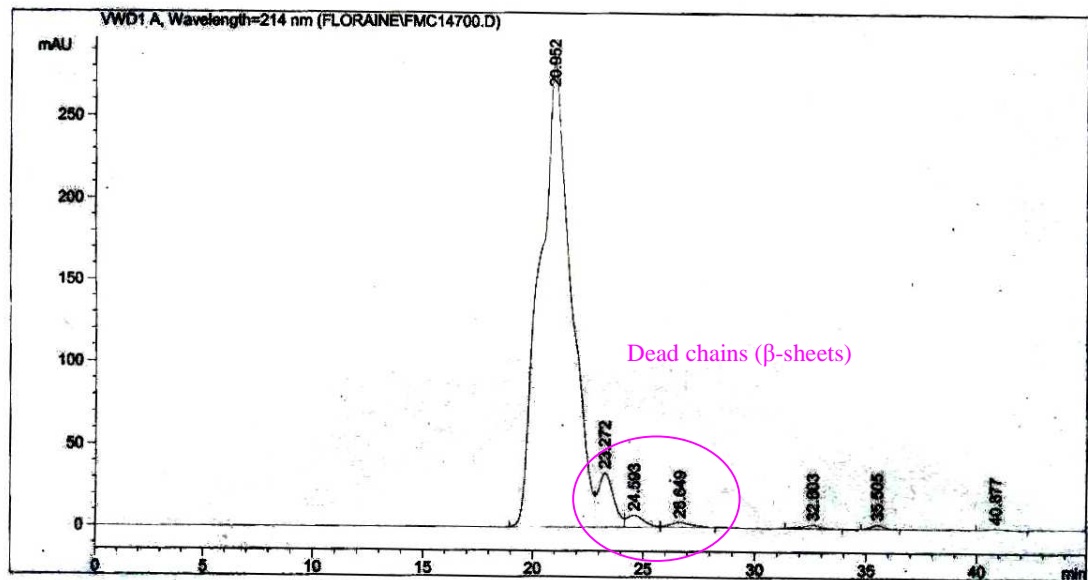


Figure 75. GPC chromatogram of polyglutamic acid (FMC 147, eluent phosphate buffer saline) showing low molecular weight chains, sign of the β -sheets formation in the poly(benzyl glutamate)

Polyglutamic acid was obtained from polybenzyl glutamic acid via a classical deprotection method used in peptide synthesis (trifluoroacetic acid, methane sulfonic acid and anisole¹⁶²) (Figure 76). The reaction can be controlled by monitoring the disappearance of the aromatic protons resonance in ¹H NMR. Initially, the deprotection was done for 3 hours but was later adjusted to 1h10 when the degree of polymerization was 100 and to 45 minutes when the degree of polymerization was 30. As shown by the GPC trace (Figure 75), the amount of low molecular weight “dead” chains is small and the polydispersity low. We can then assume that the molecular weight distribution of the polymer after deprotection is not changed.

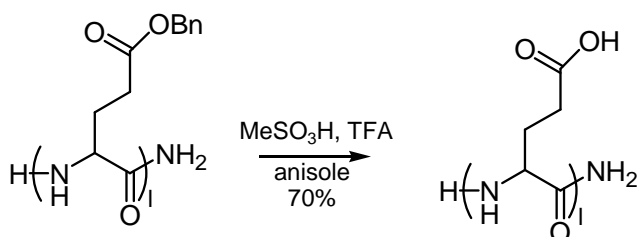


Figure 76. PGlu deprotection

The very acidic medium can cause the hydrolysis of the peptide bonds of PGlu if a small amount of water is present. This reaction was observed with long deprotection times (3 hours). Therefore, other methods of deprotection have been tried (Figure 77). The most common method for a benzyl deprotection is the use of dihydrogene gas in the presence of a Pd/C catalyst. The solvent for this hydrogenolysis is either dimethyl formamide or N-methyl pyrrolidinone in the presence of methanol. However this method is less efficient with polymers than with organic molecules and the percentage of deprotection was found to be low

(only 35% of the benzyl groups were removed, Table 5). It is believed that the PGlu strongly adsorbs at the surface of the catalyst, blocking the access to the active sites. Basic saponification,¹⁵³ acid catalyzed hydrolysis of this ester,¹⁵³ as well as the use of hydrobromic acid in the presence of trifluoroacetic acid, diethyl phosphite and methyl ethyl sulfide¹⁵³ were also explored. For later reactions, diethyl phosphite and methyl ethyl sulfide were added to prevent alkylation reactions by benzyl bromide.

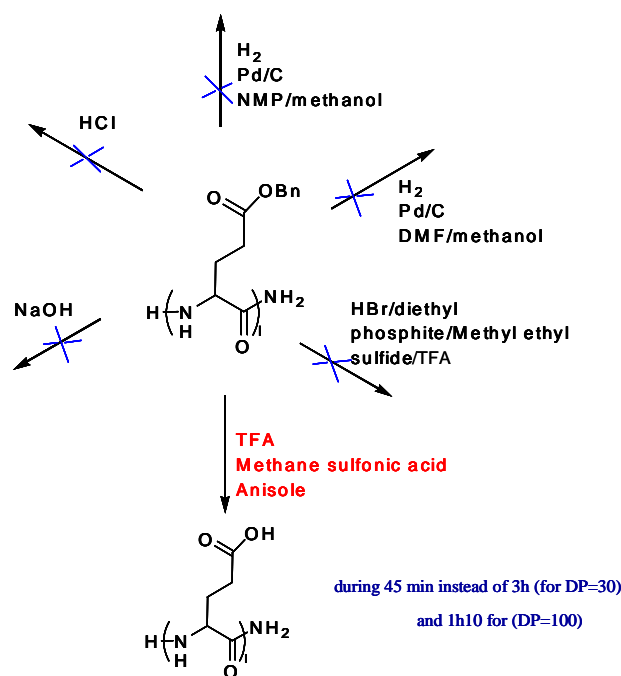


Figure 77. Different methods to deprotect the poly(benzyl glutamic acid)

The saponification and the hydrolysis of the benzyl group remained unsuccessful. On the contrary, with the use of hydrobromic acid, only 0.7% of the polymer remained protected (Table 5) but the analysis by GPC indicated that the polymer was partially hydrolyzed.

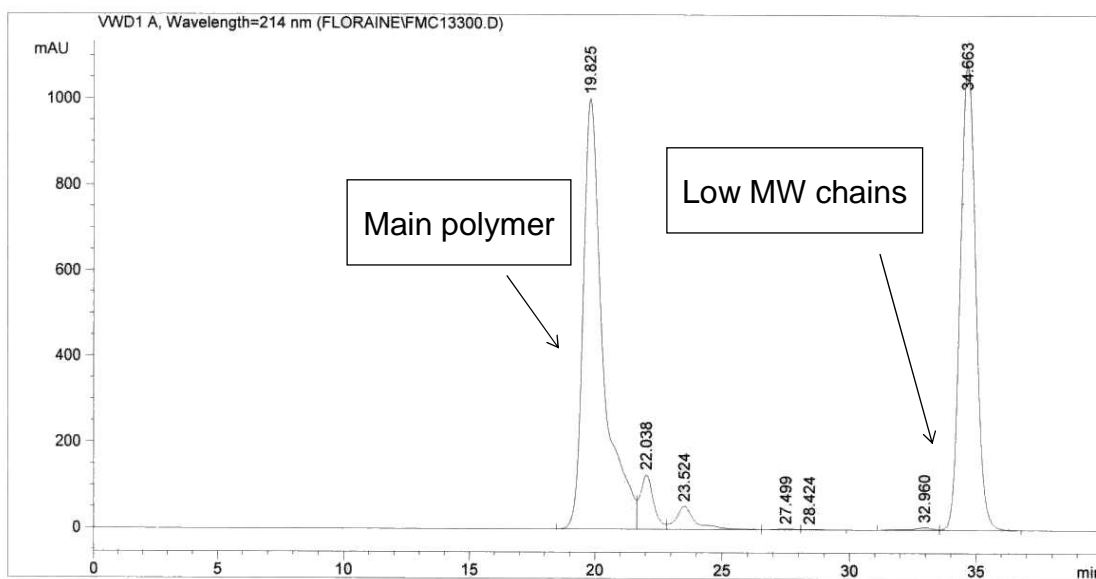


Figure 78. GPC trace of polyglutamic acid (eluent phosphate buffer saline) showing low molecular weight chains, sign of the hydrolysis of the PGLu

Table 5. Yield of the deprotection reaction

FMC	benzyl residual (%)	Deprotection method	Mn _{th} (g/mol)
133	0.7	HBr	3870
142	65	H ₂ /Pd/C	3870
147	0.9	TFA	3870
155	1	TFA	12900
170	0.2	TFA	12900
219	1.4	TFA	12900

3. Formation of the triblock copolymer PEG-PLA-PGLu

In order to obtain the triblock copolymer, a typical method of coupling¹⁵⁴ between an amino group and a carboxylic acid (used to form peptide bonds) has been adapted to couple the hydroxy group of the PLA and one of the carboxylic acid of the PGLu. In this method, dicyclohexyl carbodiimide is used as a coupling agent in the presence of N-hydroxy succinimide. The coupling reaction can occur

randomly with any carboxylic group of the PGLu, therefore, in average, a branched polymer is obtained (Figure 79). The coupling reaction was done using an excess of PGLu (2 equivalents) relative to PEG-PLA (1 equivalent). Once coupled with one diblock copolymer, the steric hindrance and the excess of PGLu most likely prevent multiple couplings (two PLA per PGLu for example).

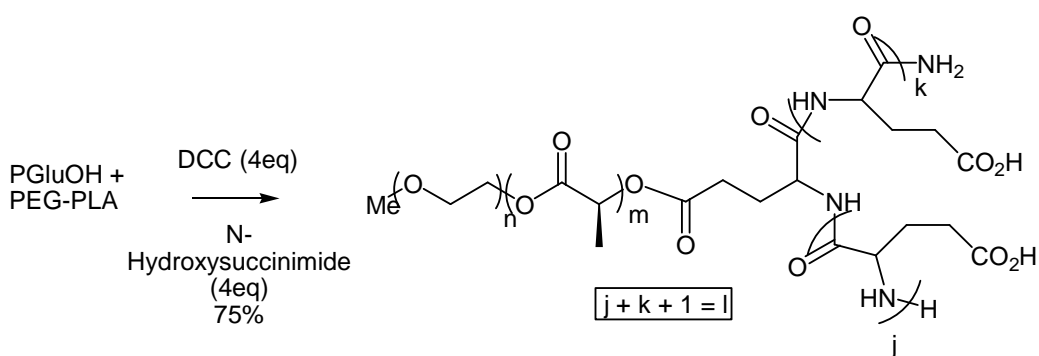


Figure 79. Coupling reaction between PGLu and the diblock copolymer

From the ^1H NMR spectrum, the molar percentage of each block can be measured. The weight percentage of each block can be calculated, using GluOK (MW=167g/mol) for the molecular weight of the glutamic unit. From this percentage, the amount of diblock PEG-PLA and PGLu in the final product is calculated and the coupling yield is found to be 75% if we considered that the coupling reaction is quantitative.

The principal side reactions are racemization and acyl transfer. In the second case, the very reactive intermediate O-acyl-urea undergoes an intramolecular transfer which competes with the desired attack of an external nucleophile. The N-acylurea obtained is much less reactive which decreases the

yield and can lead to purification problems (Figure 80). In our case, no O-acyl-urea has been seen in the final product.

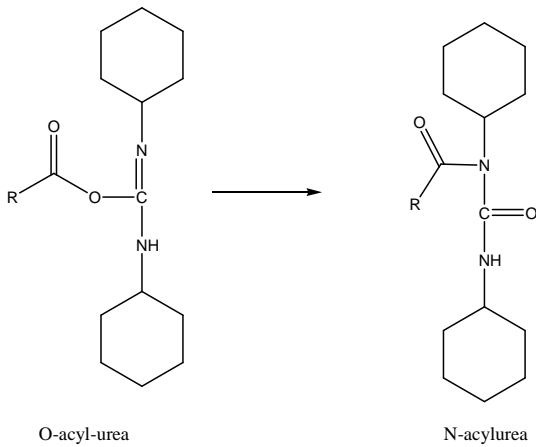


Figure 80. Side reaction occurring with DCC

After coupling, the triblock polymer was suspended in PBS and purified by ultrafiltration to remove the impurities and the solvent. The polymer was then freeze-dried (or lyophilized) and resuspended in buffer. The triblock copolymer was characterized by ^1H NMR (Figure 81) and no impurities are detected.

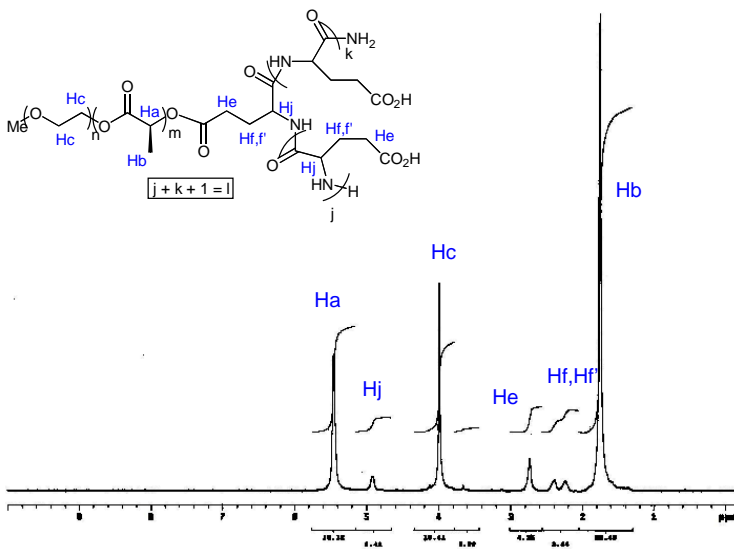


Figure 81. ^1H NMR spectrum of the branched triblock copolymer PEG₂₀₀₀-PLA₅₄₇₅-PGlu₃₈₇₀ (FMC 95)

Table 6. Recapitulative table of the branched triblock copolymers synthesized

FMC	Mn _{th} (PEG) (g/mol)	Mn _{exp} (PLA) (g/mol)	Mn _{th} (PGlu) (g/mol)
64(L)	750	13900	3900
66(L)	750	13900	3900
71(L)	750	13900	3900
73(L)	750	13900	6500
75(L)	750	7600	3900
76(L)	750	13900	6500
90(L)	2000	4300	3900
91(L)	2000	4300	6500
95(L)	2000	5500	3900
104(L)	2000	14300	3900
107(L)	2000	15900	3900
110(L)	2000	8800	3900
114(rac)	2000	9700	3900
135(sc)	2000	10000	3900
138(sc)	2000	10000	3900
146(rac)	2000	9800	8500
148(sc)	2000	9800	50000
149(rac)	2000	10000	50000
150(rac)	2000	9800	3900
160(rac)	2000	9800	12900
163, 178, 179, 182, 183, 220(rac)	2000	9800	12900

All the number average molecular weight given are theoretical for the PEG and PGlu and experimental for the PLA. Lactide used: L: L-Lactide, sc: 10% racemic lactide-90% L lactide, rac: racemic lactide

A linear polymer can be prepared by a different method (Figure 83): poly(benzyl glutamate) was first coupled with the diblock copolymer and the deprotection occurred after the coupling. As said above, the coupling method used is done between a carboxylic acid and a hydroxy group. In order to anchor the PEG-PLA to the poly(benzyl glutamate), the homopolymer has to be functionalized. For this purpose, succinic anhydride was used (Figure 82). At the end of the NCA polymerization, 10 equivalents of succinic anhydride and

triethanol amine were added. After 2 hours at 40°C, the poly(benzyl glutamate) was functionalized. Here, the triethanol amine is used as a proton trap.

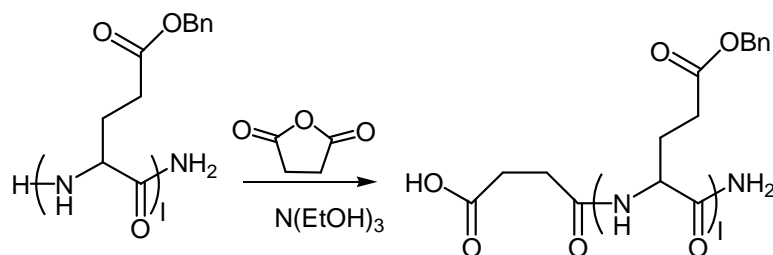


Figure 82. Functionalization of the poly(benzyl glutamate) prior coupling

After functionalization, the impurities were washed with acidic and basic water, and then with methanol. The polymer was freeze-dried and analyzed by ^1H NMR and GPC (using NMP as eluent).

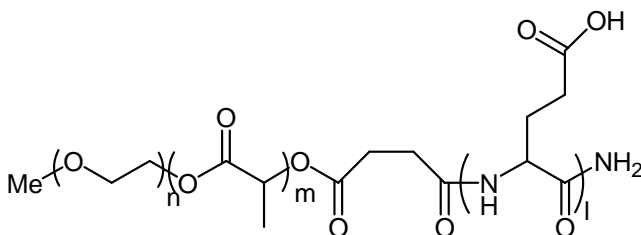


Figure 83. Linear triblock copolymer

The deprotection conditions for the triblock copolymer are very acidic (same conditions as for the poly(benzylglutamate)). PLA is a polyester and may be hydrolyzed under these conditions. When the PEG-PLA was subjected to the deprotection conditions for 2 hours, it was found to be intact (see GPC chromatogram, Figure 84). After 2 hours, the PLA was hydrolyzed.

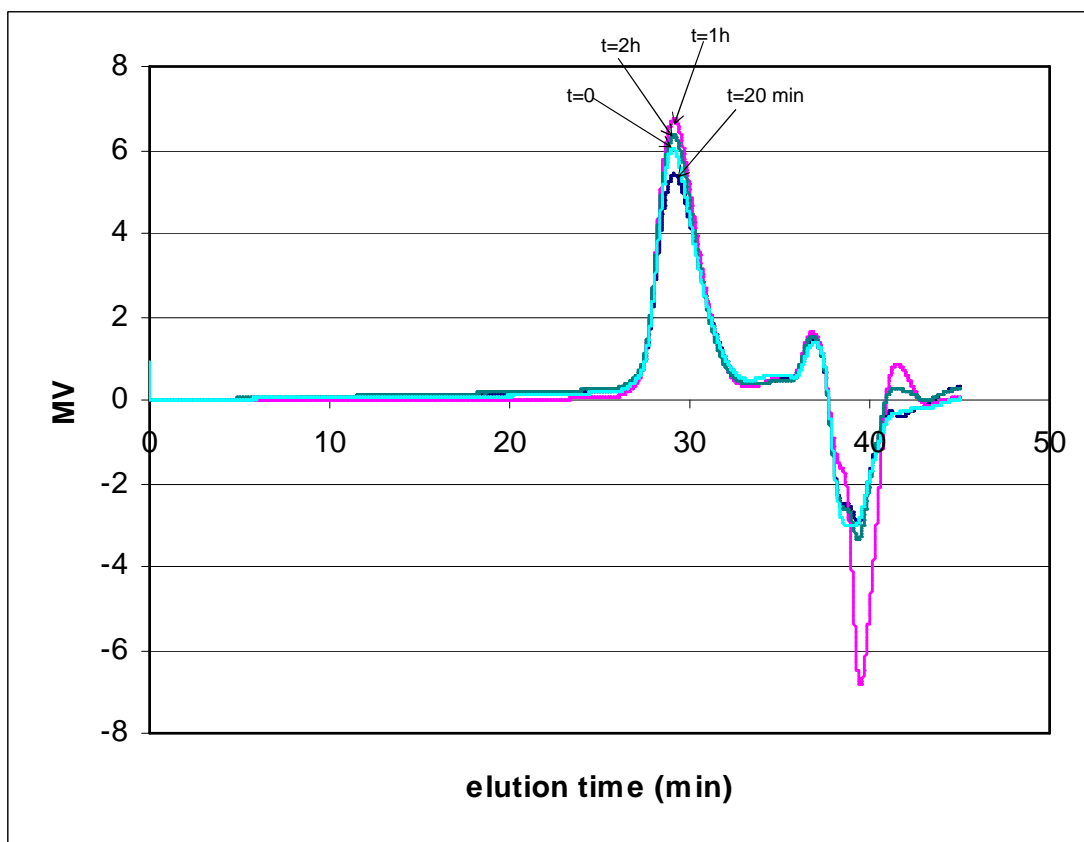


Figure 84. GPC chromatogram of the diblock copolymer PEG-PLA under deprotection condition at 20 minutes, 1 hour and 2 hours

Table 7. Recapitulative table of the linear triblock copolymers synthesized

FMC	Mn (PEG) (g/mol)	Mn (PLA) (g/mol)	Mn(Pglu) (g/mol)
18	350	5000	6450
34	750	3000	6450
46	2000	5000	6450
60	750	1500	3870

All the average number molecular weight given in this table are theoretical. All the PLA are crystalline.

4. Formation of vesicles

A. Self-assembly of vesicles and characterization

a. Self-assembly. In presence of a buffer, phosphate buffer saline (PBS) or HEPES buffer, or an aqueous solution of sodium hydroxide (pH adjusted to be between 7 and 8), the triblock copolymers self-assemble to form different nano-objects. After 30 minutes of sonication, the nano-objects scatter the light and the suspension appears to be white and no macroscopic objects can be observed. As the triblock copolymer is formed by two hydrophilic end-blocks and an internal hydrophobic block, hydrophobic interactions occur to minimize the contacts between the hydrophobic PLA and the aqueous medium. The PGlu is hydrophobic at acidic pH but is water soluble at basic pH. The presence of hydrophobic interactions is also observed in ^1H NMR: in basic water, the resonances of poly(lactide) nearly disappear (Figure 85), indicating that they have a short relaxation time T_2^* (broad resonance). This is typical of the resonance of compounds either in solid state or in a very viscous environment (no molecule mobility).

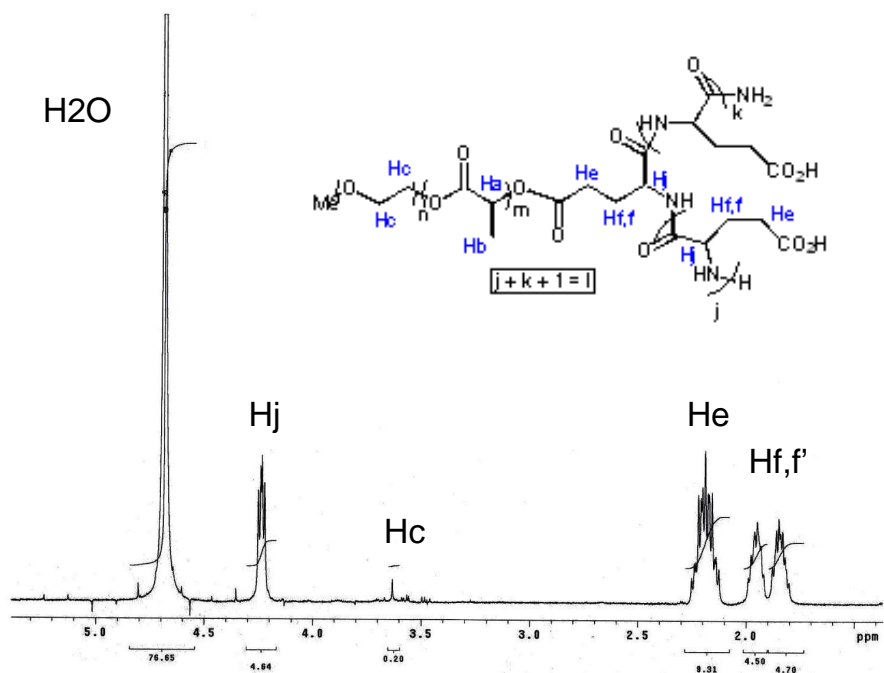


Figure 85. ¹H NMR of the vesicles in D₂O

In a slightly basic medium (pH = 7.2), most of the carboxylic groups of the PGlu block are deprotonated. The pK_a of the first deprotonated acid on the PGlu chain is around 4.4. The second carboxylic group to be deprotonated has a higher pK_a because of the electrostatic repulsions between the two carboxylates. For the same argument, the third carboxylic group will have a higher pK_a than the second one, and so on... Thus, the pK_a of a polyelectrolyte, such as PGlu, is not a defined value, but depends on numerous factors: length of the PGlu chains, ionic strength, temperature, etc... It is believed that at pH~7.2, approximately 80% of the carboxylic groups are deprotonated.¹⁶³ Due to the repulsions between the carboxylate groups, the PGlu chains are probably located on the outside face of the vesicles where each negatively charged chain has more space to minimize the interactions. The pH was selected to be almost the same than in the intestinal

lumen (pH=7.4): as the nanovesicles are going to be used for oral delivery of insulin, they need to be stable and solvated in the small intestine. Moreover, if the pH is too acidic or too basic, the PLA or the PGlu can be hydrolyzed. The self-assembly experiments were done at physiological pH and ionic strength. The typical concentrations of triblock copolymer for our experiments are 10g/L and 20g/L. The concentration of KH_2PO_4 and K_2HPO_4 in the PBS (pH=7.2) is 0.33mol/L. At a concentration of 10g/L of polymer, 0.04mol/L of “glutamic acid units” are added. A deviation of 10% of the composition of the buffer (0.033mol/L) does not result in a significant change in the pH. Therefore, adding the triblock copolymer to PBS (10g/L) does not result in a significant pH variation. At 20g/L, the pH varies slightly and needs to be adjusted with sodium hydroxide.

As an alternative to disperse the copolymer directly in a buffer, the triblock copolymer was suspended in pure water and the pH of the acidic solution was slowly adjusted until pH~7-8. When the resulting solution is freeze-dried, a white powder is obtained, which should be PEG-PLA-PGluONa. However, when redispersed in water, no vesicles are formed. It is impossible to assume that the copolymer has been partially hydrolyzed during this treatment, either at the beginning of the experiment (acidic pH) or when the NaOH solution is added (localized domain of high pH at the place the basic drop falls in the solution). For all further experiments, the vesicles were prepared using a buffer.

After ultrafiltration of the vesicles suspension, the triblock copolymer was dried either with a classical vacuum pump or with a lyophilization apparatus. The dispersion of the triblock copolymer is much easier and faster when it is

lyophilized and the suspension of the vesicles seems to be more stable. The choice of the buffer does not make any difference and the results appear to be reproducible. Suspensions of ultrafiltered vesicles stay more stable over time than suspension of redispersed triblock copolymer. The choice of the concentration of polymer does not seem to play a role but more investigation on low concentration were done by measuring the Critical Aggregation Concentration (see the CAC section).

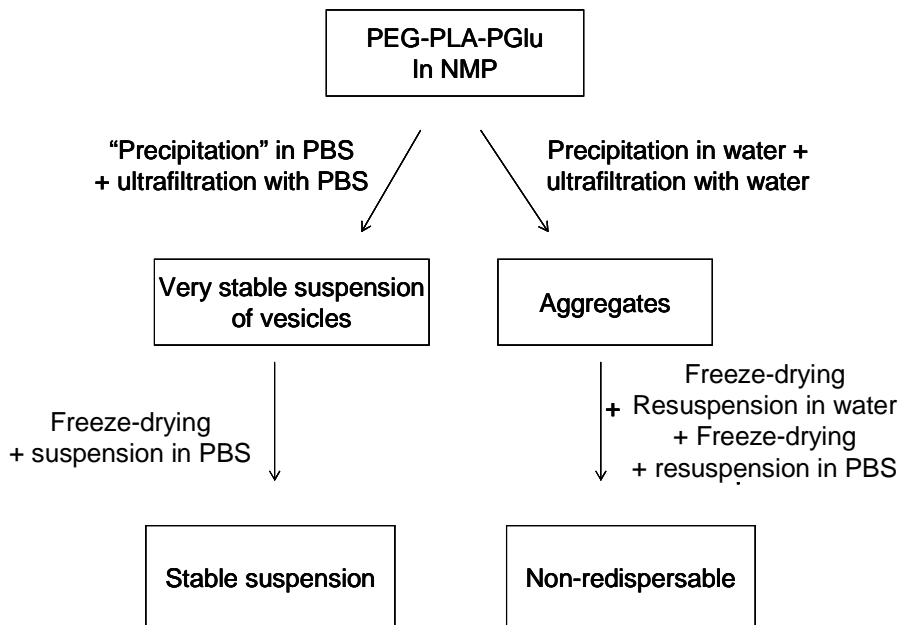


Figure 86. Different processes applied on the triblock copolymer

Self-assembly by phase inversion was also explored. The triblock copolymer was suspended in NMP and water was added dropwise to the solution. The objects obtained were analyzed by TEM (vide infra).

b. TEM. The objects formed by self-assembly have been analyzed by Transmission Electron Microscopy (TEM). In TEM, an electron beam crosses a

thin film on which vesicles have been deposited and dried. The contrast increases with the atomic number of the constituent of the cross section. The vesicles are constituted of C, H, O, N which provide low contrast. The buffer contains P, Na and K which have higher contrast. For example, we found that when PBS was deposited on a grid, dried and observed by TEM, objects which resemble a vesicle were observed. Thus, we only used a HEPES buffer for these experiments. Two types of staining agents were tried (uranyl acetate and phosphotungstic acid hydride) to enhance the contrast. The two types of triblock copolymers (linear and branched) were analyzed. The TEM samples were done on gold grids and copper grids. Several trials have been done and the best results were obtained with a concentration of 0.01-0.02% in weight, using HEPES as a buffer and a gold grid. The vesicles observed by TEM had a diameter found to be between 100 to 600 nm (Figure 88). The linear triblock copolymer forms particles by direct self-assembly (Figure 87). Experimentations by self-assembly after phase inversion (using NMP as organic solvent) were also explored. Either the TEM experiment or the phase inversion experiment stayed unsuccessful and no furthest investigation was done.

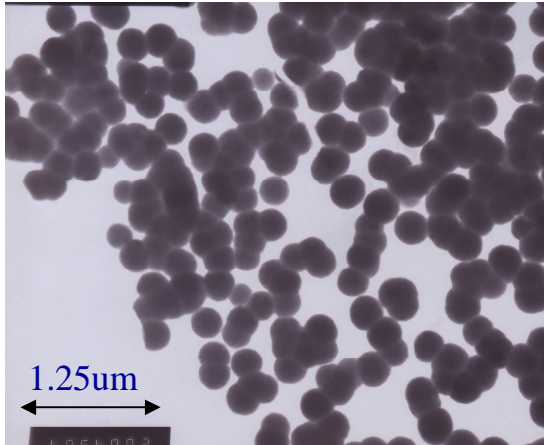


Figure 87. TEM picture of particles formed by linear triblock copolymers.

On the contrary, the branched triblock copolymer self-assembles to form vesicles which have been characterized by Transmission Electron Microscopy (TEM). Most of the work has been done using the branched copolymer PEG₂₀₀₀-PLA₉₈₀₀-PGlu₁₃₀₀₀. The rest of this chapter will be focused on the vesicles formed with this copolymer. It seems difficult to explain why the linear triblock copolymer forms particles and the branched one self-assembles in vesicles. For the branched polymer, the branched PGlu needs more space to minimize the electrostatic repulsions. By forming vesicles instead of particles, the space imparted to each branched PGlu may be larger.

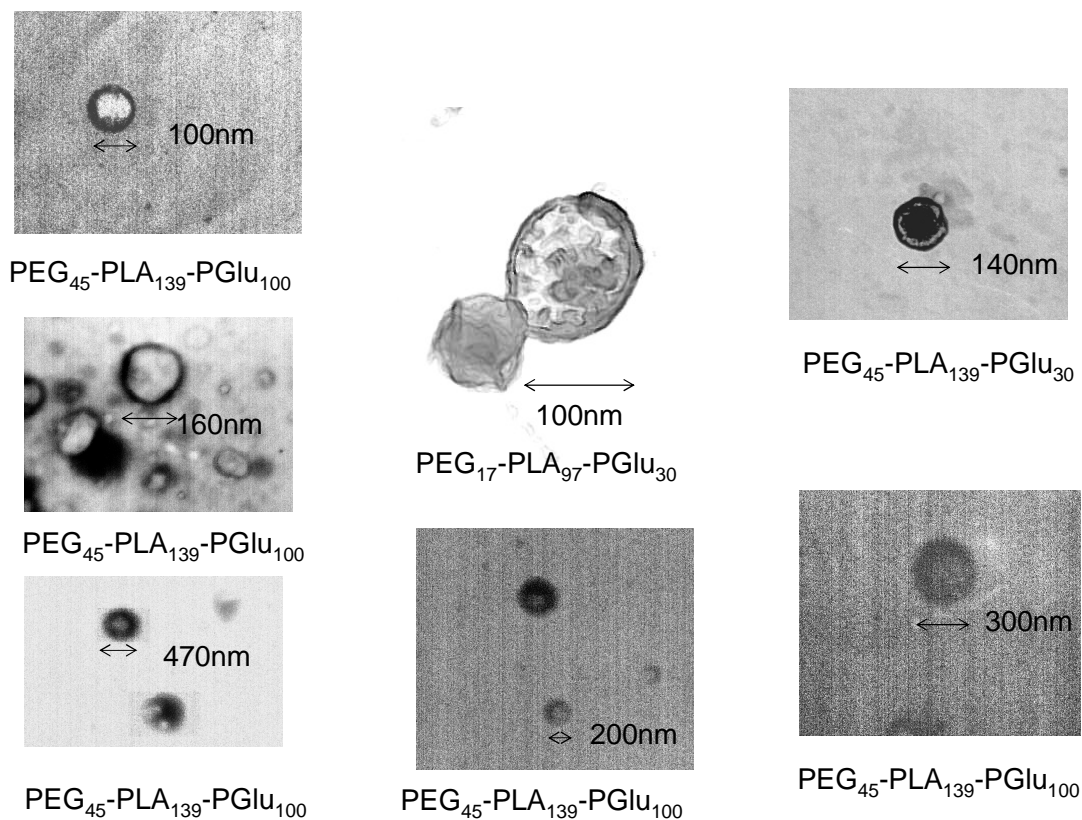


Figure 88. TEM pictures of the nanovesicles obtained by self-assembly in an HEPES buffer (The numbers correspond to the DP of each block).

The difficulty with TEM is that the sample is dried in high vacuum. What happens to a vesicle when it is submitted to high vacuum? Another technique, called cryo TEM, consists of freezing the aqueous solution in liquid ethane (to prevent the formation of ice crystals) and transfer this sample in the microscope at low temperature. This experiment was carried out in the microscopy center of Harvard University. The samples were prepared in PBS at a concentration of 1% in weight and the triblock copolymer used was freeze-dried using a lyophilization apparatus. As seen in Figure 89, vesicles of small size (between 10nm and 85nm) are observed.

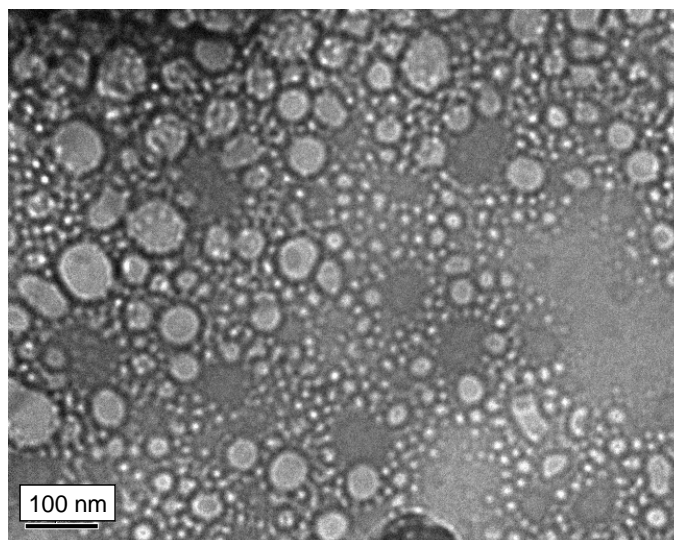


Figure 89. Cryo TEM of vesicles made by self-assembly of the triblock copolymer PEG-PLA-PGlu

c. AFM. The results found by TEM and cryo TEM have been confirmed by AFM (Atomic Force Microscopy). The glass slides were covered by a 500 angstroms gold layer and the gold was functionalized with 11-Amino-1-undecanethiol hydrochloride (SAM1), 10-carboxy-1-decanethiol (SAM2) and dodecane thiol (SAM3) to form self-assembled monolayer (SAM) (Figure 90).

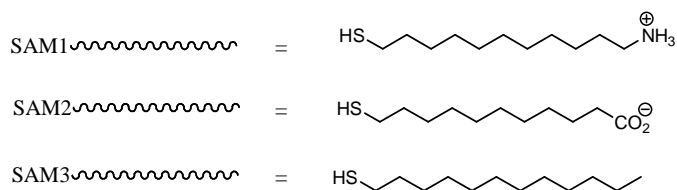
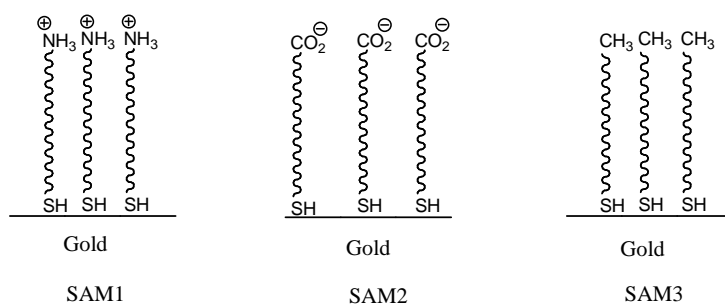


Figure 90. Self-assembled monolayers SM1, SM2 ans SM3

All the AFM measurements were done in liquid cell using contact mode. The SAM were designed to offer different interactions with the vesicles (SAM1: electrostatic attraction, SAM2: electrostatic repulsions, SAM3: Van der Waals). With an untreated gold surface, SAM2 and SAM 3, the vesicles could not be observed probably due to either the sample preparation or the fact that the vesicles could be pushed by the tip during imaging. With SAM1, which immobilize the vesicles via electrostatic interactions, vesicles were observed (Figure 91).

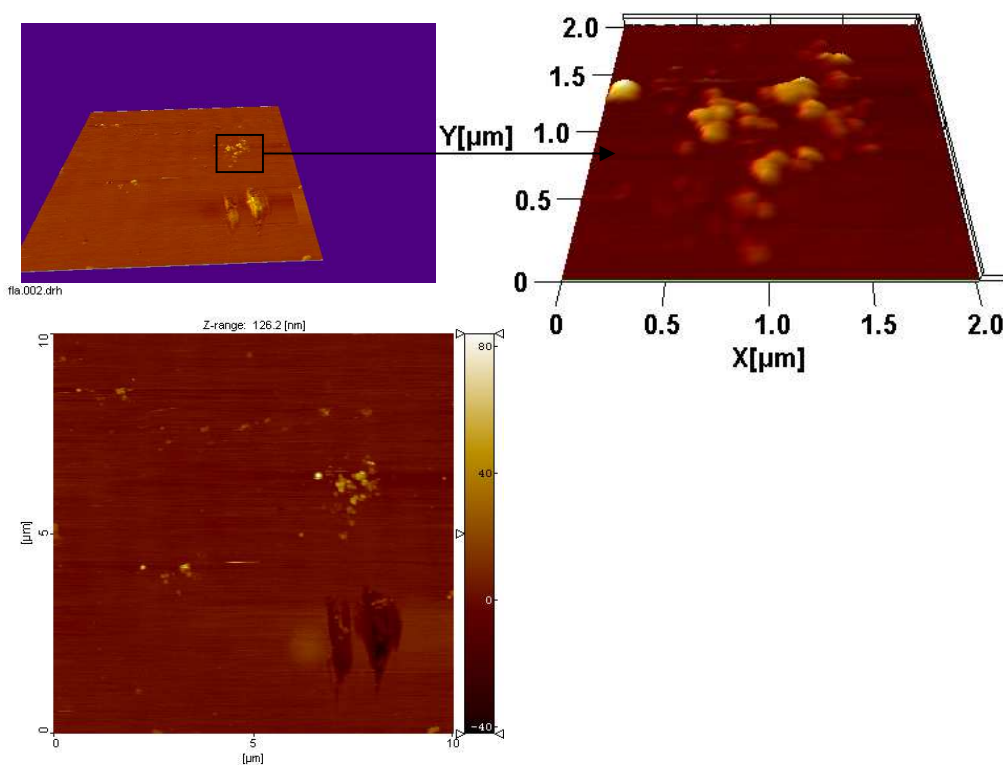


Figure 91. AFM 3D view (1:1:1) of vesicles made by self-assembly of the triblock copolymer PEG-PLA-PGlu

The average diameter was found to be around 250 nm. However, the height of the vesicles was around 80 nm. This could be explained by the fact that the vesicles are squeezed by the pressure of the tip or by the vesicles-surface interaction which would provoke the deformation of the vesicle into an ellipsoidal object. Such a phenomenon has already been observed with AFM of liposomes.¹⁶⁴ Further investigation needs to be done in particular using tapping mode. The same vesicles were analyzed by dynamic light scattering (1% in PBS) and their size was found to be around 166 nm (Figure 92).

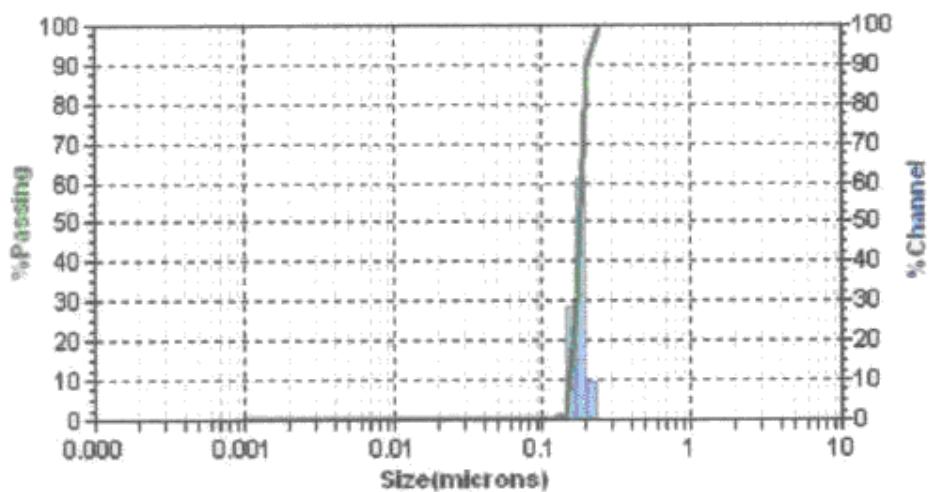


Figure 92. Light scattering spectrum of the nanovesicles

How could we explain the size discrepancy between AFM, light scattering and microscopy? Light scattering measures an hydrodynamic diameter which correspond to the “wet” diameter of the vesicles, with the hydrating water molecules around it. AFM measures a diameter for an ellipsoidal object. The volume of an ellipsoid is given by $V=4/3\pi abc$ where a, b and c are the radius of the three axis. Using $a=b=125\text{nm}$ and $c=40\text{nm}$, we find a volume of $V=2.6 \cdot 10^6$

nm³. The sphere of equivalent volume has a diameter of 171nm, which is in good agreement with the light scattering measurement. The cryo TEM gives an idea of a “solid” diameter. It is likely that all the chains of PGlu are not solvated and are collapsed at the surface of the PLA. This results in an underestimate of the radius.

d. CAC. The Critical Aggregation Concentration (CAC) has been measured using pyrene as a fluorescent marker. CMC measurement using this method has been reported by Wilhelm et al.¹⁶⁵ In this experiment, the intensity of the emission bands at 332 nm and 338nm are used as marker of the environment of the pyrene. When the pyrene is in water, it mostly emits at 332nm (Figure 93), but this emission is shifted toward 338nm in an hydrophobic environment.

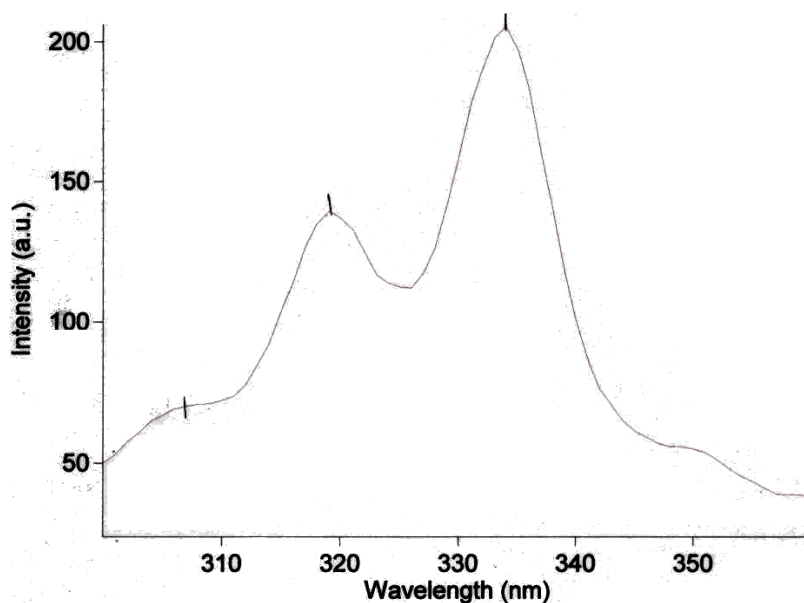


Figure 93. Emission spectrum of pyrene in presence of PEG₂₀₀₀-PLA₉₈₀₀-PGlu₁₂₉₀₀

Pyrene is solvated in water at a concentration which is less than its solubility ($4.25 \cdot 10^{-6}$ mol/mL). If no vesicles are present, then pyrene remains in water, whereas it goes in the PLA hydrophobic phase when vesicles are present. In Figure 94, it is apparent that the cac is around $2.8 \cdot 10^{-3}$ g/L. This very low cac indicates that under “in vivo” conditions, the vesicles should be stable and should not dissociate. For example, in 5 liters of blood (usual blood volume) or 1.5 L of intestinal volume, as little as 50 mg of polymer would be “self-assembled”.

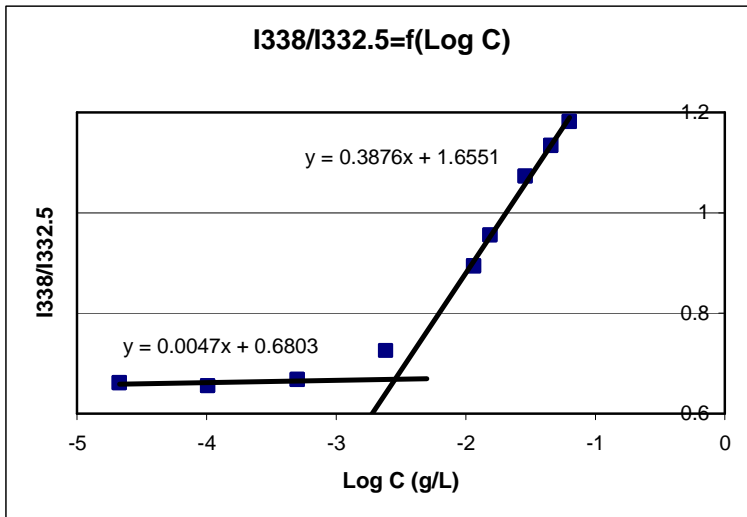


Figure 94. Ratio of the intensity of the bands located at 332.5 and 338 nm vs pyrene concentration.

B. Structure of the vesicles.

a Proteolytic degradation of the PGlu. One piece of evidence that the PGlu is located outside the vesicles is given by adding proteases to a suspension of nanovesicles. The PGlu is a polypeptide whose hydrolysis is catalyzed by proteases, in particular by pepsin. For our experiments, we used, pronase E from *Streptomyces griseus*, also called actinase E. This protease is less specific but is considered one of the most potent proteases cocktail. The effectiveness of the

proteolytic degradation has been controlled by adding pronase to a solution of PGlu. The analysis by aqueous GPC (eluent: PBS) showed a fast degradation of the PGlu. On the contrary, we checked using GPC that pronases do not degrade PEG chains. It has not been checked whether pronase degrades PLA. This experiment would be difficult to implement, because PLA is not soluble at all in water. Because proteases are selective of peptide bonds, it is possible to make the assumption that PLA is not hydrolyzed by proteases. In theory, after proteolytic degradation of the PGlu, the vesicles suspended in solution should become hydrophobic as the PLA is exposed to the buffer and the vesicles should precipitate. Pronase E (16g/L) were added to a suspension of nanovesicles (5g/L) at 37°C. Another vial was prepared with the same initial suspension of vesicles without pronase. The two vials were kept under the same conditions at 37°C and the suspensions were observed at different times (Figure 95). After a few minutes, a precipitate was observed in the vial containing the pronase and the suspension became clearer. On the contrary, in the vial containing only the vesicles, the suspension remained stable. As a precipitate was observed only when the vesicles were in presence of pronases, we can assume that a significant amount of the PGlu is located on the outside part of the vesicles.

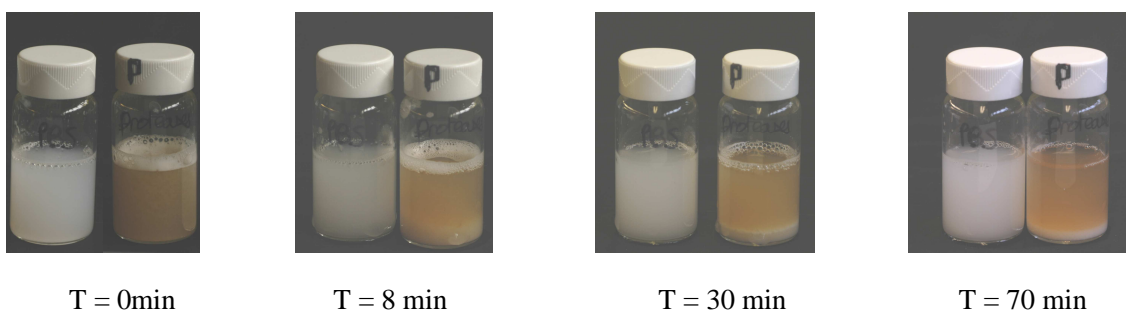


Figure 95. triblock copolymer in suspension in PBS in the presence (right side, vial labeled with a P) or without (left side) proteases

b Fluorescence experiments. Another piece of evidence concerning the PGLu location can be given by experiments with fluorescent probes. The experiments were done using Alexa Fluor 350 as a fluorescent marker (Figure 96). The PGLu chains were coupled to the fluorescent probe Alexa fluor 350 using DCC as coupling agent and NMP as solvent.

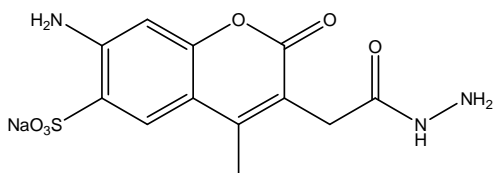


Figure 96. Formula of the Alexa fluor 350 hydrazide sodium salt

After suspension of the triblock copolymer in PBS, the vesicles were purified by ultrafiltration. In theory, if the PGLu is located at 100% on the outside of the vesicles, then when a quencher of the fluorescent dye is added, no fluorescent should be detected anymore. On the contrary, if only a part of the PGLu is located on the outside, then the fluorescence intensity is going to be proportional to the number of chains located inside the vesicles. However, an efficient quencher for the Alexa fluor 350 has yet to be found and further investigation is necessary. In the absence of vesicles, cobalt ions, nickel ions and copper ions were found to be good quenchers for Alexa fluor 350. However, the addition of the ions provokes the formation of a white cloud in the vesicle suspension which could be the sign of the vesicle precipitation. Indeed, these divalent ions are chelated by the PGLu chains. This results in the formation of crosslinks between the chains,

and the PGLu cannot play its role of outside hairy layer. For example, $2(\text{PGLuO}^-)_n(\text{Ca}^+)_n$ is insoluble in water.

Fluorescent dyes were also used to assess the capacity of the vesicles to encapsulate. For these experiments, Alexa Fluor 488 and 568 were used.

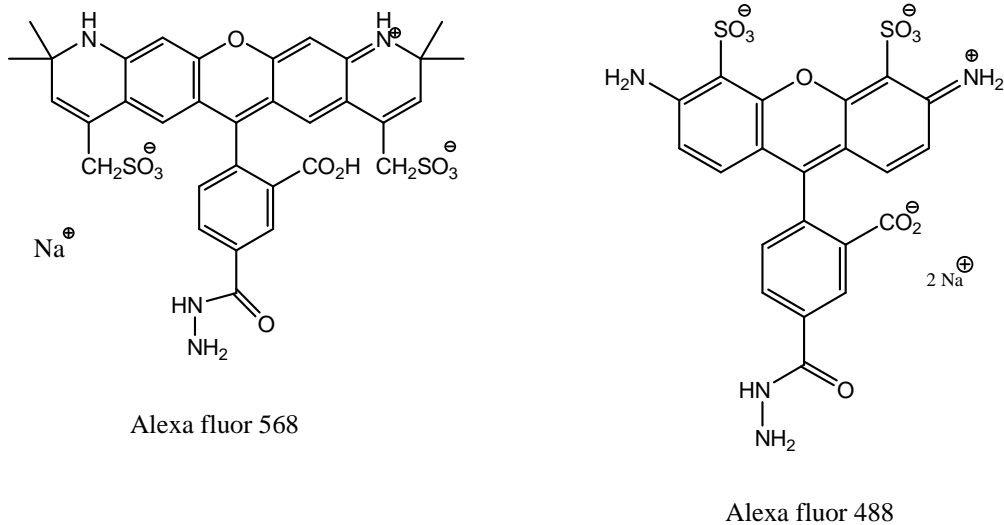


Figure 97. Formula of the Alexa fluor dyes 568 and 488

The addition of the triblock copolymer in a solution containing a fluorescent dye leads to the formation of vesicles and to the encapsulation of a part of the fluorescent dye. Upon the addition of a quencher, one expects to only observe the fluorescence due to encapsulated dye. However, once again no good quencher has been found yet and so no fluorescence was detected after addition of the quencher. This also may be due to the diffusion of the quencher through the walls of the vesicles. Further investigation needs to be done.

C. Insulin Encapsulation. In the presence of a solution of human recombinant insulin the triblock copolymer self-assembles to form vesicles and encapsulates a

part of the insulin within them. After 3 hours of incubation, the amount of free insulin, which is the non-encapsulated insulin, is quantified by HPLC (Table 8). The eluent used is acidic water and acetonitrile. As the pH is acidic, the vesicles probably precipitate in the HPLC column, releasing or not the insulin, which could explain the non-reproducibility of the results. The average percentage of encapsulation is found to be 20%. This percentage does not seem to change when phosphate buffer or an aqueous solution of sodium hydroxide (pH = 8) is used. On the contrary, the encapsulation ratio increases with the insulin concentration. This percentage also depends on whether or not the sample is filtered on mixed cellulose ester filters (0.45 μ m) prior analysis. In certain cases, a very high percentage of encapsulated insulin (above 60%) is measured. This could be due to the precipitation of a part of the insulin, caused by a decrease of pH obtained during the addition of the triblock copolymer (the pI of insulin around 6.1). In general, these encapsulation results are not very reproducible and further work is necessary to better understand the influence of each parameter.

Table 8. insulin encapsulation results

Polymer	[polymer] (mg/mL)	[insulin] (mg/mL)	% of encapsulation
FMC 146	19	10	47
FMC 150	7.9	10	56
FMC 163	8.2	10	80
FMC 178	15.3	1.54	13
FMC 179	18.3	1.54	23

In another series of experiment, vesicles were formed by self-assembly of the triblock copolymer (15 mg/mL) in the presence of insulin (0.75 mg/mL). These vesicles were ultrafiltered on a membrane (500,000 kD) which allows for the passage of insulin, but not the one of the vesicles. After several hours of ultrafiltration, only 30% of the insulin is extracted by ultrafiltration. Under the same condition, all of the insulin would be extracted if no vesicles are present (dashed line in Figure 98, calculated). This clearly indicates that insulin is encapsulated and that there exists a slow leakage of the insulin from the vesicles (as shown by the small but not zero slope of the extracted insulin versus time). Further studies need to be performed in order to precisely measure this release rate.¹⁶⁶

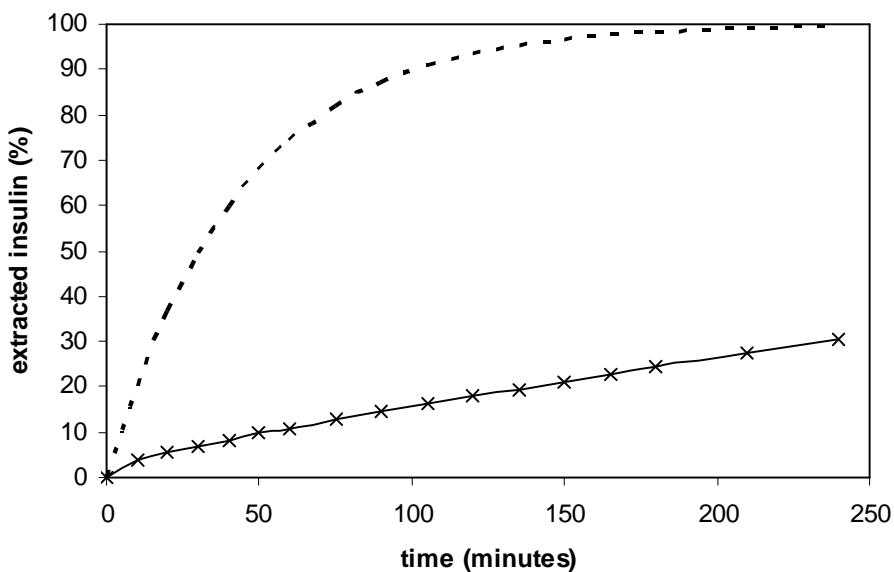


Figure 98. Amount of insulin, leaking from the vesicles (solid line) measured by HPLC, and calculated without vesicles (dash line)

5. Pharmacokinetics and pharmacodynamics

The capacity of the vesicle to vectorize insulin through the gastro-intestinal track was assessed using female Sprague-Dawley rats, which were fasted for 12 hours prior the experiment. The rats were divided in 3 groups of 4 rats:

- Group 1 : Subcutaneous injection (0.4 unit per rat) of human recombinant insulin (different from the rat insulin)
- Group 2 : Oral gavage of a solution (20 unit per rat) of human recombinant insulin
- Group 3 : Oral gavage of a suspension containing human recombinant insulin (20 unit per rat) and the triblock copolymer

The concentration of the human insulin was measured using an Elisa detection kit for human insulin. This kit is sensitive only to human recombinant insulin (insulin produced by the rat is not detected). The results, given by the level of the insulin (Figure 99) present in the blood of the rats (pharmacokinetics for the three groups), indicate that the polymer was effective in promoting the oral delivery of insulin.

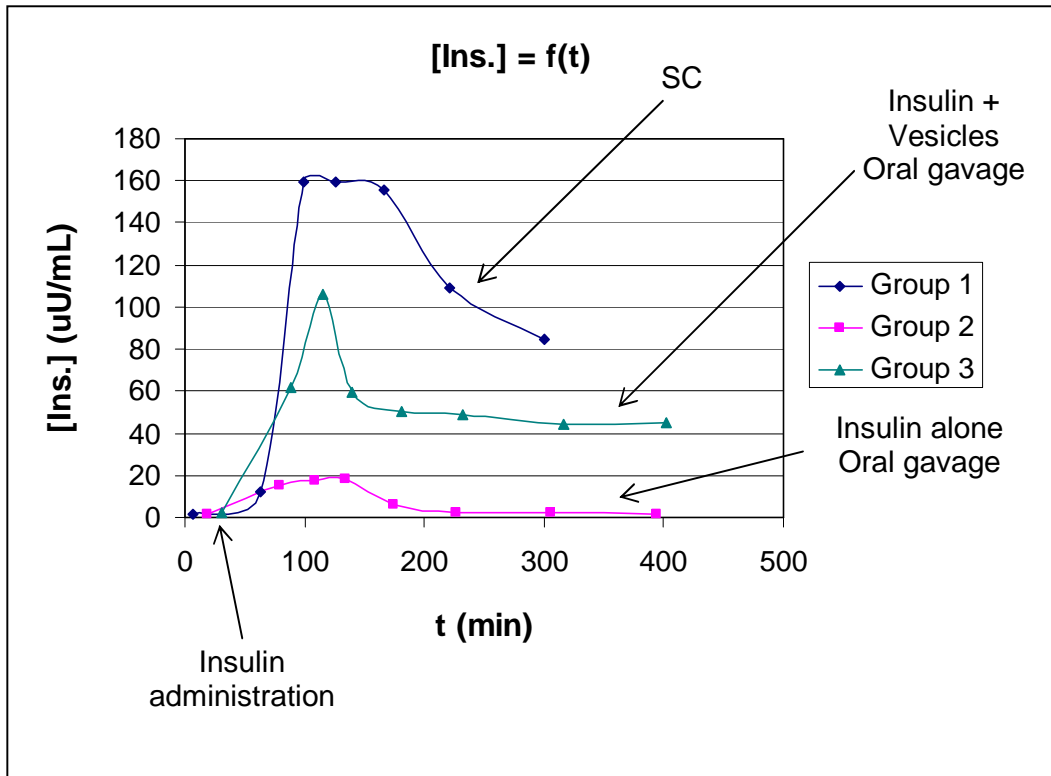


Figure 99. Average insulin concentration vs time

As expected, the level of insulin increases drastically for the first group, while the level of the second group is zero (Figure 99). For the group 3, the one with the nanovesicles, the level of insulin in the blood is significantly higher than for the group 2. Those preliminary results indicate that the encapsulation is quite efficient. The vesicles can deliver insulin through the membrane of the intestine and to be released in the blood.

Although human recombinant insulin is used for this experiment, it still presents an activity (Figure 100).

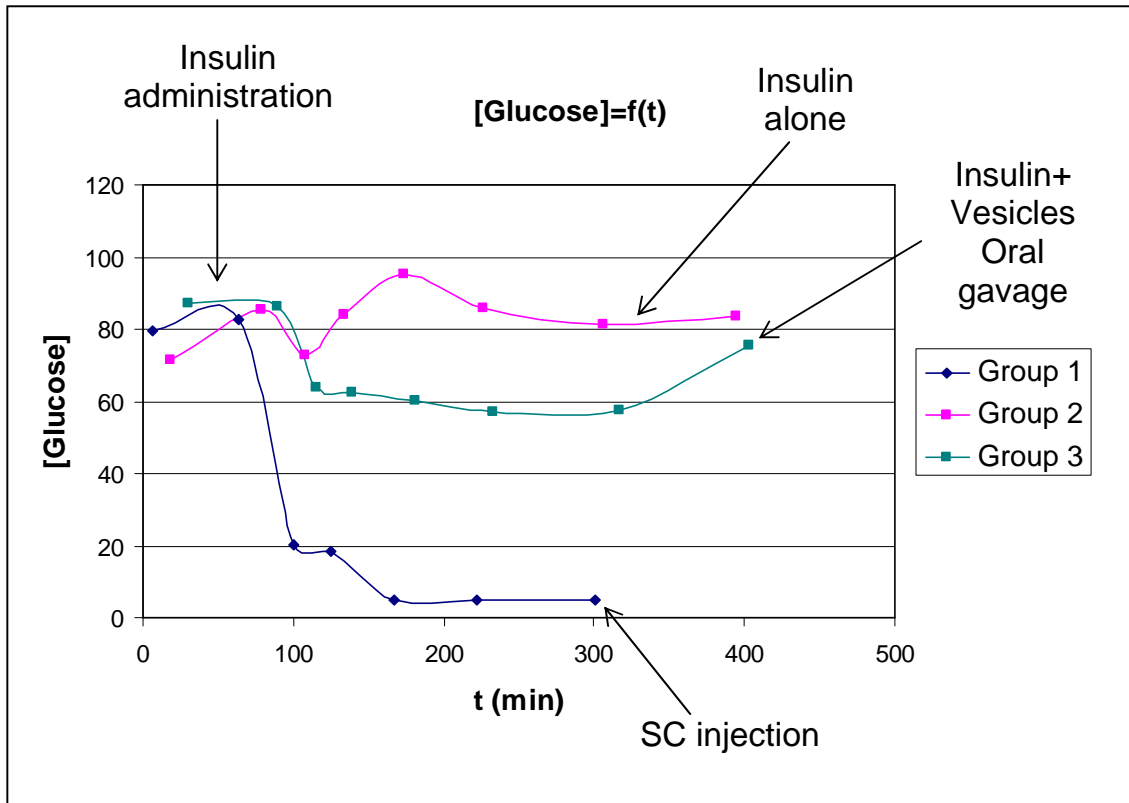


Figure 100. Average glucose concentration vs time

The blood glucose level for each group indicates that the insulin was still potent (no degradation). For the rats of group 1, the glucose level (Figure 100) decreases drastically. At some point during the experiments, the decision was taken to euthanized the rats because of their critically low glycemia. For the rats of group 2, the insulin level seems stable, or slightly increasing. When animals are fasted for a long time, their liver releases glucose in the blood in order to maintain the glycemia (gluconeogenesis¹⁶⁷). For the third group, glycemia decreases, although not as much as for the first group.

One of the causes of the low bioavailability of the vesicles could be the partial degradation of the nanovesicles in the stomach. The gastric medium is

very acidic due to the secretion of hydrochloric acid by the parietal cells (or oxyntic cells)¹⁶⁸ and the pH of the stomach may go as low as 1. One way to increase the bioavailability of the nanovesicles is to use gastro-resistant protection. For this purpose, a macroencapsulation using an enteric coating (Eudragit) is performed. In another study, in vivo tests were done again on female Sprague-Dawley rats which were fasted for 12 hours prior the experiment. However the doses used were divided by ten for the subcutaneous injection and by 5 for the three other groups. Even if the doses used for the first experiment were those found in the literature, they seemed to be too high (specially for the group 1). For the second experiment, the rats were divided in 4 groups of 4 rats:

- Group 1: Subcutaneous injection (0.04 unit per rat) of human recombinant insulin (different from the rat insulin)
- Group 2: Oral gavage of a solution (3.8 unit per rat) of human recombinant insulin
- Group 3: Oral gavage of a suspension containing human recombinant insulin (3.8 unit per rat) and the triblock copolymer
- Group 4: Oral gavage of the nanovesicles (containing some insulin) micro encapsulated in Eudragit

Once again, the concentration of the human insulin was measured using an Elisa detection kit for human insulin. The results given by the level of the insulin (Figure 101) present in the blood of the rats (for the four groups), indicate that the

polymer was effective in promoting the oral delivery of insulin. Moreover a big difference was observed when the solid form (the macroencapsulation with Eudragit) was used.

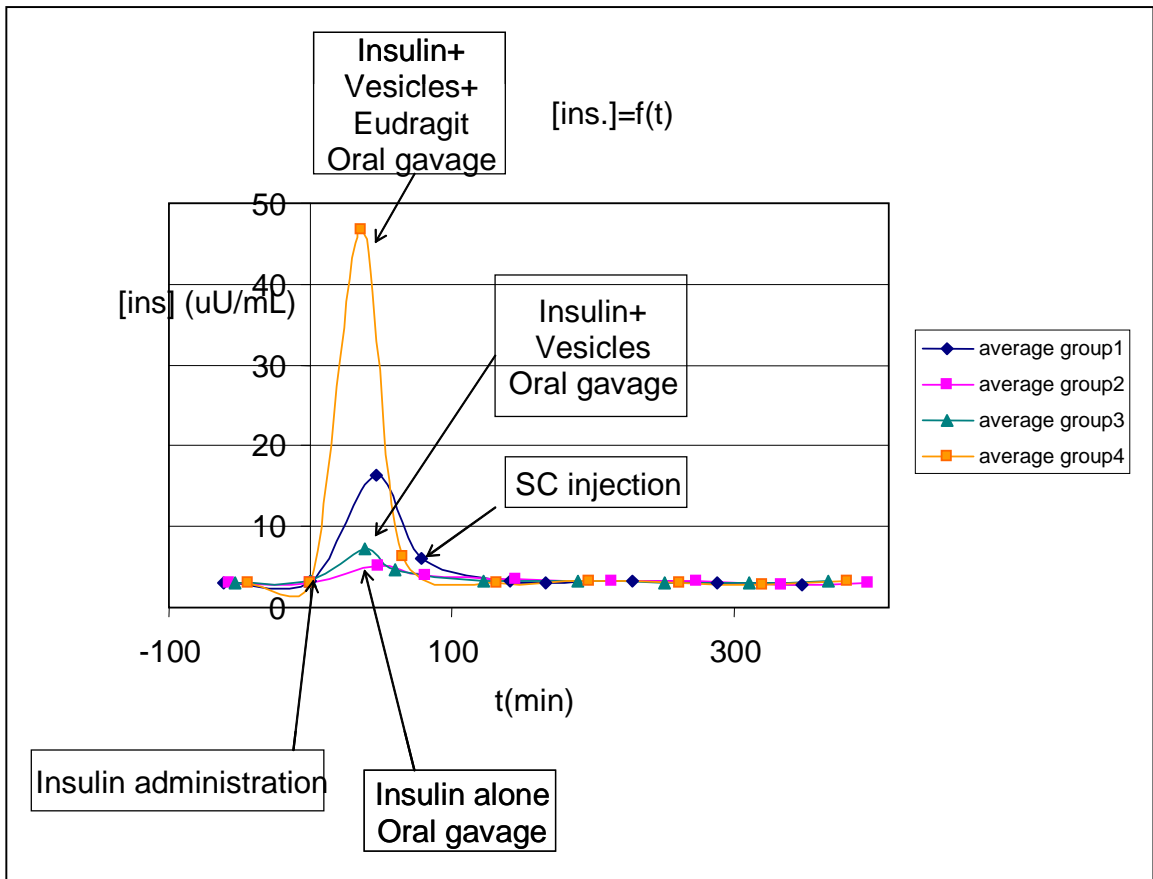


Figure 101. Average insulin concentration vs time

As expected, the level of insulin increases for the first group, while it is almost zero for the second group. In group 3, the one with the nanovesicles, the insulin level in the blood is slightly higher than for the group 2 however the difference is not very significant. This is probably due to the small doses used for this experiment. As a result, the results are very noisy and the reproducibility is low, even for the first group (subcutaneous injections) (Figure 102). Although the rat

to rat reproducibility is low, it appears that the bioavailability is higher when using a gastro-resistant protection (Group 4). These preliminary results are very encouraging and indicate that the encapsulation (nano encapsulation and micro encapsulation) is quite efficient.

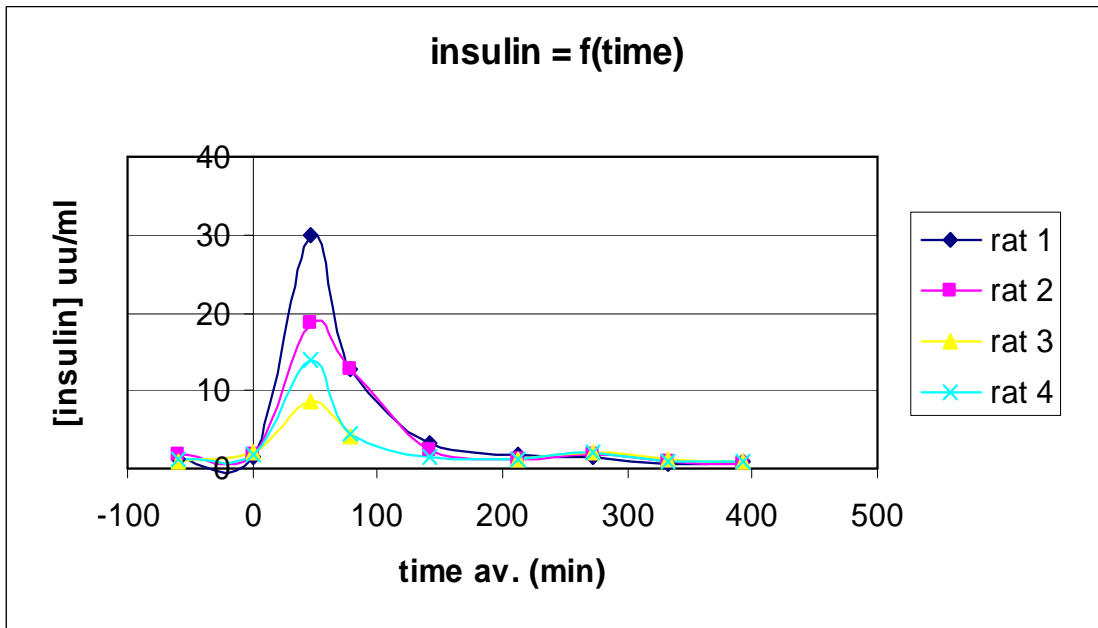


Figure 102. Insulin concentrations in function of the time for the group 1

IV. CONCLUSION

A new triblock copolymer PEG-PLA-PGlu was synthesized in three steps: formation of the diblock copolymer PEG-PLA, synthesis of the PGlu and coupling between the diblock copolymer and the homopolymer. The lactide polymerization was catalyzed by diethyl zinc in the presence of monomethyl PEG. This polymerization was living (or controlled) and rapid. Any zinc residue would not be toxic for the human body, as zinc is part of the normal metabolism. The synthesis of the PGlu was done in three steps: preparation of the monomer (NCA), polymerization of the benzyl glutamic acid NCA (which has also been proved to be living or controlled) and deprotection of the polymer. The synthetic control of those steps is important as this triblock copolymer will be used for a medical application. For both synthesis of PEG-PLA and PGlu, the polydispersity remains low. The coupling between the diblock copolymer PEG-PLA and the homopolymer PGlu was based on a usual method to form amide bonds. In an aqueous buffer, vesicles were obtained by self-assembly of the copolymer and were mainly characterized by TEM, cryo-TEM and AFM. The average diameter obtained by cryo-TEM was 100 nm. In the presence of an insulin solution, it was shown by HPLC that part of the insulin was encapsulated. These results were corroborated by animal studies. Not only insulin could be delivered in the blood via the gastro-intestinal track but also the therapeutic protein was still active (as shown by a glycemia decrease).

When using an enteric coating (EUDRAGIT) the vesicles were protected in the stomach, and the pharmacokinetics results were improved but this step still needs some improvements as the results were not reproducible.

To our knowledge, this triblock copolymer is the first example of biocompatible and biodegradable triblock copolymer. This makes it ideally suited for medicinal purposes, in particular, for the oral delivery of proteins. The insulin is encapsulated in nanovesicles which are formed by self-assembly of our triblock copolymers. In a selective solvent, triblock copolymers lead to the formation of several objects (micelles, vesicles, nanotubes...). In our case, only particles and vesicles were obtained. Particles were formed by the self-assembly of a linear triblock copolymer, while branched triblock copolymers with specific block molecular weights were needed to form vesicles. Vesicles were obtained with one combination of molecular weights ($MW_{\text{PEG}}=2000$ g/mol, $MW_{\text{PLA}}=10000$ g/mol and $MW_{\text{PGlu}}=13000$ g/mol), but other combinations should be tested in the future.

Considering that the triblock copolymer is branched and that negative repulsions occur between the carboxylates, the outside layer of the vesicles is most likely formed by the PGlu block. An indirect proof was brought by an experiment with proteases where the vesicles were found to precipitate.

At the end of this preliminary project, it seems that the preliminary success we got preparing and using these vesicles triggers a vast number of questions. First, we believe that we should concentrate on improving the control on the PGlu polymerization. Finding other deprotection methods or synthesizing PGlu by

polycondensation are strategies we are currently exploring. Synthesizing triblock copolymers PEG-PLA-PGlu with different molecular weights, while keeping a same proportion between them, could lead to the formation of vesicles with varying diameters. Moreover, triblock copolymers containing other biocompatible/biodegradable polymers (like pol(caprolactone) for example which is also a polymer approved by the FDA) could be investigated.

How do the vesicles pass through the intestinal wall and how drug is released in the blood? Histological studies in the presence of a fluorescent probe could be one way to probe this fascinating aspect of the project.

After optimizing the different synthetic steps, several studies should be done on other animals (pigs e.g., whose digestive system is much closer to that of a human). The toxicity of the vesicles must be measured before any clinical study on humans is to begin. Moreover, different parameters could be studied to see their influence on the time of release. One of them is the synthesis of PGlu using D-glutamic acid instead of the natural L-glutamic acid. The human body is also able to hydrolyze the PGlu formed with D-glutamic acid, however the time of hydrolysis will be longer, as would be the drug release.

The formulation with the enteric coating should be studied and optimized in order to obtain reproducible results. Our preliminary results were successful, but the concentration of insulin and glucose was found to vary substantially between animals. One of our concerns is to prevent the possible denaturation of the insulin during the encapsulation in the enteric coating.

This entire study has revolved around insulin as a model for therapeutic proteins. We believe that these vesicles could be equally effective for a wide range of applications such as the delivery of cytokines, growth hormones, oligonucleotides for gene therapy and vaccines.

V. EXPERIMENTAL SECTION

1. General Methods

The Gel Permeation Chromatography (GPC) instrument was constituted of an isocratic HPLC pump Waters 515, a refractometric detector Waters 2414, an autosampler Waters 717 plus, a monowavelength UV –VIS detector Waters 486, an oven (Waters temperature control module). The acquisition and treatment software was Millennium 32. The instrument was equipped with a series of four columns from Polymer Laboratories (PLgel 5um 100A, PLgel 3um 100A, PLgel 5um MIXED-C, PLgel 5um MIXED-C). Tetrahydrofuran was used as eluent at 35 °C and the flow rate was set at 1mL/min. The calibration was done using polystyrene standards ranging in molecular weight from 695 to 361,000 g/mol.

¹H NMR analysis was realized on a Varian *Mercury* 400 MHz NMR. TMS was used as reference. The Chemical shift (δ) values reported were given in part per million (ppm) relative to tetramethyl silane (TMS: Me₄Si). All the solvent used are deuterated.

¹³C NMR analysis was realized on a Varian *Mercury* 400 MHz NMR. TMS was used as reference. The Chemical shift (δ) values reported were given in part per million (ppm) relative to tetramethyl silane (TMS: Me₄Si). All the solvent used are deuterated.

The Transmission Electron Microscopy (TEM) was realized on a JEOL 100S TEM with an accelerating voltage of 80 KV. The exposure time was 2 seconds. The High Pressure Liquid Chromatography (HPLC) was an Agilent Hewlett Packard series 1100 HPLC equipped with a ZORBAX 300 SB-C8 5um column. The eluent used for the insulin detection was a combination of water/trifluoroacetic acid (TFA) (2 mL of TFA in 1L of ultra pure water) and acetonitrile/TFA (1 mL of TFA in 1L of acetonitrile). The elution consisted of a solvent gradient from 80% water/TFA (20% acetonitrile/TFA) to 50% water/TFA (50% acetonitrile/TFA) spread over 15 minutes. The flow rate was 1mL/min and the elution was done at 30 °C.

2. Solvents

Acetone (HPLC grade) was obtained from EMD Pharmaceuticals and was used without further purification.

Acetonitrile (MeCN) was obtained from Aldrich Chemical Co. and was used without further purification.

Deuterated NMR solvents were obtained from Cambridge Isotope Laboratories and were used without further purification.

Diethyl Ether (Et₂O) was obtained from Pharmaco Chemical Co. and was used without further purification.

Ethanol (95% EtOH) was obtained from Pharmaco Chemical Co. and was used without further purification.

Ethyl Acetate was obtained from Aldrich Chemical Co. and was used without further purification.

Hexanes were obtained from Aldrich Chemical Co. and were used without further purification.

Hydrochloric acid (HCl, metal grade, 35.5 % in water) was obtained from Fisher Chemical Co. and was used without further purification.

Methanol (MeOH) was obtained from EMD Pharmaceuticals and was used without further purification.

N-Methyl Pyrrolidinone (NMP) was obtained from Aldrich Chemical Co. and was used without further purification.

Tetrahydrofuran (THF) was obtained from Aldrich Chemical Co. and was used without further purification.

Toluene (C₆H₅CH₃) was obtained from Aldrich Chemical Co. and was magnetically stirred for 24 hours in the presence of calcium hydride. It was then distilled under reduced pressure, and stored under argon. The calcium hydride was also obtained from Aldrich Chemical Co.

3. Reagents

Ammonia (2 mol/L in toluene) was obtained from Aldrich Chemical Co.

Anisole was obtained from Aldrich Chemical Co.

Antifoam A was obtained from Fluka Chemical Co.

Benzyl Amine was obtained from Aldrich Chemical Co.

Benzyl glutamate was obtained from Bachem Bioscience.

Calcium Hydride was obtained from Aldrich Chemical Co.

Dicyclohexyl Carbodiimide (DCC) was obtained from Aldrich Chemical Co.

Diethyl Phosphite was obtained from Aldrich Chemical Co.

Diethyl Zinc (Et₂Zn) was obtained from Aldrich Chemical Co.

Eudragit L100 was obtained from Belmac laboratories

Hydrobromic acid (HBr) was obtained from Aldrich Chemical Co.

Hydrochloric acid (HCl, metal grade, 35.5 % in water) was obtained from Fisher Chemical Co. and was used without further purification.

L-Lactide and racemic lactide were obtained from Aldrich Chemical Co and were recrystallized three times in dried toluene.

Liquid paraffin Amojell snow-white was obtained from Aldrich Chemical Co.

Methane Sulfonic Acid was obtained from Aldrich Chemical Co.

Methyl Ethyl Sulfide was obtained from Aldrich Chemical Co.

N-hydroxysuccinimide was obtained from Aldrich Chemical Co.

Palladium over carbon (Pd/C) was obtained from Aldrich Chemical Co.

Poly(ethylene glycol) (PEG), containing one methoxy end and one hydroxy end (M_n=2000 g/mol, viscosity 54,6000 centistokes or M_n=750 g/mol, viscosity 10,500 centistokes or M_n=350 g/mol, viscosity 4,100 centistokes), was obtained from Aldrich Chemical Co.

Span 85 was obtained from Fluka Chemical Co.

Sodium Hydroxide (NaOH, 30%) was obtained from Merck Chemical Co.

Trifluoro Acetic acid was obtained from Aldrich Chemical Co.

Triphosgene was obtained from Aldrich Chemical Co.

4. Synthesis

A. Typical preparation of a diblock copolymer. The lactide polymerization was realized using standard Schlenk techniques required to manipulate air-sensitive reagents. The lactide was polymerized by ring opening polymerization using some monomethoxy PEG and using diethyl zinc as a catalyst. The lactide (10.009 g, 0.069 mol) was dissolved in 60 mL of dried toluene and the solution was then heated at 60°C prior the introduction of the Zinc compound. In a separate round bottom flask, polyethylene glycol monomethyl ether (2 g, 0.001 mol) was added in some dried toluene and was stirred until complete dissolution. Diethyl zinc was added via an argon-flushed syringe to the polyethylene glycol solution, and the mixture was stirred magnetically for one hour. Then, the zinc containing solution was transferred via a cannula to the lactide containing solution. The mixture was left to react at 60 °C for one hour. Then, 0.26 mL of an aqueous solution of hydrochloric acid were added to quench the reaction. The solvent was subsequently evaporated using a rotary evaporator. The diblock was then redissolved in 50 mL of THF. The solution was added to a magnetically stirred beaker containing 250 mL of cold ether, forcing the precipitation of the diblock. The solid was filtered off over a fritted glass filter and was washed twice with cold ether (5* 100 mL). It was then dried under vacuum for 12 hours at room temperature. The yield of the reaction was 74%.

Table 9. Synthesis of diblock copolymers

FMC	2	32	44	54	55	89	94
T (°C)	80	80	60	60	60	60	60
t _(reaction) (min)	240	120	40	40	40	40	40
Quencher Q	M	M	M	M	M	M	M
V _{Quencher} (mL)	150	500	250	585	350	392	392
m _{PEG} (g)	0.3	2.006	4.008	2.251	0.751	1.44	1.439
n _{PEG} (mol)	0.00015	0.003	0.002	0.003	0.001	0.0007	0.0007
MW (PEG)	350	750	2000	750	750	2000	2000
m _{lactide} (g)	5.59	8.064	5.041	15.12	10.08	10.79	10.78
n _{lactide} (mol)	0.039	0.056	0.035	0.105	0.07	0.075	0.075
V _{Et₂Zn} (mL)	0.5	1.21	0.45	1.36	0.45	0.33	0.33
n _{Et₂Zn} (mol)	6E-04	0.001	5E-04	0.001	5E-04	4E-04	4E-04
V _{toluene} (mL)	40	100	65	117	69	78	78
V _{ether} (mL)	/	/	150	750	750	500	500
V _{wash} (mL)	100	100	100	200	100	100	200
V _{THF} (mL)	/	/	30	150	150	100	100
lactide	L	L	L	L	L	L	L

FMC	105	109	113	117	145
T (°C)	60	60	60	60	60
t _(reaction) (min)	100	60	60	60	60
Quencher Q	HCl	HCl	HCl	HCl	HCl
V _{Quencher} (mL)	0.2	0.27	0.15	0.2	0.26
m _{PEG} (g)	1.531	2.049	1.159	1.5365	2
n _{PEG} (mol)	0.0008	0.001	0.0006	0.0008	0.001
MW (PEG)	2000	2000	2000	2000	2000
m _{lactide} (g)	11.46	10.25	5.795	7.6886	10.01
n _{lactide} (mol)	0.08	0.071	0.04	0.053393056	0.07
V _{Et₂Zn} (mL)	0.35	0.46	0.26	0.35	0.45
n _{Et₂Zn} (mol)	4E-04	5E-04	3E-04	0.000385	5E-04
V _{toluene} (mL)	84	82	46	61	79.5
V _{ether} (mL)	1000	500	250	250	250
V _{wash} (mL)	400	100	100	100	100
V _{THF} (mL)	200	100	50	50	50
lactide	L	L	rac	10%rac 90%L	rac

FMC: number of the experiment

HCl: hydrochloric acid, 35% in water

L: L-lactide

m: weight

M: Methanol

V_{wash}: Volume of ether used to wash the diblock copolymer

n: number of moles

rac: racemic lactide

T: Temperature of reaction

t: time of reaction

V: Volume

¹H NMR (400 MHz, CDCl₃) δ: 5.2 (CH, 1H, q), 3.7 (CH₂, 2H, s), 1.5 (CH₃, 3H, d)

B. Typical N-Carboxy Anhydride preparation. The Benzyl glutamate (10g, 0.042 mol) was suspended in 88 mL of ethyl acetate. One equivalent of triphosgene (12.514 g, 0.042 mol) was slowly added to the suspension previously cooled at 10°C. The solution was heated at 90°C, under 665 mm of mercury during three hours. Then 70% of the solvent was removed by distillation (62 mL), under 370 mm of mercury, and 62 mL of hexane were added under warm conditions. The solution was cooled at 2°C. The solid was separated from the liquid by filtration over a fritted glass filter and was washed twice with 100 mL of hexane. It was then dried under vacuum for 12 hours at room temperature. The yield of this reaction was 95%.

Table 10. Synthesis of N-Carboxy Anhydride (NCA)

FMC	13	25	35	96	118	140	167	173
m _{benzyl glutamate} (g)	8.014	10.06	10	51.19	12.25	9.085	25.48	10
n _{benzyl glutamate} (mol)	0.034	0.042	0.042	0.216	0.052	0.038	0.107	0.042
V _{ethyl acetate} (mL)	71	90	88.5	453	108	80	225	88
m _{triphosgene} (g)	21.66	12.59	12.51	64.15	15.31	11.37	31.87	12.51
n _{triphosgene} (mol)	0.073	0.042	0.042	0.216	0.052	0.038	0.107	0.042
V _{hexane} (mL)	20	65	60	320	70	56	160	62
V _{wash} (mL)	100	100	100	200	100	100	100	100
T (°C)	70	80	90	90	30	90	90	90
t (min)	180	240	180	180	180	180	180	180

FMC: number of the experiment

m: weight

n: number of moles

T: Temperature of reaction

t: time of reaction

V: Volume

V_{wash}: Volume of hexane used to wash the NCA

C. Typical polymerization of the NCA. The NCA obtained (3.386 g, 0.013 mol) was dissolved in 24 mL of NMP and was polymerized by ring-opening¹⁴⁸ using 64 μ L of ammonia, initiator of the polymerization. After three hours at 40°C, ten equivalents of succinic anhydride and ten equivalents of triethanol amine were added. After two hours at 40°C, the polymer was precipitated in 125 mL of ultra pure water. The polymer was filtered over a fritted glass and was purified by washing with 100 mL of basic water (pH = 10), 100 mL of acidic water (pH = 3), 100 mL of neutral water and then 100mL of ether so all the unreacted NCA was removed. The solid was then dried under vacuum for 12 hours at room temperature. The yield of this reaction was 85%.

Table 11. Synthesis of Poly(Benzyl Glutamate) (PBnGlu)

FMC	51	57	69	97	129	137	157	174	175
m_{NCA} (g)	2.008	2.845	2.64	43.12	1.576	1.976	4.662	3.386	5.095
n_{NCA} (mol)	0.008	0.011	0.01	0.164	0.006	0.008	0.018	0.013	0.019
V_{NMP} (mL)	7	9.9	13.2	150	5.5	13.8	32.6	24	36
Initiator	A	A	A	A	B	B	B	A	A
$V_{\text{initiator}}$ (μ L)	76	108	167	2730	22	27	19	64	97
t (min)	180	240	40	40	60	60	120	960	4200
$V_{\text{neutral water}}$ (mL)	135	150	166	1000	128	169	263	225	380
$V_{\text{acidic water}}$ (mL)	100	100	100	250	100	100	200	100	200
$V_{\text{basic water}}$ (mL)	100	100	100	250	100	100	200	100	200
V_{methanol} (mL)	100	100	100	250	/	/	/	/	/
V_{ether} (mL)	/	/	/	250	100	100	200	100	200

FMC: number of the experiment

m: weight

n: number of moles

T: Temperature of reaction

t: time of reaction

V: Volume

$V_{\text{neutral water}}$: cumulated volume of neutral water used for the precipitation of the polymer and for its wash

D. Typical deprotection of a poly(benzyl glutamate). The polyglutamic acid was obtained by deprotection of the poly(benzyl glutamate). The poly(benzyl glutamate) (3.475 g, 0.016 mol) was dissolved in 35 mL of trifluoroacetic acid (TFA). Then 35 mL of methane sulfonic acid (MSA) and 8.6 mL of anisole ¹⁶² were added at 10°C. After 70 minutes, the polymer was precipitated with 393 mL of cold ether, filtered over a fritted glass and washed with ether (2* 150 mL). The solid was then dried under vacuum for 12 hours at room temperature. The yield of this reaction was 99.7%.

Table 12. Synthesis of Poly(Glutamic acid) (PGlu)

FMC	58	65	70	72	74	100	147	159	176	177
m _{PBnGlu} (g)	0.48	0.149	1.568	1.082	1.147	24.58	0.444	2.443	2.392	3.475
n _{PBnGlu} (mol)	0.002	7E-04	0.007	0.005	0.005	0.112	0.002	0.011	0.011	0.016
V _{MSA} (mL)	4.83	1.5	15.8	10.9	11.5	246	4.45	24.5	24	35
V _{TFA} (mL)	4.83	1.5	15.8	10.9	11.5	246	4.45	24.5	24	35
V _{anisole} (mL)	1.19	0.37	3.87	2.67	2.85	61	1.1	6.07	6	8.6
V _{ether} (mL)	55	17	178	123	130	2765	50	275	270	393
V _{wash} (mL)	100	50	100	100	100	500	50	100	100	300
t (min)	180	180	180	180	180	180	45	70	80	70

FMC: number of the experiment

m: weight

n: number of moles

t: time of reaction

V: Volume

V_{wash}: volume of ether used to wash the polymer

¹H NMR (400 MHz, TFA) δ: 4.95 (CH, 1H, s), 2.77 (CO₂H-CH₂-CH₂-CH, 2H, s), 2.43-2.28 (CO₂H-CH₂-CH₂-CH, 2H, s)

¹H NMR (400 MHz, D₂O) δ: 4.15 (CH, 1H, s), 2.09 (CO₂H-CH₂-CH₂-CH, 2H, s), 1.87-1.76 (CO₂H-CH₂-CH₂-CH, 2H, s)

As the samples analyzed by ^1H NMR are polymeric chains, all the peaks appear as a singlet.

E. Five other methods of deprotection of the Poly(benzyl glutamate)

1) The poly(benzyl glutamate) (55.8 mg, $0.25 \cdot 10^{-3}$ mol) was dissolved in NMP (10 mL) and 10mL of methanol were added. 10 mg of palladium over carbon, which is the catalyst, were suspended and some dihydrogene bubbled in the suspension for 10 hours. Then the catalyst was removed by filtration over a buchner funnel. The polymer was precipitated in five volumes of ether (100 mL), filtered over a fritted glass and washed with ether ($2 \cdot 50$ mL). The solid was then dried under vacuum for 12 hours at room temperature.

2) The poly(benzyl glutamate) (0.72 g, $3.3 \cdot 10^{-3}$ mol) was dissolved in 20 mL of a solution of NMP/methanol (v/v: 1/1). 72.8 mg of palladium over carbon, which is the catalyst, were suspended and some dihydrogene bubbled in the suspension for 10 hours. Then the catalyst was removed by filtration over a buchner funnel and the solvent was evaporated with a rotary evaporator. The solid was then dried under vacuum for 12 hours at room temperature.

3) The poly(benzyl glutamate) (0.453 g, 0.002 mol) was dissolved in 22.6 mL of trifluoroacetic acid. 3.46 mL of diethyl phosphite and 3.46 mL of methyl ethyl sulfide were added. The solution was cooled at -5°C while protected from the light. Then 5.65 mL of a solution of hydrobromic acid in acetic acid (30wt) was slowly added. The solution was kept in a closed round bottom flask at 20°C

in the darkness. After two hours, the solvent was evaporated using a rotary evaporator and the polymer was suspended in ether. After filtration over a fritted glass, the solid was washed with ether (2*50 mL) and dried under vacuum for 12 hours at room temperature.

Table 13. Deprotection of PBnGlu with HBr

FMC	133	136
m _{PBnGlu} (g)	0.277	0.453
n _{PBnGlu} (mol)	0.001	0.002
V _{TFA} (mL)	13.84	22.6
V _{HBr anhydrous} (mL)	3.46	5.65
V _{Diethyl phosphite} (mL)	3.46	5.65
V _{Methyl Ethyl sulfide} (mL)	3.46	5.65

FMC: number of the experiment

m: weight

n: number of moles

V: Volume

4) The poly(benzyl glutamate) (0.6449 g, $2.9 \cdot 10^{-3}$ mol) was dissolved in 4.3 mL of N-Methyl Pyrrolidinone and 4.3 mL of a solution of sodium hydroxide in NMP (1N) were added. After two hours at room temperature, 4.3 mL of a solution of hydrochloric acid in NMP (1N) were added as well as 1mL of water. The suspension was heated at 80°C for one hour and then filtered over a fritted glass. The solid was washed with water (2*50 mL) and then ether (2*50 mL) and dried under vacuum for 12 hours at room temperature.

5) The poly(benzyl glutamate) (70 mg, $18 \cdot 10^{-6}$ mol) was dissolved in N-Methyl Pyrrolidinone (0.47 mL) and a solution of hydrochloric acid in NMP (1N) (90 uL) was added. After five hours at 70°C, the polymer was precipitated in five

volumes of ether (2.8 mL) and filtered over a fritted glass. The solid was washed with ether (2*50 mL) and dried under vacuum for 12 hours at room temperature.

F. Typical preparation of the branched triblock copolymer. The triblock copolymer is formed by coupling of the diblock copolymer PEG-PLA and the homopolymers PGLu. Dicyclohexyl carbodiimide (DCC) is used as an activator for coupling the diblock copolymer to one of the carboxylic groups of the poly(glutamic acid). The poly(glutamic acid) (1.105 g, $85.49 \cdot 10^{-6}$ mol), some N-hydroxysuccinimide (0.0199 g, $171 \cdot 10^{-6}$ mol) and the diblock copolymer (0.503 g, $43 \cdot 10^{-6}$ mol) were suspended in 7.8 mL of N-methyl Pyrrolidinone (NMP). Some DCC (0.037 g, $171 \cdot 10^{-6}$ mol) was dissolved in 0.2 mL of NMP, in another round bottom flask. Then the two liquids were mixed together, and stirred at 55 °C, over night. 40 mL of ultrapure water were added to the mixture, and the suspension was cleaned by ultrafiltration in order to remove the impurities and the NMP. At the end of the ultrafiltration experiment, the polymer suspension was concentrated and the concentrated solution was freeze dried to afford an off-white solid. The yield of this reaction was 75%.

Table 14. Synthesis of triblock copolymers

FMC	64	66	71c	73a	73b	73c	75
m _{diblock} (g)	0.3246	0.1354	0.719	0.0989	0.0775	0.1444	0.1479
n _{diblock} (mol)	2.22E-05	9.24E-06	4.91E-05	6.75E-06	5.29E-06	9.86E-06	1.78E-05
m _{PGlu} (g)	0.1714	0.0698	0.095	0.0871	0.0683	0.0318	0.1377
n _{PGlu} (mol)	4.43E-05	1.80E-05	2.45E-05	1.35E-05	1.06E-05	4.93E-06	3.56E-05
m _{DCC} (g)	0.0102	0.0042	0.0202	0.00278	0.00109	0.00406	0.0074
n _{DCC} (mol)	4.95E-05	2.04E-05	9.81E-05	1.35E-05	5.29E-06	1.97E-05	3.59E-05
m _{NHS} (g)	0.0097	0.0051	0.02131	0.0029	0.00115	0.0043	0.0077
n _{NHS} (mol)	4.47E-05	2.35E-05	9.82E-05	1.34E-05	5.30E-06	1.98E-05	3.55E-05
V _{NMP} (mL)	5.85	2.85	2.6	1.5	0.88	1.58	1.7
T (°C)	50	45	45	50	50	50	50
time (min)	120	120	120	120	120	120	120

FMC	76	90	91	95	104a	104b	104c
m _{diblock} (g)	0.16099	0.7024	0.1543	0.2497	0.1041	0.0952	0.1649
n _{diblock} (mol)	1.10E-05	4.13E-05	9.08E-06	1.47E-05	5.04E-06	4.61E-06	7.98E-06
m _{PGlu} (g)	0.1418	0.3198	0.1171	0.1137	0.0392	0.0359	0.0154
n _{PGlu} (mol)	2.20E-05	8.26E-05	1.82E-05	2.94E-05	1.01E-05	9.28E-06	3.98E-06
m _{DCC} (g)	0.0045	0.017	0.0062	0.0066	0.0021	0.0009	0.0033
n _{DCC} (mol)	2.18E-05	8.25E-05	3.01E-05	3.20E-05	1.02E-05	4.37E-06	1.60E-05
m _{NHS} (g)	0	0.0194	0.0057	0.0064	0.0027	0.0012	0.0035
n _{NHS} (mol)	0	8.94E-05	2.63E-05	2.95E-05	1.24E-05	5.53E-06	1.61E-05
V _{NMP} (mL)	1.88	5.97	1.82	2.26	0.9	0.83	1.07
T (°C)	25	50	50	50	50	50	50
time (min)	120	120	120	120	120	120	120

FMC	107	110	114	138	146	148	149
m _{diblock} (g)	1.1292	1.1355	0.5296	0.032	0.0163	0.0107	0.0107
n _{diblock} (mol)	6.33E-05	1.05E-04	4.53E-05	2.66E-06	1.38E-06	8.89E-07	8.89E-07
m _{PGlu} (g)	0.4908	0.8126	0.3508	0.0445	0.023	0.0847	0.0847
n _{PGlu} (mol)	1.27E-04	2.10E-04	9.06E-05	5.24E-06	2.71E-06	1.69E-06	1.69E-06
m _{DCC} (g)	0.0523	0.0865	0.0381	0.0052	0.0032	0.001	0.001
n _{DCC} (mol)	2.54E-04	4.20E-04	1.85E-04	2.52E-05	1.55E-05	4.85E-06	4.85E-06
m _{NHS} (g)	0.0549	0.0911	0.021	0.0028	0.0011	0.0008	0.0008
n _{NHS} (mol)	2.53E-04	4.20E-04	9.68E-05	1.29E-05	9.56E-06	6.95E-06	6.95E-06
V _{NMP} (mL)	16.2	10.9	4.76	0.84	0.25	1.24	1.02
T (°C)	55	55	55	55	55	55	55
time (min)	120	120	120	12	120	120	120

Table 14. (continued) Synthesis of triblock copolymers

FMC	150	160	163	178	179	182	183
m _{diblock} (g)	0.0601	0.0966	0.5169	0.3104	0.5034	1.5158	0.2732
n _{diblock} (mol)	5.10E-06	8.20E-06	4.39E-05	2.64E-05	4.27E-05	1.29E-04	2.32E-05
m _{PGlu} (g)	0.0394	0.2133	1.1325	0.6806	1.1028	3.3207	0.5964
n _{PGlu} (mol)	1.02E-05	1.65E-05	8.78E-05	5.28E-05	8.55E-05	2.57E-04	4.62E-05
m _{DCC} (g)	0.0042	0.0068	0.0364	0.022	0.0368	0.1071	0.0194
n _{DCC} (mol)	2.04E-05	3.30E-05	1.77E-04	1.07E-04	1.79E-04	5.20E-04	9.42E-05
m _{NHS} (g)	0.0027	0.0039	0.0201	0.0122	0.0199	0.0594	0.0109
n _{NHS} (mol)	2.35E-05	3.39E-05	1.75E-04	1.06E-04	1.73E-04	5.16E-04	9.47E-05
V _{NMP} (mL)	0.58	1.7	8.2	5	8	24.6	4.4
T (°C)	55	55	55	55	55	55	55
time (min)	120	120	120	1080	1080	120	120

FMC: number of the experiment
m: weight
n: number of moles

T: Temperature of reaction
t: time of reaction
V: Volume

¹H NMR (400 MHz, TFA) δ: 5.45 (CH-CH₃, 1H, q), 4.95 (HN-CH-CO, 1H, m), 3.97 (O-CH₂, 2H, s), 2.77 (CO₂H-CH₂-CH₂-CH, 2H, m), 2.43-2.28 (CO₂H-CH₂-CH₂-CH, 2H, m), 1.72 (CH-CH₃, 3H, d)

¹H NMR (400 MHz, D₂O) δ: 4.15 (HN-CH-CO, 1H, m), 3.94 (CH-CH₃, 1H, q), 3.54 (O-CH₂, 2H, s), 2.09 (CO₂H-CH₂-CH₂-CH, 2H, m), 1.87-1.76 (CO₂H-CH₂-CH₂-CH, 2H, m), 1.16 (CH-CH₃, 3H, d)

Some of the spectra show broad singlets instead of multiplets due to the fact that the product analyzed is a polymer.

G. Typical preparation of the linear triblock copolymer, typical polymerization of the NCA and functionalisation of the PBnGlu. The NCA obtained (2.5067 g, 9.53 10⁻³ mol) was dissolved in 12.5 mL of NMP and was polymerized by ring-opening¹⁴⁸ using 159 uL of ammonia, initiator of the polymerization. The solution was left at 40°C and after 90 minutes, 10 equivalents of succinic anhydride (0.3184 g, 3.177 10⁻³) and 10 equivalent of triethanol amine (0.478 g, 3.177 10⁻³) were added. After 180 minutes at 40°C, the

polymer was precipitated in 63 mL of ultra pure water. The polymer was filtered over a fritted glass and was purified by washing with 100 mL of basic water (pH = 10), 100 mL of acidic water (pH = 3), 100 mL of neutral water and then 100mL of methanol so all the unreacted NCA was removed. The solid was then dried under vacuum for 12 hours at room temperature. The yield of this reaction was 85%.

Table 15. Preparation of functionalized PBnGlu prepared

FMC	17	28	39
m_{NCA} (g)	2	4.812	2.507
n_{NCA} (mol)	0.008	0.018	0.01
V_{NMP} (mL)	10	24	12.5
V_{NH_3} (uL)	76	305	159
t (min)	180	180	90
$V_{neutral\ water}$ (mL)	150	175	160
$V_{acidic\ water}$ (mL)	100	100	100
$V_{basic\ water}$ (mL)	100	100	100
$V_{methanol}$ (mL)	100	100	100
m_{SA} (g)	7.607	0.61	0.318
n_{SA} (mol)	0.076	0.006	0.003
m_{TA} (g)	11.33	0.909	0.478
n_{TA} (mol)	0.076	0.006	0.003

FMC: number of the experiment

m: weight

n: number of moles

t: time of reaction

V: Volume

$V_{neutral\ water}$: cumulated volume of neutral water used for the precipitation of the polymer and for its wash

SA: Succinic Anhydride

TA: Triethanol Amine

H. Typical coupling reaction. The protected triblock copolymer is formed by coupling of the diblock copolymer PEG-PLA and an end-capped

homopolymers PBnGlu. Dicyclohexyl carbodiimide (DCC) is used as an activator for coupling the diblock copolymer to the carboxylic group which is at the end of the poly(benzyl glutamate). The poly(benzyl glutamate) (0.638 g, $96 \cdot 10^{-6}$ mol), some N-hydroxysuccinimide (0.0207 g, $96 \cdot 10^{-6}$ mol) and some DCC (0.037 g, $171 \cdot 10^{-6}$ mol) were suspended in 3.1 mL of N-methyl Pyrrolidinone (NMP). The diblock copolymer (0.7006 g, $48 \cdot 10^{-6}$ mol) was dissolved in 10.7 mL of NMP, in another round bottom flask. Then the two liquids were mixed together, and stirred at 55 °C, for two hours. The solution was added in 70 mL of ultrapure water and the polymer precipitated. The solid was filtered over a fritted glass, washed with 100 mL of ultrapure water and then with 100 mL of methanol. It was then dried under vacuum for 12 hours at room temperature. The yield of this reaction was 95%.

Table 16. Formation of protected triblock copolymers

FMC	18	34	46	60
m _{diblock} (g)	0.2732	0.675	0.1121	0.7066
n _{diblock} (mol)	5.11E-05	1.80E-04	1.60E-05	4.82E-05
m _{PBnGlu} (g)	1.1305	2.3963	0.2142	0.6381
n _{PBnGlu} (mol)	1.02E-04	3.59E-04	3.21E-05	9.57E-05
m _{DCC} (g)	0.0525	0.1876	0.017	0.0497
n _{DCC} (mol)	2.55E-04	9.11E-04	8.25E-05	2.41E-04
m _{NHS} (g)	0.022	0.0781	0.0071	0.0207
n _{NHS} (mol)	1.91E-04	6.79E-04	6.17E-05	1.80E-04
V _{NMP} (mL)	9	24	40.05	13.8

FMC: number of the experiment

m: weight

n: number of moles

V: Volume

I. Typical deprotection of the linear triblock copolymers. The linear triblock copolymer was obtained by deprotection of the poly(benzyl glutamate) block. The

triblock copolymer (1.2405 g, $0.058 \cdot 10^{-3}$ mol) was dissolved in 6 mL of trifluoroacetic acid (TFA). Then 3.8 mL of methane sulfonic acid (MSA) and 0.95 mL of anisole¹⁶² were added at 10°C. After 180 minutes, the polymer was precipitated with 54 mL of cold ether, filtered over a fritted glass and washed with ether (2* 50 mL). The solid was then dried under vacuum for 12 hours at room temperature. The yield of this reaction was 78%.

Table 17. Deprotection of protected triblock copolymers

FMC	21	36	47	61
m _{TB} (g)	0.1539	0.999	0.1632	1.2405
n _{TB} (mol)	9.36E-06	9.59E-05	1.20E-05	5.82E-05
V _{MSA} (mL)	1	9.4	0.79	3.85
V _{TFA} (mL)	2	11.5	1	6
V _{anisole} (mL)	0.26	1.6	0.196	0.95
V _{ether} (mL)	16	130	3	54
V _{wash} (mL)	40	100	20	100

FMC: number of the experiment

m: weight

n: number of moles

t: time of reaction

V: Volume

V_{wash}: volume of ether used to wash the polymer

TB: Protected Triblock copolymer

MSA: Methane Sulfonic Acid

TFA: Trifluoroacetic Acid

J. Typical CAC measurement experiment. A solution of pyrene in acetone (0.1674 g/L) was prepared. 2 mL of this solution were added in vials. After evaporation of this solution, 2 mL of suspensions of vesicles with different concentrations were added in each vial and the suspensions were sonicated for 70 minutes. The excitation was done at 339 nm and the emission was measured between 300 and 360 nm.

Table 18. Intensities measured at 332.5 nm and 335 nm for different concentration of PEG-PLA-PGlu in the presence of pyrene (0.1674 g/L)

FMC217x	I333	I335	I335/I333	C (g/L)	log C	[polymer](mg/mL)
FMC217e	836.3878	996.2097	1.191086	1.1930E-01	-0.92336	0.1193
FMC217f	663.942	797.1873	1.200688	6.3200E-02	-1.19928	0.0632
FMC217g	484.1377	579.8109	1.197616	4.5500E-02	-1.34199	0.0455
FMC217h	441.5533	512.2809	1.160179	2.8870E-02	-1.53955	0.02887
FMC217i	341.269	378.8298	1.110062	1.5400E-02	-1.81248	0.0154
FMC217j	325.6174	354.3131	1.088127	1.1500E-02	-1.9393	0.0115
FMC217k	251.3818	256.1551	1.018988	2.4072E-03	-2.61849	0.002407
FMC217l	221.3848	223.0407	1.00748	5.0214E-04	-3.29918	0.000502
FMC217m	236.1921	236.1921	1	1.0229E-04	-3.99017	0.000102
FMC217n	241.6612	240.7575	0.99626	2.1169E-05	-4.6743	2.12E-05

K. Typical insulin encapsulation experiment. A solution of human recombinant insulin in HEPES buffer (Aldrich, pH=8.2, [insulin] = 10mg/mL) was diluted ten times with a phosphate buffer (pH = 7.4, 300 mOsm). The polymer synthesized in the experiment 2.2 was dissolved in this solution (8.2 mg/mL). The pH was adjusted to a value between 7 and 8 using a solution of sodium hydroxide (10 mol/L). The suspension was sonicated for 20 minutes in a sonicating bath at room temperature. After incubation for 3h, the amount of residual insulin in the suspension was then analyzed in a high pressure liquid chromatography (HPLC). The HPLC is calibrated with insulin solutions of different concentration. Thus, the concentration of free insulin is obtained from the area of the insulin peak. The concentration of free insulin in solutions containing vesicles is measured via the area of the insulin peak. The peak of insulin was monitored at 9.6 min, which corresponds to the peak of a non-encapsulated. The amount was obtained from the area under the curve. The proportion of encapsulated insulin, 20%, was

obtained from the mass balance between encapsulated and non-encapsulated insulin.

L. Animal experiments

1) The experiment was done with female Sprague-Dawley rats (weight between 180 and 200g). The rats were delivered with one of their jugular vein cathetered (Charles River company) and were fasted for 12 hours prior the experiment. They were separated into three groups:

Table 19. Treatments given to the three groups of rats

Group	Type of delivery	# Rat
1	Subcutaneous injection	1 to 4
2	Gavage with insulin solution	5 to 8
3	Gavage with insulin encapsulated in polymer	9 to 11

Blood samples (200 microliters) were taken at -30, 0, 30, 60, 90, 150, 210, and 330 min. For each sample, the glucose level was measured with a glucometer (Freestyle, Therasense). The blood was poured in EDTA coated tubes (Microvette 200um, Sarstedt Inc.) and was centrifuged at 3000 rpm during 15 min. The plasma was isolated and analyzed using an insulin ELISA kit (Human Insulin Elisa Kit, #EZHI-14K, Linco Research, Inc.).

For the each rat of group 1, 140 microliters of a solution of human recombinant insulin ([insulin] = 0.107 mg/mL) were injected via the catheter. This solution of human recombinant insulin was obtained from a commercially available solution

of human recombinant insulin ([insulin] = 10 mg/mL, 25mM Hepes, pH=8.2, sterile-filtered) which was diluted 93 times with a HEPES buffer (pH = 8.2, 25 millimolar of HEPES in water). For the rats of the second group, 500 microliters of a solution of human recombinant insulin ([insulin] = 1.54 mg/mL) were fed by oral gavage. This solution of human recombinant insulin was obtained from a commercially available solution of human recombinant insulin ([insulin] = 10 mg/mL, 25mM Hepes, pH=8.2, sterile-filtered) which was diluted 6.5 times with a HEPES buffer (pH = 8.2, 25 millimolar of HEPES in water). Rats of the third group were fed by oral gavage with 500 microliters of a suspension containing insulin and the polymer. This suspension was prepared by mixing the insulin solution used for the rats of group 2 to polymer 2.1 (polymer concentration = 15 g/L). The suspension was sonicated for 10 minutes in a Branson 2210 ultrasonic cleaner at room temperature prior to gavage.

2) The experiment was done with female Sprague-Dawley rats (weight between 180 and 200g). The rats were delivered with one of their jugular vein cathetered (Charles River company) and were fasted for 12 hours prior the experiment. They were separated into four groups:

Table 20. Treatments given to the three groups of rats

Group	Type of delivery	# Rat
1	Subcutaneous injection	1 to 4
2	Gavage with insulin solution	5 to 8
3	Gavage with insulin encapsulated in polymer	9 to 12
4	Gavage with insulin encapsulated in polymer under a solid form (Eudragit)	13 to 16

Blood samples (150 microliters) were taken at -60, 0, 40, 70, 135, 200, 265, 325 and 385 min. For each sample, the glucose level was measured with a glucometer (Freestyle, Therasense). The blood was poured in EDTA coated tubes (Microvette 200um, Sarstedt Inc.) and was centrifuged at 3000 rpm during 15 min. The plasma was isolated and analyzed using an insulin ELISA kit (Human Insulin Elisa Kit, #EZHI-14K, Linco Research, Inc.).

For the each rat of group 1, 100 microliters of a solution of human recombinant insulin ([insulin] = 0.015 mg/mL) were injected via the catheter. This solution of human recombinant insulin was obtained from a commercially available solution of human recombinant insulin ([insulin] = 10 mg/mL, 25mM HEPES, pH=8.2, sterile-filtered) which was diluted 668 times with a HEPES buffer (pH = 8.2, 25 millimolar of HEPES in water). For the rats of the second group, 500 microliters of a solution of human recombinant insulin ([insulin] = 0.292 mg/mL) were fed by oral gavage. This solution of human recombinant insulin was obtained from a commercially available solution of human recombinant insulin ([insulin] = 10 mg/mL, 25mM HEPES, pH=8.2, sterile-filtered) which was diluted 35 times with a HEPES buffer (pH = 8.2, 25 millimolar of HEPES in water). Rats of the third group were fed by oral gavage with 500 microliters of a suspension containing insulin and the polymer. This suspension was prepared by mixing the insulin solution used for the rats of group 2 to the triblock copolymer (polymer concentration = 15 g/L). The suspension was sonicated for 10 minutes in a Branson 2210 ultrasonic cleaner at room temperature prior to gavage. For the

rats of the fourth group, a solid form of the nanovesicles containing some insulin was fed by oral gavage. A solution of human recombinant insulin was obtained from a commercially available solution of human recombinant insulin ([insulin] = 10 mg/mL, 25mM Hepes, pH=8.2, sterile-filtered) which was diluted 3.4 times with a HEPES buffer (pH = 8.2, 25 millimolar of HEPES in water). Some Eudragit L100 (643 mg) was dissolved in a solution of Ethanol (2.15 mL)/Acetone (4.3 mL) and the suspension of vesicles previously made was poured in it under stirring. Some span 40 (0.904 g) and Antifoam A (91.7 mg) were added. Then the suspension was poured in 90.51 g of liquid paraffin. The homogenizer was used three times during 20 seconds, leaving one minute between each use of the homogenizer, and the system was heated at 40°C under magnetic stirring. After three hours, the paraffin was dissolved in 300 mL of hexane. The “capsules” were filtered over a buchner funnel, washed with hexane (2*100 mL) and then dried under vacuum for 12 hours at room temperature.

LIST OF REFERENCES

1. Type-2 Diabetes – the Expected Adaptation to Overnutrition. *The McDougall Newsletter* **2004**, 3, (2).
2. Rocchiccioli, J. T.; O'Donoghue, C. R., Diabetes Mellitus: Toward a Federal Policy. *Policy, Politics and Nursing Practice* **2004**, 5, (4), 237-242.
3. www.doctissimo.fr.
4. Kochanek, K.D.; Smith, B.L., Deaths: Preliminary Data for 2002. *National Vital Statistics Reports* **2004**, 52, (13).
5. The Challenge of Poorly Controlled Diabetes Mellitus. *Diabetes Metab* **2003**, 29, 101-109.
6. www.pfizerhealthsolutions.com.
7. Weir, G. C.; Bonner-Weir, S., Islets of Langerhans: the puzzle of intraislet interactions and their relevance to diabetes. *J. Clin. Invest.* **1990**, 85, (4), 983-987.
8. static.howstuffworks.com.
9. Florence, J. A.; Yeager, B. F., Treatment of Type 2 Diabetes Mellitus. *American Family Physician* **1999**, 59, (10).
10. Reasner, C. A., Treatment of Type 2 Diabetes Mellitus: A Rational Approach Based on Its Pathophysiology. *American Family Physician* **2001**, (May 1, 2001).
11. Wright, J. R., Almost Famous: E. Clark Noble, the Common Thread in the Discovery of Insulin and Vinblastine. *CMAJ* **2002**, 167, (12), 1391-1396.
12. Ortiz, C.; Zhang, D.; Xie, Y.; Davisson, V. J.; Ben-Amotz, D., Identification of insulin variants using Raman spectroscopy. *Anal. Biochem.* **2004**, 332, 245-252.
13. Strachan, T.; Read, A. P., *Human Molecular Genetics 2*. Bios scientific: 1999;
14. Smith, G. D.; Swenson, D. C.; Dodson, E. J.; Dodson, G. G.; Reynolds, C. D., Structural Stability in the 4-zinc Human Insulin Hexamer. *Biophys.* **1984**, 81, 7093-7097.
15. Uversky, V. N.; Garriques, L. N.; Millett, I. S.; Frokjaer, S.; Brange, J.; Doniach, S.; Fink, A. L., Prediction of the Associate State of Insulin Using Spectral Parameters. *J. Pharm. Sci.* **2002**, 92, (4), 847-858.
16. Xu, B.; Hu, S.; Chu, Y.; Wang, S.; Wang, R.; Nakagawa, S. H.; Katsoyannis, P. G.; Weiss, M. A., Diabetes-Associated Mutations in Insulin Identify In variant Receptor Contacts. *Diabetes* **2004**, 53, 1599-1602.

17. Meyts, P. D., Insulin and its Receptor: Structure, Function and Evolution. *BioEssays* **2004**, 26, 1351–1362.
18. www.ianblumer.com/new%20technologies.htm.
19. Waitz, G., Insulin: An In-Depth Look. Part 2. *Iron Magazine Online L.L.C.* **2000**, september 2000.
20. Tarr, B. D.; Campbell, R. K.; Workman, T. M., Stability and Sterility of Biosynthetic Human Insulin Stored in Plastic Insulin Syringes for 28 Days. *American Journal of Hospital Pharmacy* **1991**, 48, (12), 2631-2634.
21. Nielsen, L.; S. Frokjaer; J. Carpenter; Brange, J., Studies of the Structure of Insulin Fibrils by Fourier Transform Infrared (FTIR) Spectroscopy and Electron Microscopy. *J. Pharm. Sci.* **2001**, 90, (1), 29-37.
22. *Physician Desk Reference*. Thomson PDR: 2004;
23. Marcel Dekker, I., *Treatise on controlled drug delivery*. Princeton, 1991;
24. Garcia-Contreras, L.; Morçöl, T.; Bell, S. J. D.; Hickey, A. J., Evaluation of Novel Particles as Pulmonary Delivery Systems for Insulin in Rats. *AAPS PharmaSci* **2003**, 5, (2), Article 9.
25. Corkery, K., Inhalable Drugs for Systemic Therapy. *Respiratory Care* **2000**, 45, (7), 831-835.
26. Crockford, D. R., Adaptive Aerosol Delivery (AAD™) Technology: Approaching Drug Delivery From the Patient's Perspective. *Drug Delivery Technology* **2002**, 2, (2).
27. Bogner, R. H.; Wilkosz, M. F., Transdermal Drug Delivery. *US Pharmacist* **2003**, 28, (5).
28. www.bentleypharm.com.
29. Tang, P. Compounds and Compositions for Delivering Active Agents. WO 0216309, 2002.
30. Bermudez, H.; Brannan, A. K.; Hammer, D. A.; Bates, F. S.; Discher, D. E., Molecular weight dependence of Polymersome Membrane Structure, Elasticity and Stability. *Macromolecules* **2002**, 35, 8203-8208.
31. Damgé, C.; Vranckx, H.; Balschmidt, P.; Couvreur, P., Poly(alkyl cyanoacrylate) Nanospheres for Oral Administration of Insulin. *J. Pharm. Sci.* **1997**, 86, (12), 1403-1409.

32. Zhang, Q.; Dunbar, D.; Ostrowska, A.; Zeisloft, S.; Yang, J.; Kaminsky, L., Characterization of Human Small Intestinal Cytochromes P-450. *Drug Metabolism and Disposition* **1999**, 27, (7), 804-809.
33. Arnold, F. H.; Cirino, P. C. Thermostable peroxide-driven cytochrome P450 oxygenase variants and methods of use. US20050037411, February 17, 2005, 2005.
34. Lewis, D. F. V., Human Cytochromes P450 Associated with the Phase I Metabolism of Drugs and other Xenobiotics: A Compilation of Substrates and Inhibitors of the CYP1, CYP2 and CYP3 Families. *Current Medicinal Chemistry* **2003**, 10, 1955-1972.
35. medicine.iupui.edu/flockhart/table.htm.
36. www.preadme.bmdrc.org/preadme/help/absorption/images/intestinal.gif.
37. Madara, J. L., Loosening Tight Junction. *J. Clin. Invest.* **1989**, 83, 1089-1094.
38. A. Sood, R. P., Peroral Route: An Opportunity for Protein and Peptide Drug Delivery. *Chem. Rev.* **2001**, 101, 3275-3303.
39. Bernkop-Schnurch, A.; Clausen, A. E.; Guggi, D., The Use of Auxiliari Agents to Improve the Mucosal Uptake of Peptides. *Medicinal Chemistry Reviews* **2004**, 1, 1-10.
40. Kooshapur, H.; Chaideh, M., Intestinal Transport of Human Insulin in Rat. *Medical Journal of IAS* **1999**, 12, (1).
41. Vermehren, C.; Johansen, P.; Hansen, H., Absorption and Metabolism of the Absorption Enhancer Didecanoylphosphatidylcholine in Rabbit Nasal Epithelium *In Vivo*. *Drug Metabolism and Disposition* **1997**, 25, (9), 1083-1088.
42. Russell-Jones, G. J.; Westwood, S. W.; Habberfields, A. D., Vitamin B12 Mediated Oral Delivery Systems for Granulocyte-Colony Stimulating Factor and Erythropoietin. *Bioconjugate Chem.* **1995**, 6, (4), 459-465.
43. Russell-Jones, G. J.; Westwood, S. W.; Farnworth, P. G.; Findlay, J. K.; Burger, H. G., Synthesis of LHRH Antagonists Suitable for Oral Administration via the Vitamin B12 Uptake System. *Bioconjugate Chem.* **1995**, 6, (1), 34-42.
44. Bré, M.; Redeker, V.; Quibell, M.; Darmanaden-Delorme, J.; Bressac, C.; Cosson, J.; Huitorel, P.; Schmitter, J.; Rossier, J.; Johnson, T.; Adoutte, A.; Levilliers, N., Axonemal tubulin polyglycylation probed with two monoclonal antibodies: widespread evolutionary distribution, appearance during spermatozoan maturation and possible function in motility. *Journal of Cell Science* **1996**, 109, 727-738.
45. Lee, Y.; Perry, B. A.; Sutyak, J. P.; Stern, W.; Sinko, P. J., Regional Differences in Intestinal Spreading and pH Recovery and the Impact on Salmon Calcitonin Absorption in Dogs. *Pharm. Res.* **2000**, 17, (3), 284-290.

46. Madsen, F.; Peppas, N. A., Complexation graft copolymer networks: Swelling properties, calcium binding and proteolytic inhibition. *Biomaterials* **1999**, 20, 1701-1708.
47. Sleiman, O.; Murin, J.; Ghanem, W., Angiotensin-Converting Enzyme Inhibitors: Do We Utilize Our Knowledge in Heart Failure Patients? *J Clin Basic Cardiol* **2001**, 4, 279-283.
48. Cadman, J., Debate Widens Over Protease Inhibitor Side Effects. *Treatment Issues* **1998**, 12, (7/8).
49. Vandenberg, G. W.; Désormeaux, A.; V. Dallaire; Munger, G.; Chabot, B.; Trépanier, D. *Oralject™: A Novel System for Oral Furunculosis Vaccine Delivery to Salmonids*; www.perosbio.com/sites/1649/Vaccine%20Poster.pdf.
50. Karlsson, N. G.; Johansson, M. E.; Asker, N.; Karlsson, H.; Gender, S. J.; Carlstedt, I.; Hansson, G. C., Molecular characterization of the large heavily glycosylated domain glycopeptide from the rat small intestinal Muc2 mucin. *Glycoconj. J.* **1996**, 13, 823-831.
51. Gu, J.; Robinson, J. R.; Leung, S. S., Binding of acrylic polymers to Mucin/Epithelial surfaces: structure-property relationships. *Crit. Rev. Ther. Drug carrier Syst.* **1988**, 5, (1), 21-67.
52. Ascentiis, A. D.; deGrazia, J. L.; Bowman, C. N.; P.Colombo; Peppas, N. A., Mucoadhesion of poly(2-hydroxyethyl methacrylate) is improved when linear poly(ethylene oxide) chains are added to the polymer network. *J. Con. Rel.* **1995**, 33, 197-201.
53. Peppas, N. A.; Huang, Y., Nanoscale technology of mucoadhesive interactions. *Adv. Drug Deliv. Rev.* **2004**, 56, 1675-1687.
54. Jiang, W. W. J.; Ballard, C. E.; Wang, B., Prodrug Approaches to the improved Delivery of Peptide Drugs. *Cur. Pharmaceut. Des.* **1999**, 5, 265-287.
55. Shibata, H.; Nakagawa, S.; Tsutsumi, Y., Optimization of Protein Therapies by Polymer-Conjugation as an Effective DDS. *Molecules* **2005**, 10, 162-180.
56. Kozlowski, A.; Charles, S. A.; Harris, J. M., Development of Pegylated Interferons for the Treatment of Chronic Hepatitis C. *BioDrugs* **2001**, 15, (7), 419-429.
57. Kozlowski, A.; Harris, J. M., Improvements in protein PEGylation: pegylated interferons for treatment of hepatitis C. *J. Con. Rel.* **2001**, 72, 217-224.
58. Harris, J. M.; Chess, R. B., Effect of Pegylation on Pharmaceuticals. *Nat. Rev. Drug Discov.* **2003**, 2, 214-221.
59. pharmalicensing.com/company/disprelease/1087505455_40d2042fec5b.

60. Clement, S.; Still, J. G.; Kosutic, G.; McAllister, R. G., Oral Insulin Product Hexyl-Insulin Monoconjugate 2 (HIM2) in Type 1 Diabetes Mellitus: The Glucose Stabilization Effects of HIM2. *Diabetes Technology & Therapeutics* **2002**, 4, (4), 459-466.
61. Florence, A. T., The Oral Absorption of Micro- and Nanoparticulates: Neither Exceptional Nor Unusual. *Pharm. Res.* **1997**, 14, (3), 259-266.
62. Hillyer, J.; Albrecht, R., Gastrointestinal Persorption and Tissue Distribution of Differently Sized Colloidal Gold Nanoparticles. *J. Pharm. Pharmaceut. Sci.* **2001**, 90, (12), 1927-1936.
63. Eldridge, J. H.; Hammond, C. J.; Meulbroek, J. A.; Staas, J. K.; Gilley, R. M.; Tice, T. R., Controlled Vaccine Release in the Gut-associated lymphoid tissues. Orally Administered Biodegradable Microsphere target the Peyer's Patches. *J. Con. Rel.* **1990**, 11, 205-214.
64. Desai, M.; Labhasetwar, V.; Amidon, G.; Levy, R., Gastrointestinal Uptake of Biodegradable Microparticles: Effect of Particles Size. *Pharm. Res.* **1996**, 13, (12), 1838-1845.
65. Clark, D. E., Prediction of Intestinal Absorption and Blood-Brain Barrier Penetration by Computational Methods. *Combinatorial Chemistry & High Throughput Screening* **2001**, 4, 477-496.
66. Lian, T.; Ho, R. J. Y., Trends and Developments in Liposome Drug Delivery Systems. *J. Pharmaceut. Sci.* **2001**, 90, (6), 667-680.
67. Mainardes, R. M.; Urban, M. C. C.; Cinto, P. O.; Khalil, N. M.; Chaud, M. V.; Evangelista, R. C.; Gremião, M. P. D., Colloidal Carriers for Ophthalmic Drug Delivery. *Current Drug Targets* **2005**, 6, 363-371.
68. Basu, M. K.; Lala, S., Macrophage Specific Drug Delivery in Experimental Leishmaniasis. *Current Molecular Medicine* **2004**, 4, 681-689.
69. www.answers.com.
70. Blazek-Welsh, A. I.; Rhodes, D. G., Maltodextrin-Based Proniosomes. *AAPS Pharmsci* **2001**, 3, (1), 1-8.
71. Chourasia, M. K.; Jain, S. K.; Gour, H. S., Pharmaceutical Approaches to Colon Targeted Drug Delivery Systems. *J. Pharm. Pharmaceut. Sci.* **2003**, 6, (1), 33-66.
72. Andrade, J. D.; V. Hlady, A. P. W., Adsorption of complex proteins at interfaces. *Pure Appl. Chem.* **1992**, 64, (11), 1777-1781.
73. Trapani, G.; Franco, M.; Trapani, A.; Lopodota, A.; Latrofa, A.; Gallucci, E.; Micelli, S.; Liso, G., Frog Intestinal Sac: A New In vitro Method for the Assessment of Intestinal Permeability. *J. Pharm. Sci.* **2004**, 93, (12), 2909-2919.

74. users.rcn.com/jkimball.ma.ultranet/BiologyPages/G/GITract.html.
75. arbl.cvmbms.colostate.edu.
76. Neutra, M. R.; Padykula, H. A., *Histology, Cell and Tissue Biology*. Elsevier Biomedical: New York, 1983;
77. Alberts, B.; Johnson, A.; Lewis, J.; Raff, M.; Roberts, K.; Walter., P., *Molecular Biology of the cell*. Garland Publishing: New York, 2002;
78. www.kalergroup.che.udel.edu/Research/vesicles.htm.
79. Grumelard, J.; Taubert, A.; Meier, W., Soft nanotubes from amphiphilic ABA triblock macromonomers. *Chem. Comm.* **2004**, (13), 1462-1463.
80. www.chem.ucalgary.ca/courses/351/Carey5th/Ch26/ch26-1-2.html.
81. Dhara, D.; Shah, D. O., Stability of Sodium Dodecyl Sulfate Micelles in the Presence of a Range of Water-Soluble Polymers: A Pressure-Jump Study. *J. Phys. Chem. B* **2001**, 105, 7133-7138.
82. Henry, M. C.; Hsueh, C.; Timko, B. P.; M. S. Freunda, Reaction of Pyrrole and Chlorauric Acid A New Route to Composite Colloids. *J. Electrochem. Soc.* **2001**, 148, (11), D155-D162.
83. Grotha, C.; Nydéna, M.; Holmberga, K.; Kanickyb, J. R.; Shahc, D. O., Kinetics of the Self-Assembly of Gemini Surfactants. *J. Surfactants Deterg.* **2004**, 7, (3), 247-255.
84. Hamley, I. W., Nanoshells and nanotubes from block copolymers. *Soft Matter* **2005**, 1, 36-43.
85. Photos, P.; Bacakova, L.; Discher, B.; Bates, F.; Discher, D., Polymer vesicles in vivo: correlations with PEG molecular weight. *J. Con. Rel.* **2003**, 90, 323-334.
86. Patty, P.; Frisken, B., The Pressure-Dependence of the Size of Extruded Vesicles. *Biophys.* **2003**, 85, 996-1004.
87. Nakhla, T.; Marek, M.; Kovalcik, T., Issues Associated with Large-Scale Production of Liposomal Formulations. *Drug Delivery Technology* **2002**, 2, (4).
88. Bovill, J. G. In *Recent Advances in Slow Release Drug Formulations*, EUROANESTHESIA 2005, Vienna, Austria, 2005; Vienna, Austria, 2005.
89. Torquato, S.; Hyun, S.; Donev, A., Multifunctional Composites: Optimizing Microstructures for Simultaneous Transport of Heat and Electricity. *Phys. Rev. Lett.* **2002**, 89, (26), 266601-1,266601-4.

90. Schwarz, U.; Gompper, G., Bicontinuous Surfaces in Self-assembling Amphiphilic Systems. In *LMP 600*, ed.; Mecke, K. R.; Stoyan, D., Springer-Verlag: Berlin Heidelberg, 2002; p 107-151.
91. Nakanishi, T.; Fukushima, S.; Okamoto, K.; Suzuki, M.; Matsumura, Y.; Yokoyama, M.; Okano, T.; Sakurai, Y.; Kataoka, K., Development of the polymer micelle carrier system for doxorubicin. *J. Con. Rel.* **2001**, 74, 295-302.
92. Nishiyama, N.; Okazaki, S.; Cabral, H.; Miyamoto, M.; Kato, Y.; Sugiyama, Y.; Nishio, K.; Matsumura, Y.; Kataoka, K., Novel Cisplatin-Incorporated Polymeric Micelles Can Eradicate Solid Tumors in Mice. *Cancer Research* **2003**, 63, 8977-8983.
93. Matsumura, Y.; Hamaguchi, T.; T. Ura, K. M.; Yamada, Y.; Shimada, Y.; Shirao, K.; Okusaka, T.; Ueno, H.; Ikeda, M.; Watanabe, N., Phase I clinical trial and pharmacokinetic evaluation of NK911, a micelle-encapsulated doxorubicin. *British Journal Cancer* **2004**, 91, 1775-1781.
94. Garrec, D. L.; Ranger, M.; Leroux, J., Micelles in Anticancer Drug Delivery. *Am J Drug Deliv* **2004**, 2, (1), 15-42.
95. Duncan, R., The Dawning Era of Polymer Therapeutics. *Nature Reviews* **2003**, 2, 347-360.
96. Scott, J. C. In *Spheres*, UCLA NanoSystems Seminar Series, Los Angeles, California, 2003; CNSI Young Investigators Society: Los Angeles, California, 2003; p[^]pp.
97. Thurmond-2nd, K.; Remsen, E.; Kowalewski, T.; Wooley, K., Packaging of DNA by shell crosslinked nanoparticles. *Nucleic Acids Research* **1999**, 27, (14), 2966-2971.
98. Aggerbeck, L.; Yates, M.; Tardieu, A.; Luzzati, V., Density-Contrast Studies of Macromolecules in Solution. Cross Verification of X-ray Scattering and Pycnometry Experiments. *J. Appl. Cryst.* **1978**, 11, 466-472.
99. P. Widlak, DNA microarrays, a novel approach in studies of chromatin structure. *Acta Biochimica Polonica* **2004**, 51, (1), 1-8.
100. Wooley, K., Shell Crosslinked Polymer Assemblies: Nanoscale Constructs Inspired from Biological Systems. *J. Polym. Sci. A* **2000**, 38, 1397-1407.
101. Ahmed, F.; Hategan, A.; Discher, D. E.; Discher, B. M., Block Copolymer Assemblies with Cross-Link Stabilization: From Single-Component Monolayers to Bilayer Blends with PEO-PLA. *Langmuir* **2003**, 19, 6506-6511.
102. Porjazoska, A.; Dimitrov, P.; Dimitrov, I.; Cvetkovska, M.; Tsvetanov, C. B., Synthesis and aqueous solution properties of functionalized and thermoresponsive poly(D,L-lactide)/polyether block copolymers. *Macromol. Symposia* **2004**, 210, (Reactive Polymers 2003), 427-436.

103. Discher, B. M.; Won, Y.-Y.; Ege, D. S.; Lee, J. C.-M.; Bates, F. S.; Discher, D. E.; Hammer, D. A., Polymersomes: Tough vesicles made from diblock copolymers. *Science* **1999**, 284, (5417), 1143-1146.
104. Discher, D. E.; Eisenberg, A., Polymer Vesicles. *Science* **2002**, 297, 967-973.
105. Wang, X.; Shen, Y.; Pan, Y.; Liang, Y., Spontaneous Formation of Vesicles and Monolayer Membranes in Organic Solvents by Long-Chained Bisschiff Base or Its Organometallic complexes. *Langmuir* **2000**, 16, 7538-7540.
106. Jeong, B.; Bae, Y. H.; Lee, D. S.; Kim, S. W., Biodegradable block copolymers as injectable drug-delivery systems. *Nature* **1997**, 388, 860-862.
107. Dai, Z.; Piao, L.; Zhang, X.; Deng, M.; Chen, X.; Jing, X., Probing the Micellization of Diblock and Triblock Copolymers of Poly(L-lactide) and Poly(ethylene glycol) in Aqueous and NaCl Salt Solutions. *Coll. Pol. Sci.* **2004**, 282, (4), 343-350.
108. Jule, E.; Y.Nagasaki; Kataoka, K., Lactose-Installed Poly(ethylene glycol)-Poly(D,L-lactide) Block copolymer Micelles Exhibit Fast-Rate Binding and high affinity toward a protein bed simulating a cell surface. A surface Plasmon resonance study. *Bioconjugate Chem.* **2003**, 14, 177-186.
109. Kipkemboi, P.; Khan, A.; Lindman, B.; Alfredsson, V., Phase behavior and structure of amphiphilic poly(ethylene oxide)-poly(propylene oxide) triblock copolymers ((EO)₄(PO)₅₉(EO)₄ and (EO)₁₇(PO)₅₉(EO)₁₇) in ternary mixtures with water and xylene. *Canadian J. Chem.* **2003**, 81, (8), 897-908.
110. Li, J.; Ni, X.; Li, X.; Zhou, Z.; Leong, K. W., New biodegradable amphiphilic triblock copolymers consisting of poly[(R)-3-hydroxybutyrate] and poly(ethylene oxide) and their association behavior in aqueous solution. *Polymer Preprints (American Chemical Society, Division of Polymer Chemistry)* **2003**, 44, (2), 707-708.
111. Meier, W.; Nardin, C.; Winterhalter, M., Reconstitution of channel proteins in (polymerized) ABA triblock copolymer membranes. *Angew. Chem., Int. Ed.* **2000**, 39, (24), 4599-4602.
112. Fujiwara, T.; Miyamoto, M.; Kimura, Y., Self-organisation of diblock and triblock copolymers of Poly(L-lactide) and Poly(oxethylene) into nanostructured bands and their network system. Proposition of a doubly twisted chain conformation of Poly(L-lactide). *Macromolecules* **2001**, 34, 4043-4050.
113. Bryskhe, K.; Jansson, J.; Topgaard, D.; Schillen, K.; Olsson, U., Spontaneous Vesicle Formation in a Block Copolymer System. *J. Phys. Chem. B* **2004**, 108, (28), 9710-9719.
114. Nardin, C.; Meier, W., Hybrid materials from Amphiphilic Block Copolymers and Membrane Proteins. *Rev. Mol. Biotech.* **2002**, 90, (1), 17-26.

115. Zhang, J.; Yu, Y.; Wan, X.; Chen, X.; Zhou, Q., A novel optically active rod-coil-rod triblock copolymer forms vesicles in dioxane/water. *Polymer Preprints (American Chemical Society, Division of Polymer Chemistry)* **2004**, 45, (2), 640-641.
116. Nardin, C.; Hirt, T.; Leukel, J.; Meier, W., Polymerized ABA triblock copolymer vesicles. *Langmuir* **2000**, 16, 1035.
117. Nardin, C.; Thoeni, S.; Widmer, J.; Winterhalter, M.; Meier, W., Nanoreactors based on Polymerized ABA-triblock copolymer vesicles. *Chem. Comm.* **2000**, 1433.
118. Sauer, M.; Haeefele, T.; Graff, A.; Nardin, C.; Meier, W., Ion-carrier controlled precipitation of calcium phosphate in giant ABA triblock copolymer vesicles. *Chem. Comm.* **2001**, 2452-2453.
119. Schillen, K.; Bryskhe, K.; Mel'nikova, S., Vesicles Formed from a Poly(ethylene oxide)-Poly(propylene oxide)-Poly(ethylene oxide) Triblock Copolymer in Dilute Aqueous Solution. *Macromolecules* **1999**, 32, (20), 6885-6888.
120. Stoenescu, R.; Meier, W., Vesicles with asymmetric membranes from amphiphilic ABC triblock copolymers. *Chem. Comm.* **2002**, 24, 3016-3017.
121. Graff, A.; Sauer, M.; Van Gelder, P.; Meier, W., Virus-assisted loading of polymer nanocontainer. *Proc. Acad. Sci.* **2002**, 99, (8), 5064-5068.
122. Harris, J. K.; Rose, G. D.; Bruening, M. L., Spontaneous Generation of Multilamellar vesicles from Ethylene oxide/Butylene oxide diblock copolymers. *Langmuir* **2002**, 18, 5337-5342.
123. Yu, K.; Bartels, C.; Eisenberg, A., Vesicles with Hollow Rods in the Walls: A Trapped Intermediate Morphology in the Transition of Vesicles to Inverted Hexagonally Packed Rods in Dilute Solutions of PS-b-PEO. *Macromolecules* **1998**, 31, (26), 9399-9402.
124. Won, Y.-Y.; Brannan, A. K.; Davis, H. T.; Bates, F. S., Cryogenic Transmission Electron Microscopy (cryo-TEM) of Micelles and Vesicles formed in Water by Poly(ethylene oxide)-Based Block Copolymers. *J. Phys. Chem. B* **2002**, 106, 3354-3364.
125. Vriezema, D. M.; Hoogboom, J.; Velonia, K.; Takazawa, K.; Christianen, P. C. M.; Maan, J. C.; Rowan, A. E.; Nolte, R. J. M., Vesicles and polymerized vesicles from thiophene-containing rod-coil block copolymers. *Angew. Chem., Int. Ed.* **2003**, 42, (7), 772-776.
126. Terreau, O.; Luo, L.; Eisenberg, A., Effect of Poly(acrylic acid) block length distribution on Polystyrene-b-Poly(acrylic acid) Aggregates in Solution. 1. Vesicles. *Langmuir* **2003**, 19, 5601-5607.

127. Santore, M. M.; Disher, D. E.; Won, Y.; Bates, F. S.; Hammer, D. A., Effect of Surfactant on Unilamellar Polymeric vesicles: Altered Membranes Properties and Stability in the limit of weak surfactant Partition. *Langmuir* **2002**, 18, 7299-7308.
128. Photos, P. J.; Bacakova, L.; Disher, B.; Bates, F. S.; Disher, D. E., Polymer vesicles in vivo: correlation with PEG molecular weight. *J. Con. Rel.* **2003**, 90, 323-334.
129. Shen, H.; Eisenberg, A., Morphological Phase Diagram for a Ternary System of Block Copolymer PS₃₁₀-b-PAA₅₂/Dioxane/H₂O. *J. Phys. Chem. B* **1999**, 103, 9473-9487.
130. Morris, W., *The american heritage dictionary of the english language*. Houghton Mifflin Compagny: 1982;
131. Lim, A. L., Biocompatibility of Stent Materials. *MURJ* **2004**, 11, 33-37.
132. Bero, M.; Kasperczyk, J.; J.Jedlinski, Z., Coordination polymerization of lactides, 1 structure determination of obtained polymers. *Makromol. Chem* **1990**, 191, 2287-2296.
133. Chabot, F.; Vert, M.; Chapelle, S.; Granger, P., Configurational structures of lactic acid stereocopolymers as determined by ¹³C-¹H NMR. *Polymer* **1983**, 24, 53-59.
134. Jonga, S. J. d.; Ariasa, E. R.; Rijkersb, D. T. S.; C.F. van Nostruma; Boschc, J. J. K.-v. d.; Hennink, W. E., New insights into the hydrolytic degradation of poly(lactic acid): participation of the alcohol terminus. *Polymer* **2001**, 42, 2795-2802.
135. Gill, T. J.; Doty, P., *Biochim. Biophys. Acta* **1962**, 60, 450.
136. Shalaby, S. W., *Biomedical Polymers designed-to-degrade systems*. Hanser Verlag: New York, 1994;
137. Mehvar, R., Modulation of the pharmacokinetics and pharmacodynamics of proteins by polyethylene glycol conjugation. *J. Pharm. Pharmaceut. Sci.* **2000**, 3, (1), 125-136.
138. Caillol, S.; Lecommandoux, S.; Mingotaud, A.; Schappacher, M.; Soum, A.; Bryson, N.; Meyrueix, R., Synthesis and Self-Assembly Properties of Peptide-Polylactide Block. *Macromolecules* **2003**, 36, 1118-1124.
139. Stridsberg, K. M.; Ryner, M.; Albertsson, A. C., Controlled Ring-Opening Polymerization: Polymers with designed Macromolecular Architecture. *Ad. in Pol. Sci.* **2002**, 157, 41-65.
140. Piao, L.; Z. Dai, M. D.; Chen, X.; Jing, X., Synthesis and characterization of PCL/PEG/PCL triblock copolymers by using calcium catalyst. *Polymer* **2003**, 44, 2025-2031.
141. Hamley, I. W.; Castelletto, V.; Castillo, R. V.; Müller, A. J.; Martin, C. M.; Pollet, E.; Dubois, P., Crystallization in Poly(L-lactide)-b-poly(-caprolactone) Double

Crystalline Diblock Copolymers: A Study Using X-ray Scattering, Differential Scanning Calorimetry, and Polarized Optical Microscopy. *Macromol.* **2005**, 38, (2), 463-472.

142. Stridsberg, K. M.; Ryner, M.; Albertsson, A. C., Controlled Ring-Opening Polymerization: Polymers with designed Macromolecular Architecture. *Advances in Polymer Science* **2002**, 157, 41-65.

143. Wang, C.-H.; Hsiue, G.-H., New amphiphilic poly(2-ethyl-2-oxazoline)/ poly(L-lactide) triblock copolymers. *Biomacromol.* **2003**, 4, (6), 1487-1490.

144. Williams, C. K.; Breyfogle, L. E.; Choi, S. Y.; Nam, W.; Young, V. G.; Hillmyer, M. A.; Tolman, W. B., A Highly Active Zinc Catalyst for the Controlled Polymerization of Lactide. *J. Am. Chem. Soc.* **2003**, 125, 11350-11359.

145. Kasperczyk, J. E., HETCOR NMR study of poly(rac-lactide) and poly(meso-lactide). *Polymer* **1999**, 40, 5455-5458.

146. Zell, M. T.; Padden, B. E.; Paterick, A. J.; Thakur, K. A. M.; Kean, R. T.; Hillmyer, M. A.; Munson, E. J., Unambiguous determination of the ¹³C and ¹H NMR Stereosequence Assignment of Polylactide using High-Resolution Solution NMR Spectroscopy. *Macromolecules* **2002**, 35, (20), 7700-7707.

147. Chamberlain, B. M.; Cheng, M.; Moore, D. R.; Ovitt, T. M.; Lobkovsky, E. B.; Coates, G. W., Polymerization of Lactide with Zinc and Magnesium beta-Diiminato Complexes: Stereocontrol and Mechanism. *J. Am. Chem. Soc.* **2001**, 123, 3229-3238.

148. Kricheldorf, H. R., *alpha-Aminoacid-N-CarboxyAnhydrides and related heterocycles*. Springer-Verlag: Berlin, 1987;

149. Cornille, F.; Lebon, M. Process for the preparation of N-carboxyanhydrides. US 2002/0183551 A1, Dec. 5, 2002, 2002.

150. Deming, T. J.; Yu, M.; Curtin, S. A.; Hwang, J.; Wyrsta, M. D.; Nowak, A.; Seidel, S. W. Methods and compositions for controlled polypeptides synthesis. US 2002/0032309, 03/14/2002, 2002.

151. Kricheldorf, H. R.; Uryu, T.; Borgne, A. L.; Spassky, N.; Penczek, S.; Klosinski, P., *Models of biopolymers by ring-opening polymerization*. 1990;

152. Deming, T. J., Methodologies for preparation of synthetic block copolypeptides: materials with future promise in drug delivery. *Adv. Drug Delivery Rev.* **2002**, 54, 1145.

153. Bodanszky, M.; Bodanszky, A., *The practice of peptide synthesis*. Springer-Verlag: Berlin, 1994;

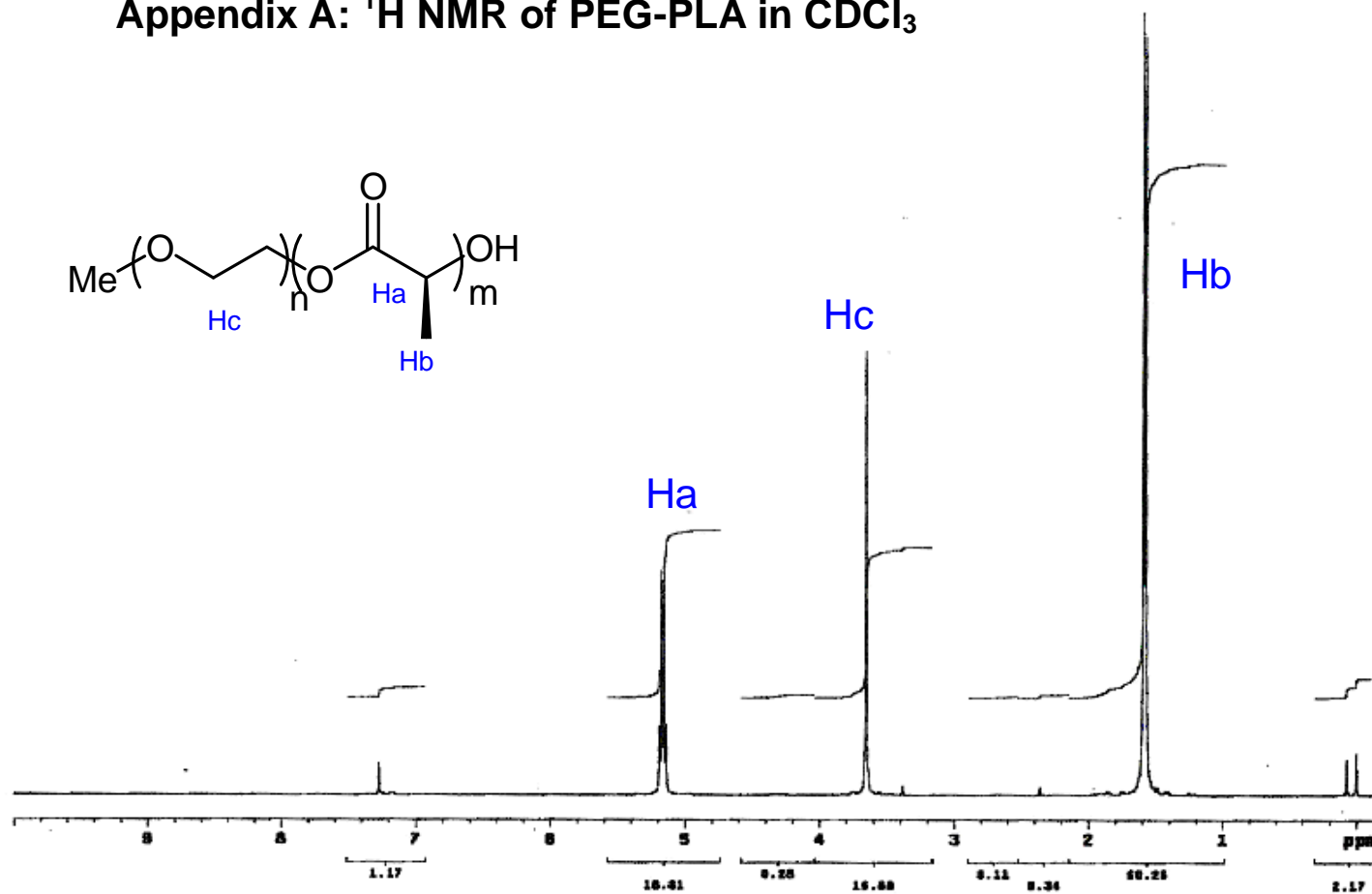
154. Jones, J., *Amino Acid and Peptide Synthesis*. Oxford University Press Inc.: Oxford, 2002;

155. DeVries, S., K. Preparation of polylactic acid and copolymers of lactic acids. 4797468, 1989.
156. Dutkiewicz, S.; D. Grochowska-Lapienis; Tomaszewski, W., Synthesis of Poly(L(+) Lactic Acid) by Polycondensation Method in Solution. *FIBRES & TEXTILES in Eastern Europe* **2003**, 11, (4), 66-70.
157. Zhangide, L.; Shen, Z.; Yu, C.; Fan, L., Ring-opening polymerization of D,L-lactide by rare earth 2,6-dimethylarylox. *Polym. Int.* **2004**, 53, 1013-1016.
158. O'Keefe, B. J.; Hillmyer, M. A.; Tolman, W. B., Polymerization of Lactide and Related Cyclic Esters by Discrete Metal Complexes. *J. Chem. Soc., Dalton Trans.* **2001**, 2215-2224.
159. Chisholm, M. H.; Delbridge, E. E., A study of the ring-opening polymerization (ROP) of L-lactide by Ph₂SnX₂ precursors (x = NMe₂, OPr): the notable influence of initiator group. *New J. Chem.* **2003**, 27, 1177-1183.
160. Auras, R.; Harte, B.; Selke, S.; Hernández, R., Mechanical, Physical, and Barrier Properties of Poly(lactide). *Journal of Plastic Films and Sheeting* **2003**, 19, (2), 123-135.
161. www.chembio.uoguelph.ca/educmat/phy456/456lec01.htm.
162. Kato, Y.; Umemoto, N.; Y. Kayama, H. F.; Takeda, Y.; Hara, T.; Tsukada, Y., A novel method of conjugation of Daunomycin with antibody with a Poly-L-glutamic acid derivative as intermediate drug carrier. An anti-alfa-fetoprotein antibody-Daunomycin conjugate. *J. Med. Chem.* **1984**, 27, 1602-1607.
163. Paoletti, S.; Cesaro, A.; Samper, C. A.; Benegas, J. C., Conformational transition of poly(alpha-L-glutamic acid). A polyelectrolytic approach. *Biophys Chem.* **1989**, 34, (3), 301-309.
164. Souza, E. F. d.; Teschke, O., Liposome Stability Verification by Atomic Force Microscopy. *Rev. Adv. Sci.* **2003**, 5, 34-40.
165. Wilhelm, M.; Zhao, C.; Wang, Y.; Xu, R.; Winnik, M., Poly(styrene-ethylene oxide) Block Copolymer Micelle Formation in Water: A Fluorescence Probe Study. *Macromolecules* **1991**, 24, 1033-1040.
166. Hays, L. M.; Crowe, J. H.; Wolkers, W.; Rudenko, S., Factors Affecting Leakage of Trapped Solutes from Phospholipid Vesicles during Thermotropic Phase Transitions. *Cryobiology* **2001**, 42, (2), 88-102.
167. Champagne, C. D.; Houser, D. S.; Crocker, D. E., Glucose production and substrate cycle activity in a fasting adapted animal, the northern elephant seal. *J. Exp. Biol.* **2005**, 208, 859-868.

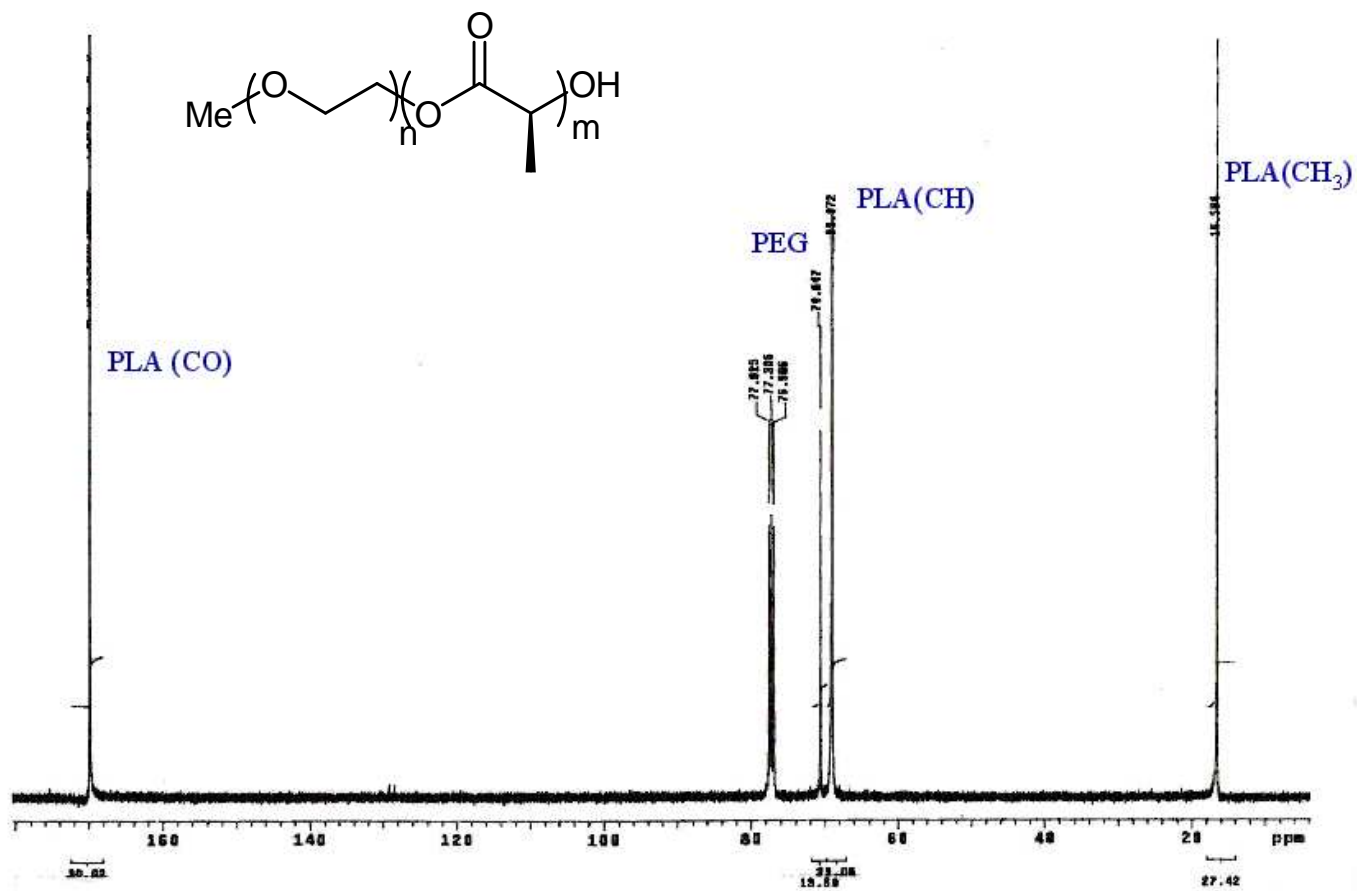
168. Kelly, G. S., Hydrochloric Acid: Physiological Functions and Clinical Implications. *Alternative Medicine Review* **1997**, 2, (2), 116-127.

APPENDICES

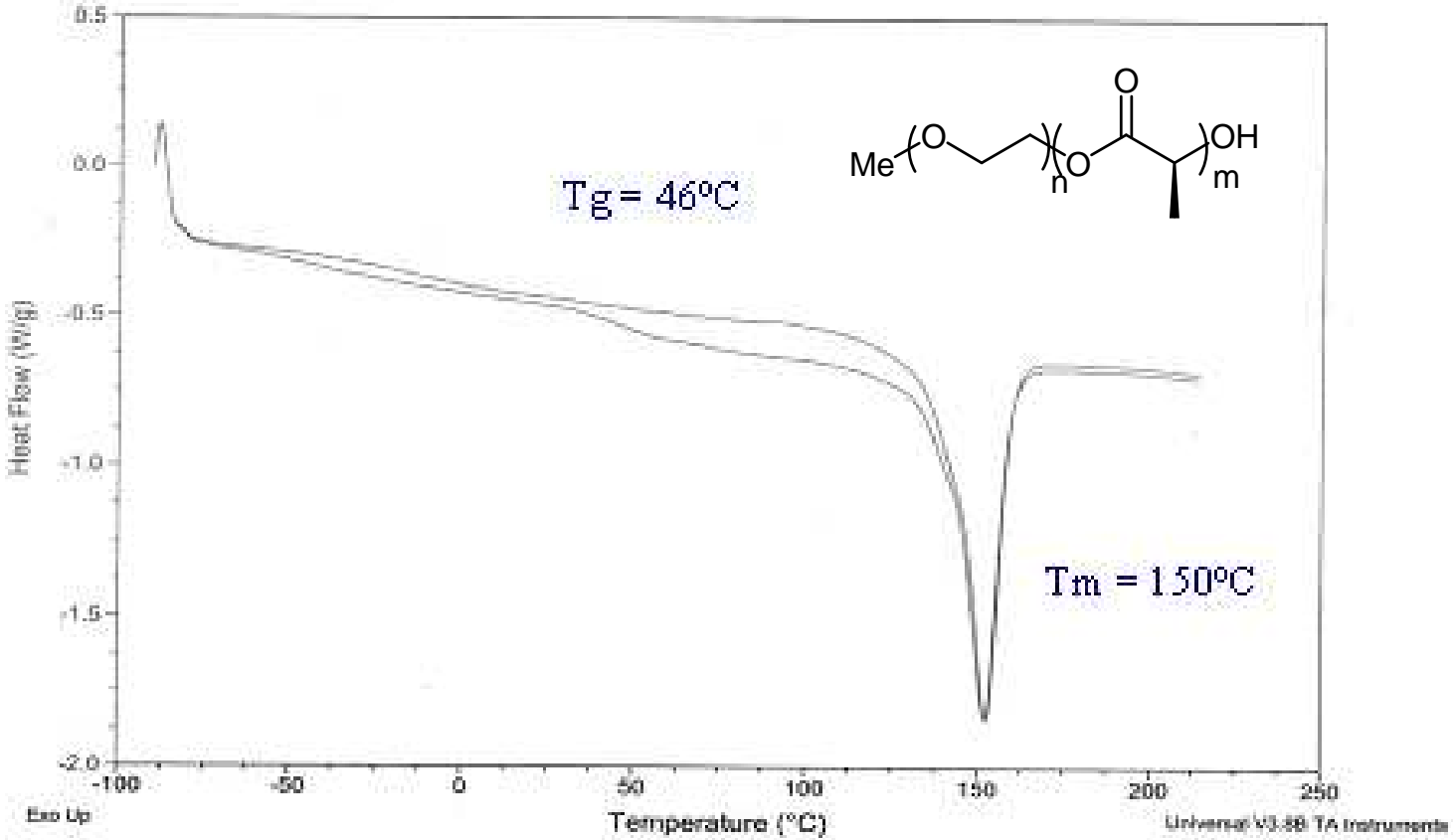
Appendix A: ^1H NMR of PEG-PLA in CDCl_3



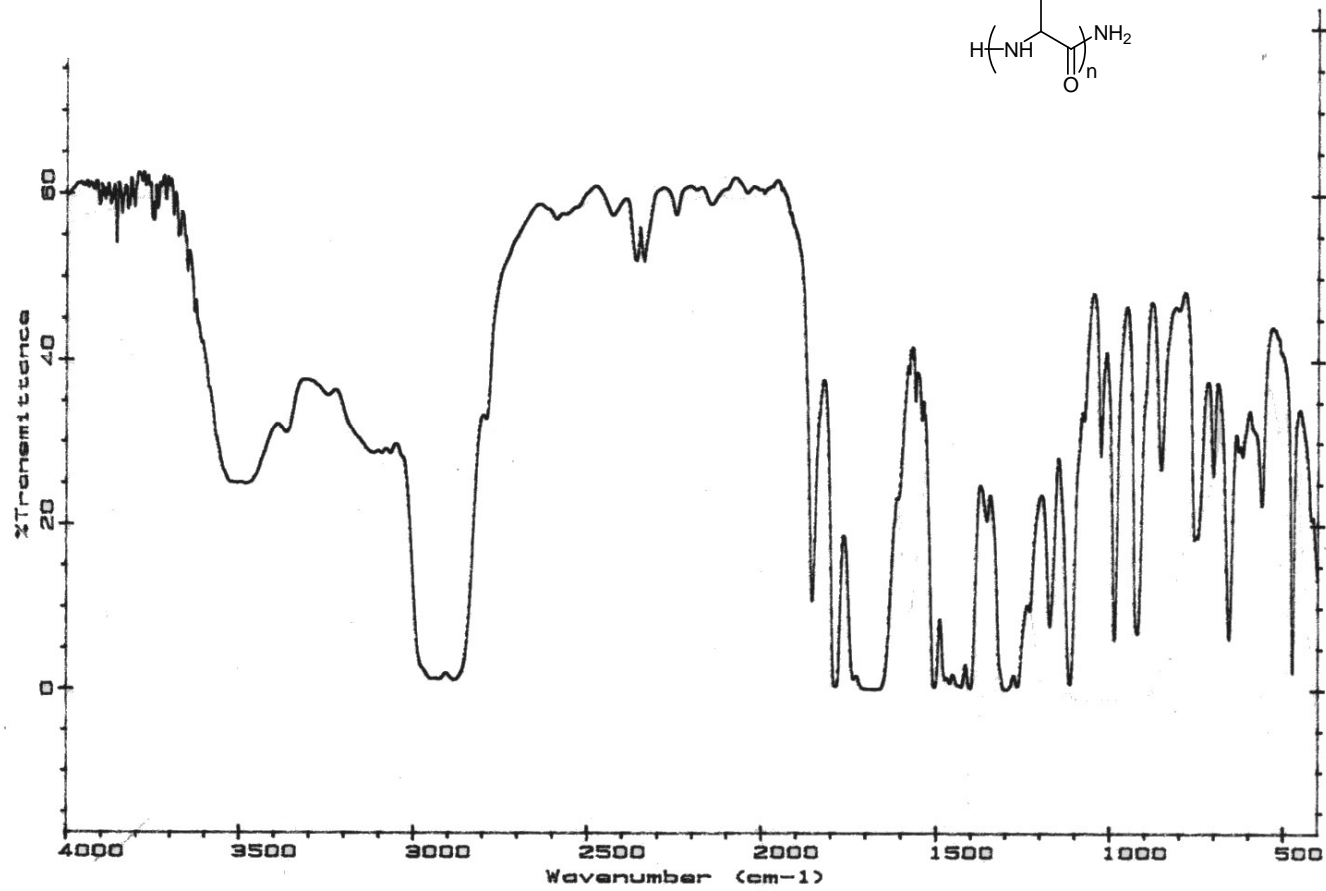
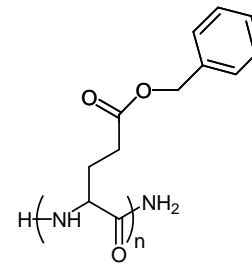
Appendix B: ^{13}C NMR of PEG-PLA in CDCl_3



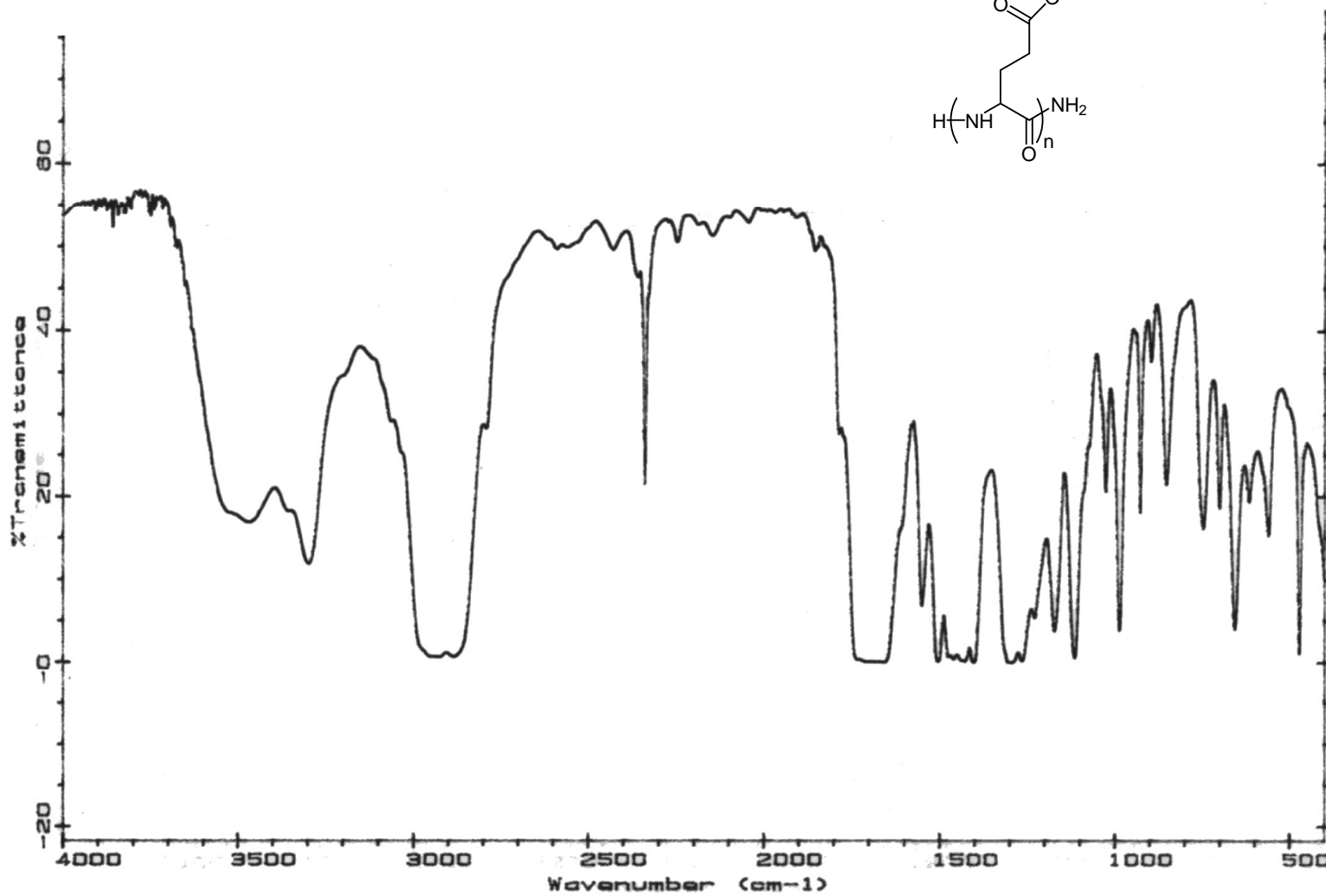
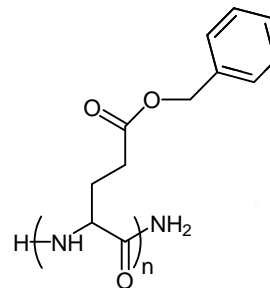
Appendix C: DSC spectrum of PEG-PLA



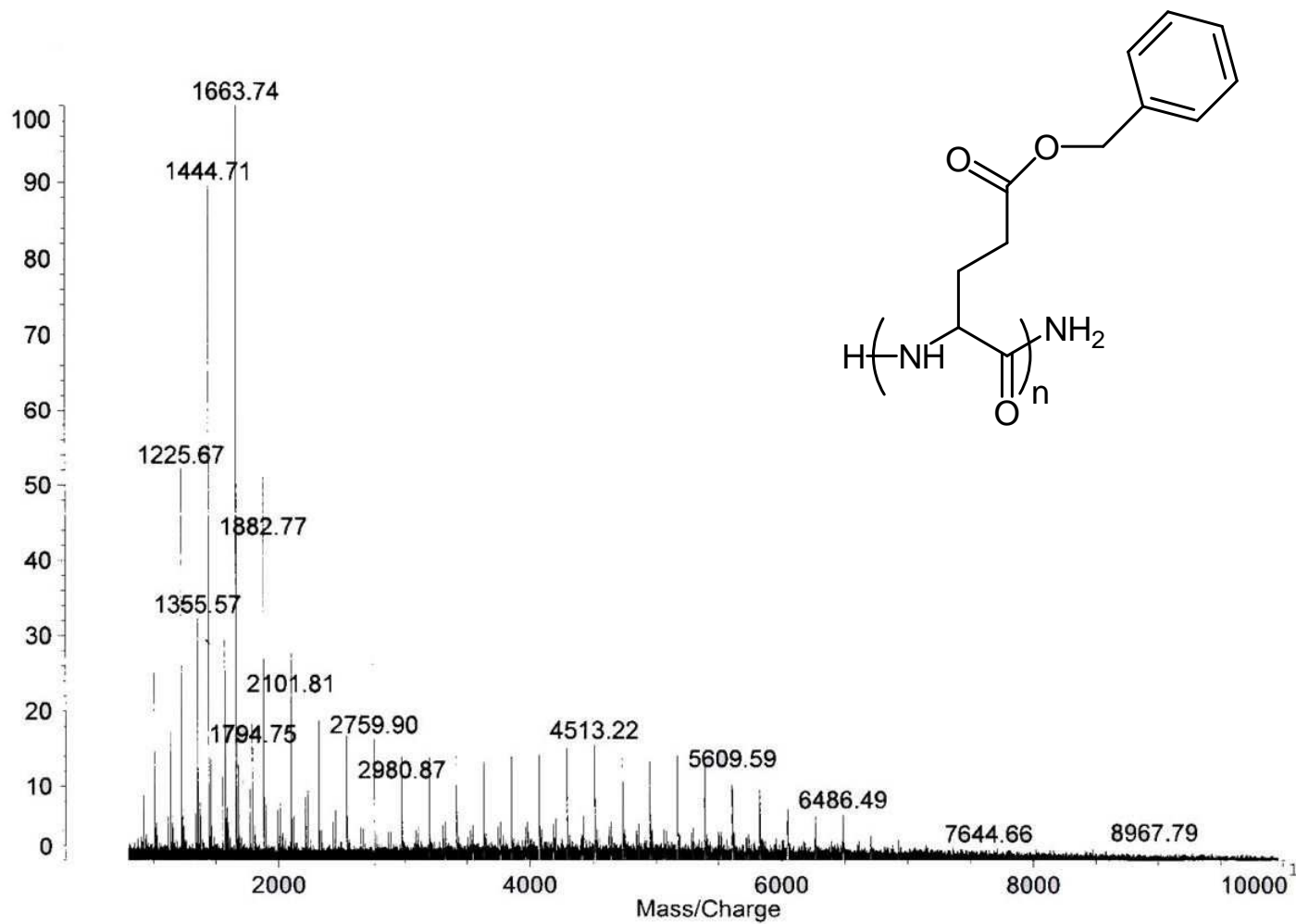
Appendix D: IR of the NCA polymerization at t=0



Appendix E: IR of the NCA polymerization at t=3h17




Appendix F: Maldi-Tof spectrum of the P(Bn)Glu

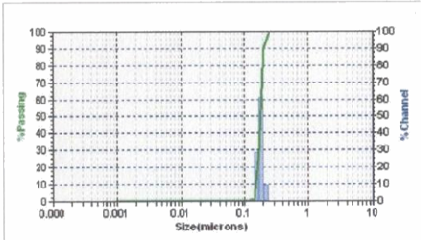


Appendix G: Light scattering of the triblock copolymer PEG₂₀₀₀-PLA₉₈₀₀-PGlu₁₃₀₀

154

FMC182	
	FMC182-Freshly prepared sonic 5 min-0.5% - filt 0.22
04/01/2005 09:20 Nanotrac S/N:U1730	

Distribution:	Monodisperse	Run Time:	30 Sec	Fluid:	CURRENT	Reflected Power (mJ):	339
Progression:	Standard	Run Num:	1 of 1	Fluid Ref. Index:	1.333	Loading Index:	0.040
Upper Edge:	6.54	Particle:	FLO'S VESICLES	Above Residual:	0	Conc. Index:	0.0365
Lower Edge:	0.0001	Transparency:	Transparent	Below Residual:	0	Cell Temp (C):	26.71
Residual:	Disabled	Part. Ref. Index:	1.63			Viscosity (cP):	0.9576
Num. Channels:	52	Part. Shape:	Spherical	Nano Ring Opt:	Disabled		
Mix:	Monodisperse	Density:	1.05 g/cc	Recirc. Status:		Serial Num:	U1730
Fiber Resolution:	Standard Form	DB Record:	95				
Sensitivity:	Standard	Database:	C:\Program Files\Microtrac\FLEX 10.3.10\Database\UHM.MDB				

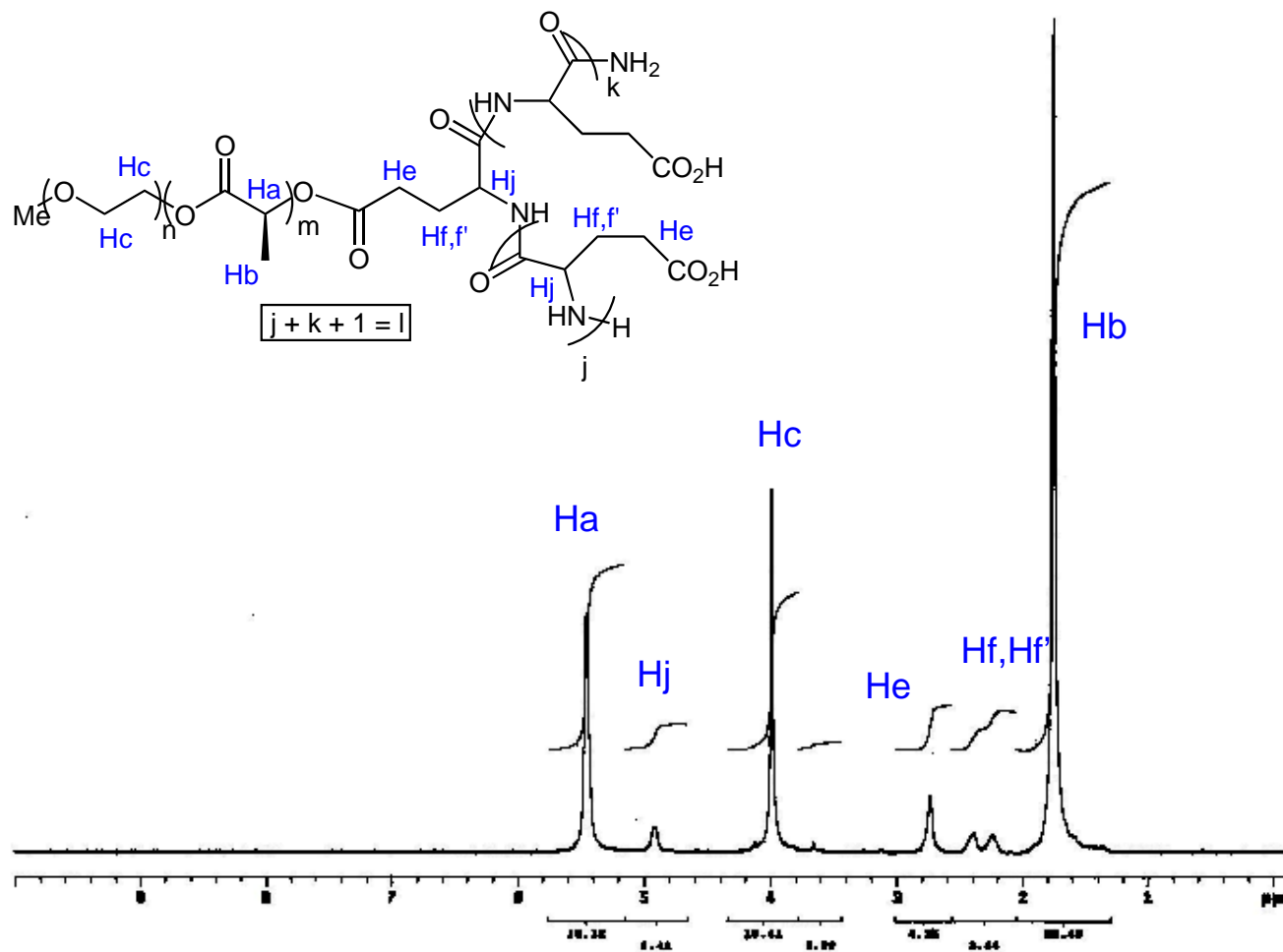


Data Item	Value	% Tile	Size(um)	Dia	Vol%	Width
MV (um):	0.1816	10.00	0.1568	0.1819	100.0	0.04
MN (um):	0.1761	20.00	0.1656			
MA (um):	0.1798	30.00	0.1721			
CS:	33.37	40.00	0.1771			
SD:	0.01874	50.00	0.1819			
MW:	1.99E+09	60.00	0.1866			
		70.00	0.1916			
		80.00	0.1971			
		90.00	0.2040			
		95.00	0.2113			

Size(um)	%Chan	% Pass	Size(um)	%Chan	% Pass	Size(um)	%Chan	% Pass	Size(um)	%Chan	% Pass
6.54	0.00	100.00	0.01806	0.00	0.00						
5.50	0.00	100.00	0.01819	0.00	0.00						
4.62	0.00	100.00	0.01277	0.00	0.00						
3.89	0.00	100.00	0.01074	0.00	0.00						
3.27	0.00	100.00	0.00903	0.00	0.00						
2.750	0.00	100.00	0.00780	0.00	0.00						
2.312	0.00	100.00	0.00639	0.00	0.00						
1.944	0.00	100.00	0.00537	0.00	0.00						
1.835	0.00	100.00	0.00452	0.00	0.00						
1.375	0.00	100.00	0.00380	0.00	0.00						
1.156	0.00	100.00	0.00319	0.00	0.00						
0.972	0.00	100.00	0.00269	0.00	0.00						
0.818	0.00	100.00	0.00226	0.00	0.00						
0.687	0.00	100.00	0.00190	0.00	0.00						
0.578	0.00	100.00	0.00160	0.00	0.00						
0.486	0.00	100.00	0.00134	0.00	0.00						
0.409	0.00	100.00	0.00113	0.00	0.00						
0.344	0.00	100.00	0.00095	0.00	0.00						
0.2890	0.00	100.00									
0.2430	9.41	100.00									
0.2044	61.09	90.59									
0.1719	28.42	29.50									
0.1445	1.08	1.08									
0.1216	0.00	0.00									
0.1022	0.00	0.00									
0.0859	0.00	0.00									
0.0723	0.00	0.00									
0.0608	0.00	0.00									
0.0511	0.00	0.00									
0.0430	0.00	0.00									
0.0361	0.00	0.00									
0.0304	0.00	0.00									
0.02555	0.00	0.00									
0.02148	0.00	0.00									

Warnings: NONE 04/01/2005 09:20

Appendix H: ^1H NMR of PEG-PLA-PGlu in TFA



Appendix I: Approval Letter IACUC #030302



UNIVERSITY of NEW HAMPSHIRE

May 24, 2005

Jerome Claverie
Materials Science
Parsons Hall
Durham, NH 03824

IACUC #: 030302
Original Approval Date: 06/09/2003 **Next Review Date:** 06/09/2006
Review Level: C

Project: Nanoparticle Mediated Peroral Delivery of Insulin

The Institutional Animal Care and Use Committee (IACUC) has reviewed and approved your request for a time extension for this protocol with the following comment(s):

- *The Committee checked "no" for #4*

Approval is granted until the "Next Review Date" indicated above. You will be asked to submit a report with regard to the involvement of animals in this study before that date. If your study is still active, you may apply for extension of IACUC approval through this office.

The appropriate use and care of animals in your study is an ongoing process for which you hold primary responsibility. Changes in your protocol must be submitted to the IACUC for review and approval prior to their implementation.

Please Note:

1. All cage, pen, or other animal identification records must include your IACUC # listed above.
2. Use of animals in research and instruction is approved contingent upon participation in the UNH Occupational Health Program for persons handling animals. Participation is mandatory for all principal investigators and their affiliated personnel, employees of the University and students alike. A Medical History Questionnaire accompanies this approval; please copy and distribute to all listed project staff who have not completed this form already. Completed questionnaires should be sent to Dr. Gladi Porsche, UNH Health Services.

If you have any questions, please contact either Van Gould at 862-4629 or Julie Simpson at 862-2003.

For the IACUC,

Handwritten signature of Robert G. Mair in black ink.

Robert G. Mair, Ph.D.
Chair

cc: File

Research Conduct and Compliance Services, Office of Sponsored Research, Service Building,
51 College Road, Durham, NH 03824-3585 * Fax: 603-862-3564

Appendix J: Approval Letter IACUC #030302



UNIVERSITY of NEW HAMPSHIRE

June 24, 2004

Claverie, Jerome
Parsons Hall
Durham, NH 03824

IACUC #: 030302
Original Approval Date: 06/09/2003 **Next Review Date:** 06/09/2005
Review Level: C

Project: Nanoparticle mediated Peroral Delivery of Insulin

The Institutional Animal Care and Use Committee (IACUC) has reviewed and approved your request for a time extension for this protocol. Approval is granted until the "Next Review Date" indicated above. You will be asked to submit a report with regard to the involvement of animals in this study before that date. If your study is still active, you may apply for extension of IACUC approval through this office.

The appropriate use and care of animals in your study is an ongoing process for which you hold primary responsibility. Changes in your protocol must be submitted to the IACUC for review and approval prior to their implementation.

Please Note:

1. All cage, pen, or other animal identification records must include your IACUC # listed above.
1. Use of animals in research and instruction is approved contingent upon participation in the UNH Occupational Health Program for persons handling animals. Participation is mandatory for all principal investigators and their affiliated personnel, employees of the University and students alike. A Medical History Questionnaire accompanies this approval; please copy and distribute to all listed project staff who have not completed this form already. Completed questionnaires should be sent to Dr. Gladi Porsche, UNH Health Services.

If you have any questions, please contact either Van Gould at 862-4629 or Julie Simpson at 862-2003.

For the IACUC,

Robert G. Mair, Ph.D.
Chair

cc: File

Research Conduct and Compliance Services, Office of Sponsored Research, Service Building,
51 College Road, Durham, NH 03824-3585 * Fax: 603-862-3564

Appendix K: Approval Letter IACUC #030302

UNIVERSITY OF NEW HAMPSHIRE

Office of Sponsored Research
Service Building
51 College Road
Durham, New Hampshire 03824-3585
(603) 862-3564 FAX

LAST NAME	Claverie	FIRST NAME	Jerome
DEPT	Materials Science Program, 137 Parsons Hall	APP'L DATE	6/9/2003
OFF-CAMPUS ADDRESS (if applicable)	Materials Science Program 137 Parsons Hall	IACUC #	030302
		REVIEW LEVEL	C
		TODAY'S DATE	6/11/2003
PROJECT TITLE	Nanoparticle mediated Peroral Delivery of Insulin		

All cage, pen or other animal identification records must include your IACUC Protocol # as listed above.

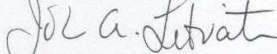
The Institutional Animal Care and Use Committee (IACUC) has reviewed and approved the protocol submitted for this study under Category C on Page 4 of the "Application for Review of Animal Use in Research or Instruction" – the research potentially involves minor short-term pain, discomfort or distress which will be treated with appropriate anesthetics/analgesics or other assessments.

Approval is granted for a period of three years from the approval date above. Continued approval throughout the three year period is contingent upon completion of annual reports on the use of animals. At the end of the three year approval period you may submit a new application and request for extension to continue this project. Requests for extension must be filed prior to the expiration of the original approval.

Please note: Use of animals in research and instruction is approved contingent upon participation in the UNH Occupational Health Program for persons handling animals. *Participation is mandatory* for all principal investigators and their affiliated personnel, employees of the University and students alike. A Medical History Questionnaire accompanies this approval; please copy and distribute to all listed project staff who have not completed this form already. Completed questionnaires should be sent to Dr. Gladi Porsche, UNH Health Services.

If you have any questions, please contact either Van Gould at 862-4629 or Julie Simpson at 862-2003.

For the IACUC,



John A. Litvaitis, Ph.D.
Chair

cc: File